SEQUENCE STRATIGRAPHY OF NIGER DELTA, ROBERTKIRI FIELD, ONSHORE NIGERIA

A Thesis

by

OLUSOLA AKINTAYO MAGBAGBEOLA

Submitted to the Office of Graduate Studies of
Texas A&M University
in partial fulfillment of the requirements for the degree of

MASTER OF SCIENCE

December 2005

Major Subject: Geology

SEQUENCE STRATIGRAPHY OF NIGER DELTA, ROBERTKIRI FIELD, ONSHORE NIGERIA

A Thesis

by

OLUSOLA AKINTAYO MAGBAGBEOLA

Submitted to the Office of Graduate Studies of
Texas A&M University
in partial fulfillment of the requirements for the degree of

MASTER OF SCIENCE

Approved by:

Chair of Committee,	Brian J. Willis
Committee Members,	Steven L. Dorobek
	William. Bryant
Head of Department,	Richard F. Carlson

December 2005

Major Subject: Geology

ABSTRACT

Sequence Stratigraphy of Niger Delta, Robertkiri Field, Onshore Nigeria.

(December 2005)

Olusola Akintayo Magbagbeola, B.Sc. (Honors);

University of Ilorin, Ilorin, Nigeria;

M.Sc., University of Ibadan, Ibadan, Nigeria

Chair of Advisory Committee: Dr. Brian J. Willis

Deposits of Robertkiri field, in the central offshore area of Niger Delta, comprise a 4 km thick succession of Pliocene to Miocene non-marine and shallow marine deposits. A sequence stratigraphic framework for Robertkiri field strata was constructed by combining data from 20 well logs and a seismic volume spanning 1400 km^2. Major sequences, hundreds of meters thick, define layers of reservoir and sealing strata formed during episodic progradation and retrogradation of deltaic shorelines. These deposits progress upward from fine-grained prodelta and deep water shales of the Akata Formation through paralic sandstone-shale units of the Agbada Formation and finally to sandy non-marine deposits of the Benin Formation. The Agbada Formation is divided into six third-order sequences starting at the first seismic reflection that can be mapped across the seismic volume. The Agbada Formation under Robertkiri field is complexly deformed across a succession of major, cuspate, offshore-dipping, normal faults, and associated antithetic faults and rollover anticlines within down-dropped blocks.

Thickening of intervals between some reflections across major faults and away from the crests of adjacent rollover anticlines suggest syndepositional displacement. Relationships between major faults and the thickness of transparent seismic facies that comprise lower parts of the seismic record suggest faulting was associated with movement of undercompacted shales within the Akata and lower Agbada Formations.

Robertkiri field is located along the proximal margin of the Coastal Swamp I depobelt, a subbasin within the Niger Delta clastic wedge formed by margin collapse into underlying undercompacted shale. Accommodation and sequence development in this setting is controlled by both structural faulting and sea level fluctuations. Upsection, sequences become thinner, more laterally uniform in thickness, less structurally deformed and contain less growth strata. Erosion along sequence boundaries becomes progressively shallower and broader, as accommodation under Robertkiri field declined and more sediment was bypassed basinward. Incisions along the base of older sequences (>100 m) is greater than 3rd order sea level falls reported to occur during the Miocene, which suggests that there were local areas of tectonic uplift within this dominantly extensional setting.

DEDICATION

I dedicate this thesis to God, my darling wife, OluwaToyin Rita Magbagbeola and son, OluwaLONImi (LONI). ‘Tayo (jr). Magbagbeola.

ACKNOWLEDGMENTS

Many thanks to Dr. Brian Willis, the chair of my thesis committee for his tireless contributions to the success of this study. I owe a debt of gratitude to Dr. Steve Dorobek and Dr. William Bryant for the assistance and contribution in reviewing the manuscript. I thank my employer, Chevron Nigeria Limited, for providing a scholarship and resources for this program. I am equally grateful for my manager in Nigeria, Mr. A. J. Akinwale, for his support and encouragement always. Thanks to ‘Dayo Adeogba and Monsur Akinyele for their wealth of knowledge and support at all times. Finally, I appreciate my wife OluwaToyin Rita Magbagbeola, son Loni Magbagbeola and parents Deacon and Deaconess E. Magbagbeola.

TABLE OF CONTENTS

Page

LIST OF FIGURES

FIGURE Page

FIGURE Page

FIGURE Page

FIGURE Page

LIST OF TABLES

INTRODUCTION

Sequence stratigraphic concepts defining sediment accumulation and preservation trends within basin fills have become a highly successful exploration technique in the search for natural resources. Classical sequence stratigraphy for deltaic successions assumes that depositional processes across linked system tracts produces an equilibrium offshore depositional gradient, that shifts in position as sediments fill accommodation generated by gradual subsidence and sea-level variations. Sequence stratigraphic analysis of these successions define key stratal surfaces at abrupt dislocations of system tracts to delineate broad-scale facies trends formed by along-basin shifts in depositional environments and changes in preservation within system tracts (Vail et al., 1977; Posamentier et al., 1988; Postma, 1995). Higher-frequency progradation and transgression of deltaic systems tracts has been related to both random autocyclic channel avulsion and associated delta lobe switching, and to allocyclic processes like sea-level fluctuations and climate changes (Thorne and Swift, 1991). The internal architecture of deltaic successions that prograde onto mobile shale substrates can be significantly complicated by structural collapse of the delta front. Despite extensive literature on large delta deposits, little attention has been focused on influence of mobile substrates on the resulting sequence stratigraphy.

The Niger Delta has a distinctive structural and stratigraphic zonation. Regional and counter-regional growth faults, developed in an outer-shelf and upper-slope setting, are linked via a translational zone containing shale diapirs to a contractional zone

---

This thesis follows the style and format of the American Association of Petroleum Geologists Bulletin.

defined by a fold-thrust belt developed in a toe-of-slope setting (Hooper, 2002). Damuth (1994) considered Neogene gravity tectonics and depositional processes on the modern deep Niger Delta continental margin. He recognized three regional structural styles; (1) an upper extensional zone of listric growth faults beneath the outer shelf, (2) a translational zone of diapirs and shale ridges beneath the upper slope; and (3) a lower compressional zone of imbricate thrust structures (toe thrusts) beneath the lower slope and rise. He suggested these areas with different structural style are linked together on a regional scale and that these variations in style suggest that large portions of this thick sediment prism are slowly moving downslope by gravity collapse. Cohen and Ken McClay (1994) discussed sedimentation and shale tectonics of the northwestern Niger Delta front. Morgan (2004) examined relationships between mobile shale structure and channel formation above the compressional toe of Niger Delta and highlighted the importance of transfer zones within the toe thrust belt as a control on the underlying structural framework. Adeogba et al. (2005) discussed transient fan architecture and depositional controls from near-surface 3-D seismic data of Niger Delta continental slope. Corredor et al. (2005) related structural styles in the deep-water fold and thrust belts of the Niger Delta and concluded that there are two complex, imbricate fold and thrust belt systems (the inner and outer fold and thrust belts) that are the product of contraction caused by gravity-driven extension on the shelf. Hoover et al., (2001) explained the role of deformation in controlling depositional patterns in the south-central Niger Delta, their work was however focused mainly at the compressional toe of the delta, and they concluded that structural elements are the primary control of accommodation changes on the slope and toe of the delta.

Other examples of deltaic systems that rapidly prograded onto mobile substrates include: the Baram delta, offshore Brunei (Rensbergen et al., 1999), Caspian Sea (Khalivov and Kerimov 1983), and Alboran Sea (Morley 1992). Daily (1976) synthesized relationships between progradation, subsidence, basal undercompacted shale wedge, growth faulting, shale diapirism and overthrusting within the Mississippi, Niger and Mackenzie Delta systems. Morley et al. (1998) related shale tectonics to deformation associated with active diapirism within the Jerudong anticline, Brunei Darussalam. They established that shale diapirs and associated growth faults exerted an important influence on large- and small-scale bedding geometries and facies changes of syntectonic shallow-marine, shoreface and tidal strata for the area. Edwards (2000) reviewed the origin and significance of failed shelf margins of Tertiary northern Gulf of Mexico basin and recognized the role of slumping in forming unconformities of regional extent along retrograde failed shelf margins. Rensbergen and Morley (2000) discussed a 3D Seismic study of a shale expulsion syncline at the base of the Champion delta, offshore Brunei and its implications for the early structural evolution of large delta systems.

Most work on depositional sequences above mobile substrates has focused on slope and deep water environments. Robertkiri field lies in a shelfal depositional setting and the focus of this study is to investigate the effect of mobile shale substrate on the nature of depositional sequence developed within this shallow water setting. The Niger Delta clastic wedge is complicated by listric normal faults that formed as prograding deltaic sediments loaded underlying undercompacted prodelta and deeper marine shales. Overpressured shale has been related to some combination of burial compaction, diagenesis of clays, kerogen maturation, and compressive tectonics. The active fluid

migration necessary to maintain shale movement can form vents for hydrocarbon migration from deeply buried source rocks to shallower reservoirs and traps (Rensbergen et al., 1999). Movement of undercompacted mobile shale beneath prograding deltaic successions can cause delta margins to collapse, altering depositional slopes and complicating sediment transport paths and patterns of deposition.

One of the poorly understood features of Agbada Formation stratigraphy is the occurrence of deep incision surfaces into these prograding deltaic successions that locally cut hundreds of meters into underlying deposits. Such incision depths are significantly greater than estimates of Miocene-aged fluctuations in sea level (Talling, 1998; Posamentier and Vail, 1988; Van Wagoner et al., 1990), which suggests they could not have formed by eustatic sea level falls alone. The rise of underlying shale and associated structural faulting of overlying strata can alter depositional sequences by increasing rates of local sediment accumulation above down dropped fault blocks as footwall blocks are eroded. A sequence stratigraphic framework is developed for Robertkiri field (Figure 1) to interpret long-term patterns of deposition along this deltaic margin. This framework is used to examine relationships between sequence boundary erosion, spatial changes in sequence thickness and internal facies trends, and patterns of syndepositional deformation.

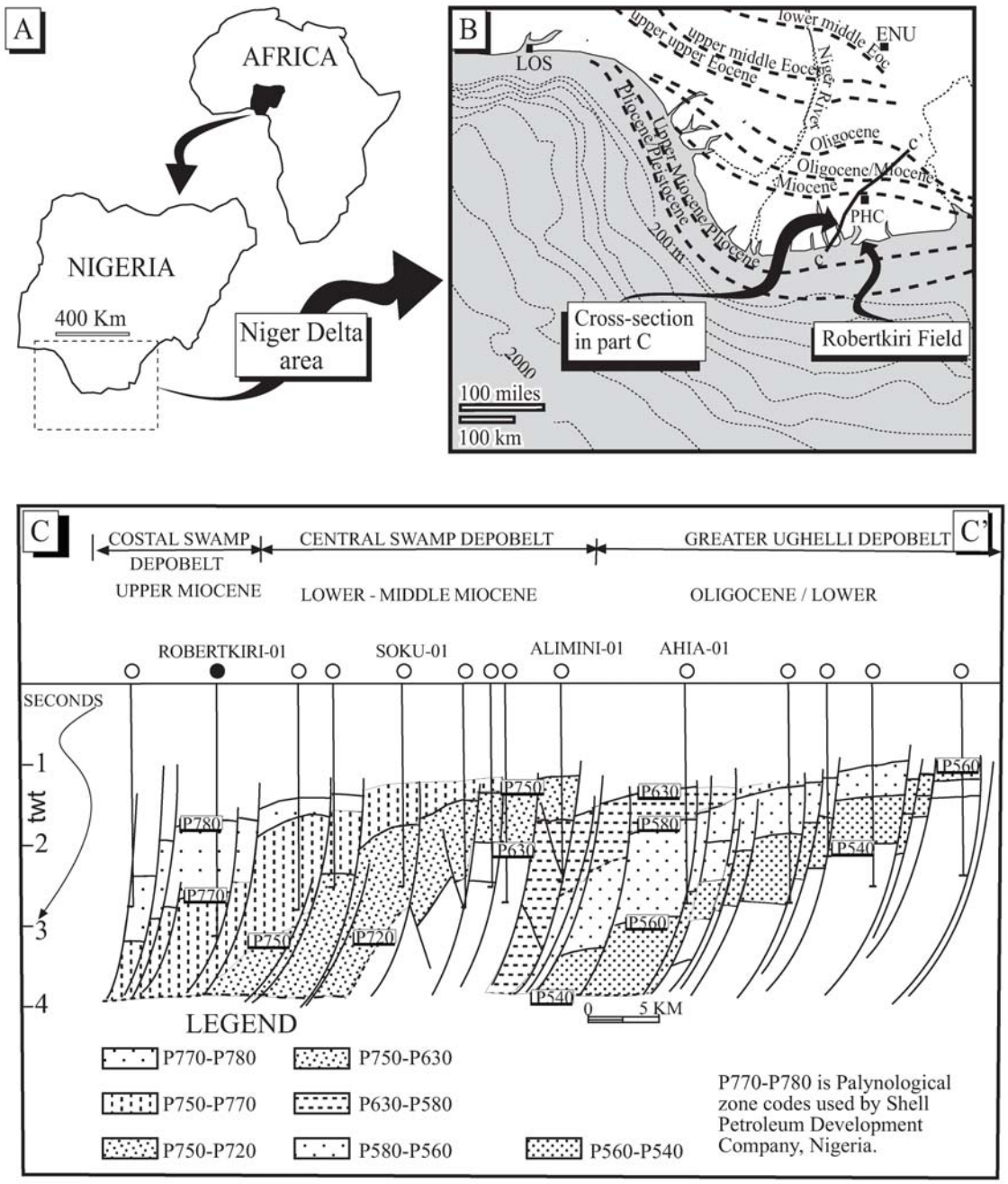

Figure 1. Location map of study area. (A) Location of Niger Delta along the west coast of Africa. (B) Location of Robertkiri field offshore Niger delta. Thick dashed lines show location of the prograding delta front at different times during the Tertiary (from Doustand Omatsola, 1990). Thin dashed lines show modern offshore bathymetry. Line C-C' shows position of cross section regional cross section below. (C) Stratigraphic cross section from NNE to SSW shows the prograding geometry of Niger Delta deposits (modified fromDoust and Omatsola, 1990). See location of cross section in part B.

THE NIGER DELTA

REGIONAL SETTING

Niger Delta covers a 70,000 square kilometer area within the Gulf of Guinea, West Africa, Nigeria (Figure 1). Although the modern Niger Delta formed in the early Tertiary, sediments began to accumulate in this region during Mesozoic rifting associated with the separation of the African and South American continents (Weber and Daukoru, 1975; Evamy et al., 1978; Doust and Omatsola, 1990). Synrift marine clastics and carbonates accumulated during a series of transgressive-regressive phases between the Cretaceous to early Tertiary; the oldest dated sediments are Albian age (Doust and Omatsola, 1989). These synrift phases ended with basin inversion in the Late Cretaceous (Santonian). Proto-Niger Delta regression continued as continental margin subsidence resumed at the end of the Cretaceous (Maastritchian). Niger Delta progradation into the Gulf of Guinea accelerated from the Miocene onward in response to evolving drainages of the Niger, Benue and Cross rivers and continued continental margin subsidence.

Tertiary Niger Delta deposits are characterized by a series of depobelts that strike northwest-southeast, sub-parallel to the present day shoreline (Figure 2). Depobelts become successively younger basinward, ranging in age from Eocene in the north to Pliocene offshore of the present shoreline. Depobelts, tens of kilometers wide, are bounded by a growth fault to the north and a counter-regional fault seaward. Each sub-basin contains a distinct shallowing-upward depositional cycle with its own tripartite assemblage of marine, paralic, and continental deposits. Depobelts define a series of punctuations in the progradation of this deltaic system. As deltaic sediment loads

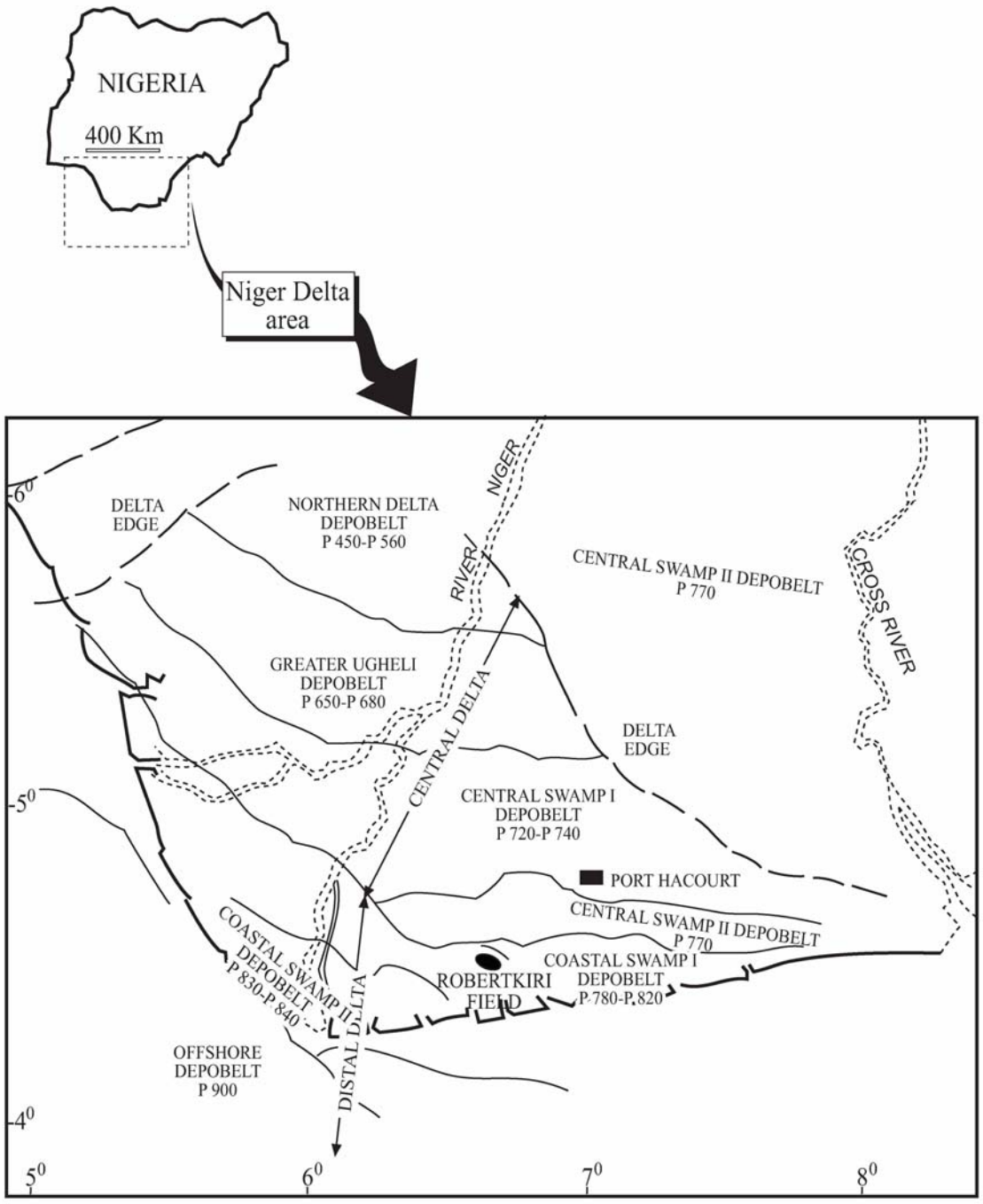

Figure 2. Depobelts with their relative ages striking northwest - southeast. Depobelts are sub-parallel to the present coastlines and become successively younger basinward. Three broad areas are distinguished: the delta edge, central delta and distal delta. Robertkiri field is located on the proximal side of the Coastal Swamp I depobelt. Modified from Doust and Omatsola (1990).

increase, underlying delta front and prodelta marine shale begin to move upward and basinward. Mobilization of basal shale caused structural collapse along normal faults, and created accommodation for additional deltaic sediment accumulation. As shale withdrawal nears completion, subsidence slows dramatically, leaving little room for further sedimentation. As declining accommodation forces a basinward progradation of sediment, a new depocenter develops basinward. Most Niger Delta faulting is due to extensional deformation. The exception is in the distal section, where overthrust faults form in the toe of the proto-Niger Delta. These extensional faults are normal and generally listric, comprising syndepositional growth faults and crestal tensional relief faults. These faults are synthetic or antithetic, running sub-parallel to the strike of the sub-basins. These synsedimentary faults exhibit growth strata above the downthrown block, as well as anticlinal (rollover) closures. Most hydrocarbon bearing structures in Niger Delta deposits are close to these structure-building faults, in complexly collapsed crest and faulted anticlinal structures. Growth faults and antithetic faults play an essential role in trap configuration. Growth faults exhibit significant throw (up to several hundred meters), are arcuate in plan view, concave basinward and may be several tens of kilometers in length. Antithetic faults have less throw (generally less than a hundred meters), can be linear or arcuate in plan view and they rarely exceed ten kilometers in length (Cathles et al., 2003).

FORMATIONS AND DEPOSITIONAL ENVIRONMENTS

The morphology of the Niger Delta changed from an early stage, spanning the Paleocene to early Eocene, to a later stage of delta development beginning in Miocene time. Early coastlines were concave to the sea and depositional patterns were strongly influenced by basement topography (Doust and Omatsola, 1989). Delta progradation occurred along two major axes. The first paralleled the Niger River, where sediment supply exceeded subsidence rate. The second, smaller than the first, became active basinward of the Cross River during the Eocene to early Oligocene. Late stages of deposition began in the early to middle Miocene, as these separate eastern and western depocenters merged. In late Miocene the delta prograded far enough that shorelines became broadly concave into the basin. Accelerated loading by this rapid delta progradation mobilized underlying unstable shales. These shales rose into diapiric walls, deforming overlying strata. The resulting complex deformation structures caused local uplift, which resulted in major erosion events into the leading progradational edge of the Niger Delta. Several deep canyons, now clay filled, cut into the shelf are commonly interpreted to have formed during sea level lowstands. The best known are the Afam, Opuama, and Qua Iboe Canyon fills (Figure 3; Reijers, et al., 1999 and Tuttle, et al., 1999).

Short and Stauble (1967) defined formations within the Niger Delta clastic wedge based on sand/shale ratios estimated from subsurface well logs. The three major lithostratigraphic units defined in the subsurface of Niger Delta (Akata, Agbada and Benin formations, Figure 4; Lawrence, et al., 2002) reflect a gross upward-coarsening clastic wedge. These Formations were deposited in dominantly marine, deltaic

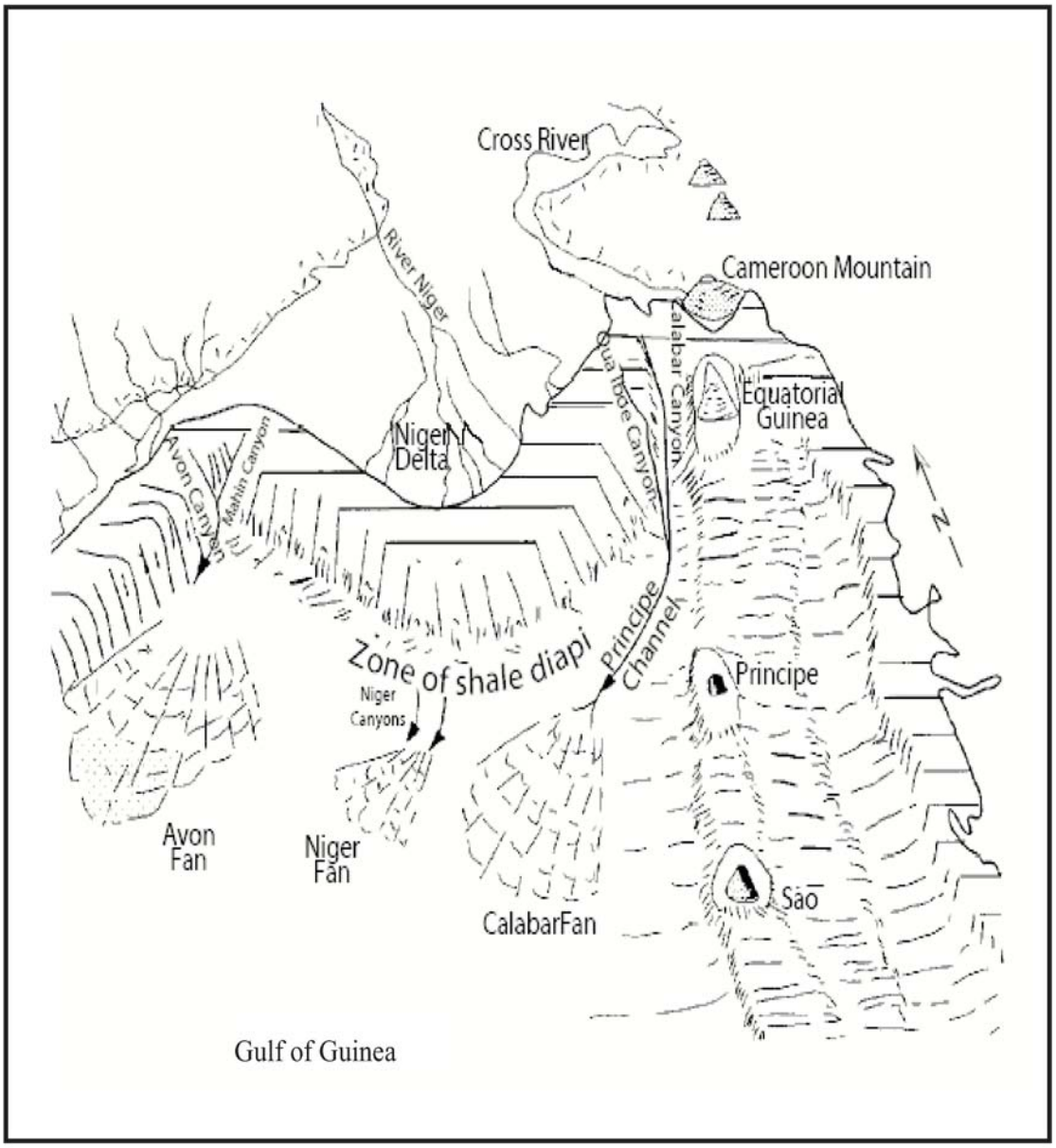

Figure 3. Physiographic sketch of the deep marine sediments in the Gulf of Guinea offshore Niger Delta (modified from Reijers et al., 1997).

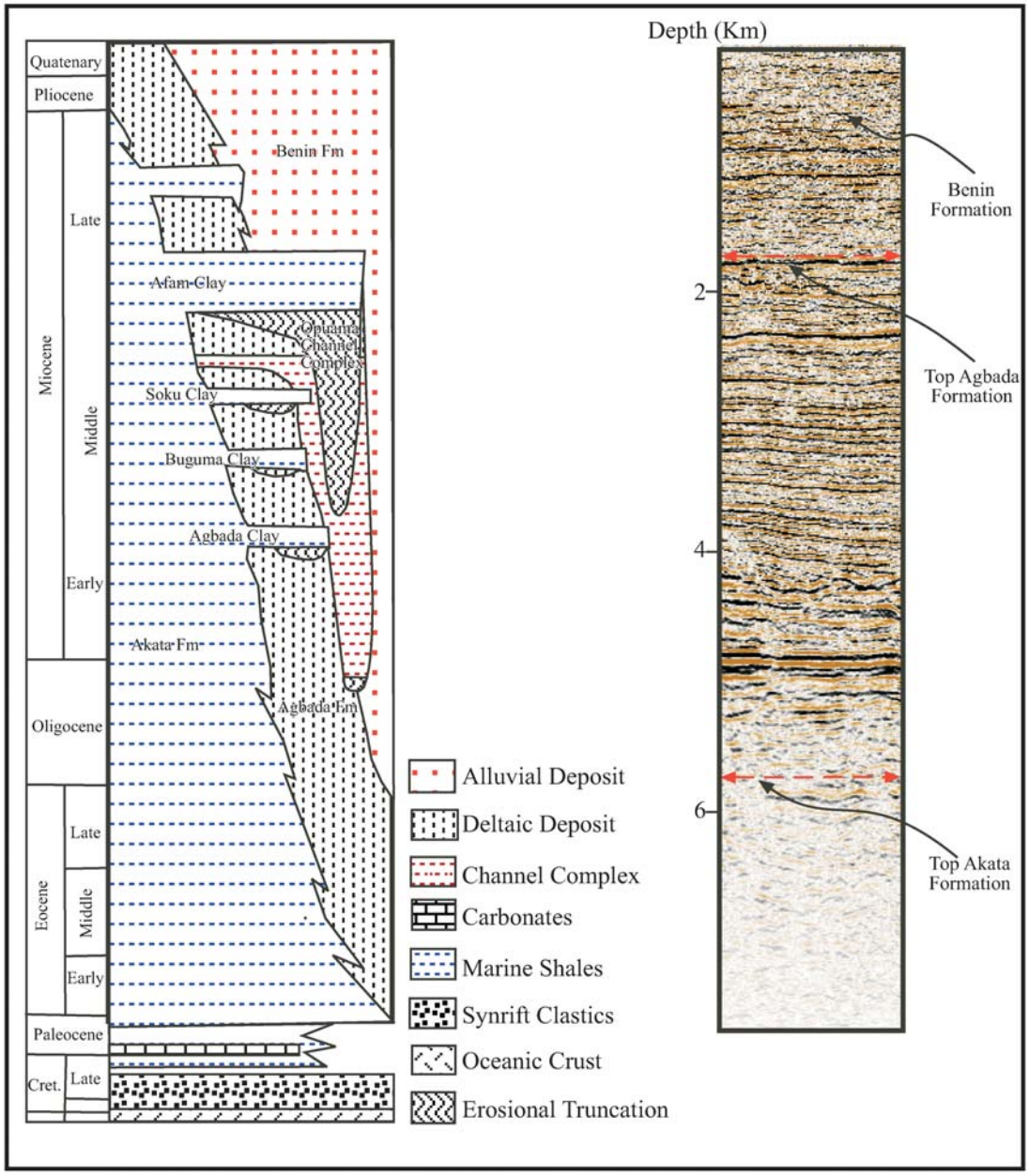

Figure 4. Schematic diagram of Niger Delta regional stratigraphy, and variable density seismic display of the main stratigraphic units with corresponding reflections (modified from Lawrence et al., 2002).

and fluvial environments, respectively (Weber and Daukoru, 1975; Weber, 1986). Stratigraphically equivalent units to these three formations are exposed in southern Nigeria (Table 1; Short and Stauble, 1967).

The Akata Formation, dark gray shales and silts with rare streaks of sand of probable turbidite flow origin, is estimated to be 6,400 m thick in the central part of this clastic wedge (Doust and Omatsola, 1989). Marine planktonic foraminifera suggest a shallow marine shelf depositional setting ranging from Paleocene to Recent in age (Doust and Omatsola, 1989). These shales are exposed onshore in the northeastern part of the delta, where they are referred to as the Imo Shale. This formation also crops out offshore in diapirs along the continental slopes. Where deeply buried, Akata shales are typically overpressured. Akata shales have been interpreted to be prodelta and deeper water deposits that shoal vertically into the Agbada Formation (Stacher, 1995, Doust and Omatsola, 1989).

The Agbada Formation occurs throughout the Niger Delta clastic wedge, has a maximum thickness of about 3,900 m and ranges in age from Eocene to Pleistocene (Doust and Omatsola, 1989). It crops out in southern Nigeria, where it is called the Ogwashi-Asaba Formation. The lithologies consist largely of alternating sands, silts and shales with progressive upward changes in grain size and bed thickness. The strata are generally interpreted to have formed in fluvial-deltaic environments (Stacher, 1995, Doust and Omatsola, 1989).

Table 1: Stratigraphic units of Niger Delta area, Nigeria. Modified from Short and Stauble (1967).

Subsurface			**Surface Outcrops**		
Youngest known Age		**Oldest known Age**	**Youngest Known Age**		**Oldest Known Age**
Recent	Benin Formation (Afam clay member)	Oligocene	Plio/Pleistocene	Benin Formation	
Recent	Agbada Formation	Eocene	Miocene Eocene	Ogwashi-Asaba Formation Ameki Formation	Oligocene Eocene
Recent	Akata Formation	Eocene	lower Eocene	Imo shale Formation	Paleocene
	Unknown		Paleocene Maestrichtian Campanian Campanian/Maestrichtian Coniacian/Santonia Turonian Albian	Nsukka Formation Ajali Formation Mamu Formation Nkporo Shale Awgu Shale Eze Aku Shale Asu River Group	Maestrichtian Maestrichtian Campanian Santonian Turonian Turonian Albian

The Benin Formation comprises the top part of the Niger Delta clastic wedge, from the Benin-Onitsha area in the north to beyond the present coastline (Short and Stauble, 1967). The top of the formation is the current subaerially-exposed delta top surface and its base, defined by the top of the youngest underlying marine shales, extends to a depth of about 1400m. The age of the formation is thought to range from Oligocene to Recent (Short and Stauble, 1967). Shallow parts of the formation are composed entirely of non-marine sands deposited in alluvial or upper coastal plain environments

during progradation of the delta (Doust and Omatsola, 1989). The formation thins basinward and ends near the shelf edge.

The modern Niger Delta is a mixed wave, tide and fluvial deltaic system. The delta is reworked by wave action along an arcuate coast with barrier islands, back-barrier lagoons, and chennier ridges. Thick mangroves border the coastline of the lower Niger Delta plain. Incised into this coastline are numerous tide-dominated coastal estuaries that have gradually been infilled with sediment following the Holocene sea level highstand (Figure 5). The modern delta front and continental slope is characterized by localized slumps and canyons that bypass sediments into deeper waters. Although details of deltaic features are difficult to decipher within reservoir intervals of Niger Delta deposits, the modern distribution of distributary channels, estuary fills, shoreface, back barrier lagoonal sediments, and delta plain deposits are assumed to be a good analog.

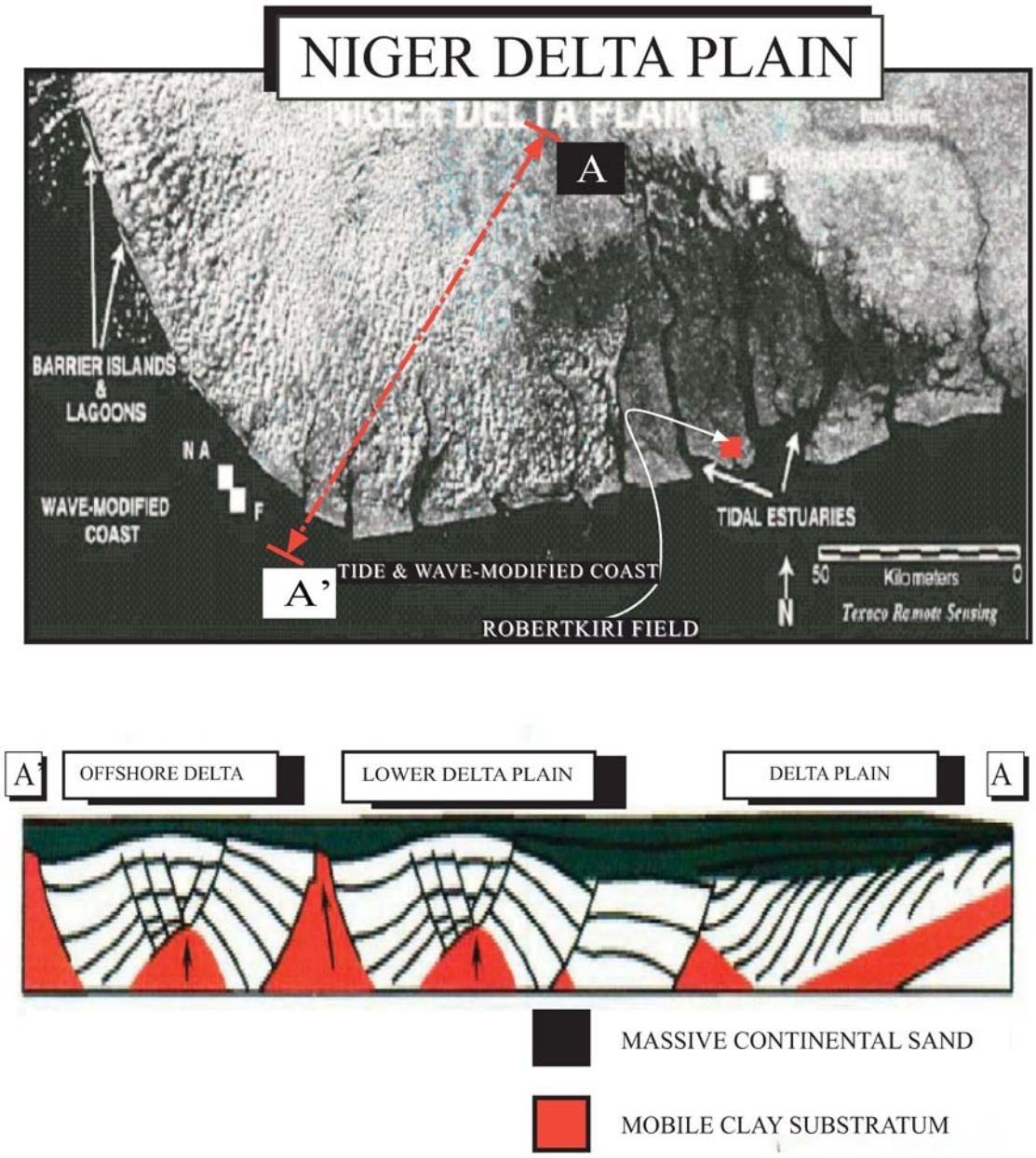

Figure 5. LANDSAT TM mosaic of mixed wave, tide, and fluvial influenced Niger Delta. River channels rework coastal plain sediments. Tide and wave action produce estuaries at the mouth of distributaries (dark gray areas in the image to the right of center). Tides have a greater effect along coasts to the east (right) and wave have greater influence to the west (left). Near the center of the mossaic, where the delta is prograding, accommodation space declines in response to increased sediment input from the active distributaries. Modified from Cathles et al.(2003).

DATA AND METHODOLOGY

DATA

Robertkiri oil field is located southeast of Port Harcourt, Nigeria, at the eastern end of the Niger Delta (Figure 1). It covers 1400 km^2 within the proximal part of the Coastal Swamp I depobelt (Figure 2). The field was discovered in 1964 by Gulf Oil Company well Robertkiri-01 and is currently operated by Chevron Nigeria Limited. The data used for this research include 20 wireline logs, a biostratigraphic interpretation of samples from the Robertkiri-01 well, and a 3-D seismic volume that covers 1400 km^2.

LOG DESCRIPTION

The 20 wells of Robertkiri field are all located in the southwest corner of the seismic volume (Figure 6). A typical gamma ray well log through the Agbada Formation in Robertkiri field has higher average values near the base of the Formation and values increase upward on average over 2.7 km to the base of the Benin Formation (Figure 7a). Within the Benin Formation gamma ray values are uniformly low. This vertical trend reflects a large-scale coarsening of the clastic wedge. Within the Agbada Formation four general log signatures are defined over stratigraphic intervals ranging from several tens to hundreds of meters thick: (1) Intervals that start with an abrupt decrease of gamma ray values and then gradually increase upward, interpreted to indicate an abrupt coarsening followed by a gradual fining-upward trend (Figure 7b, a), (2) Intervals with decreasing gamma ray values that end where values abruptly increase, interpreted to indicate an upward-coarsening trend (Figure 7b, b), (3) Symmetric patterns defined by initial gradual decrease and then increase in gamma ray values interpreted to record a gradual

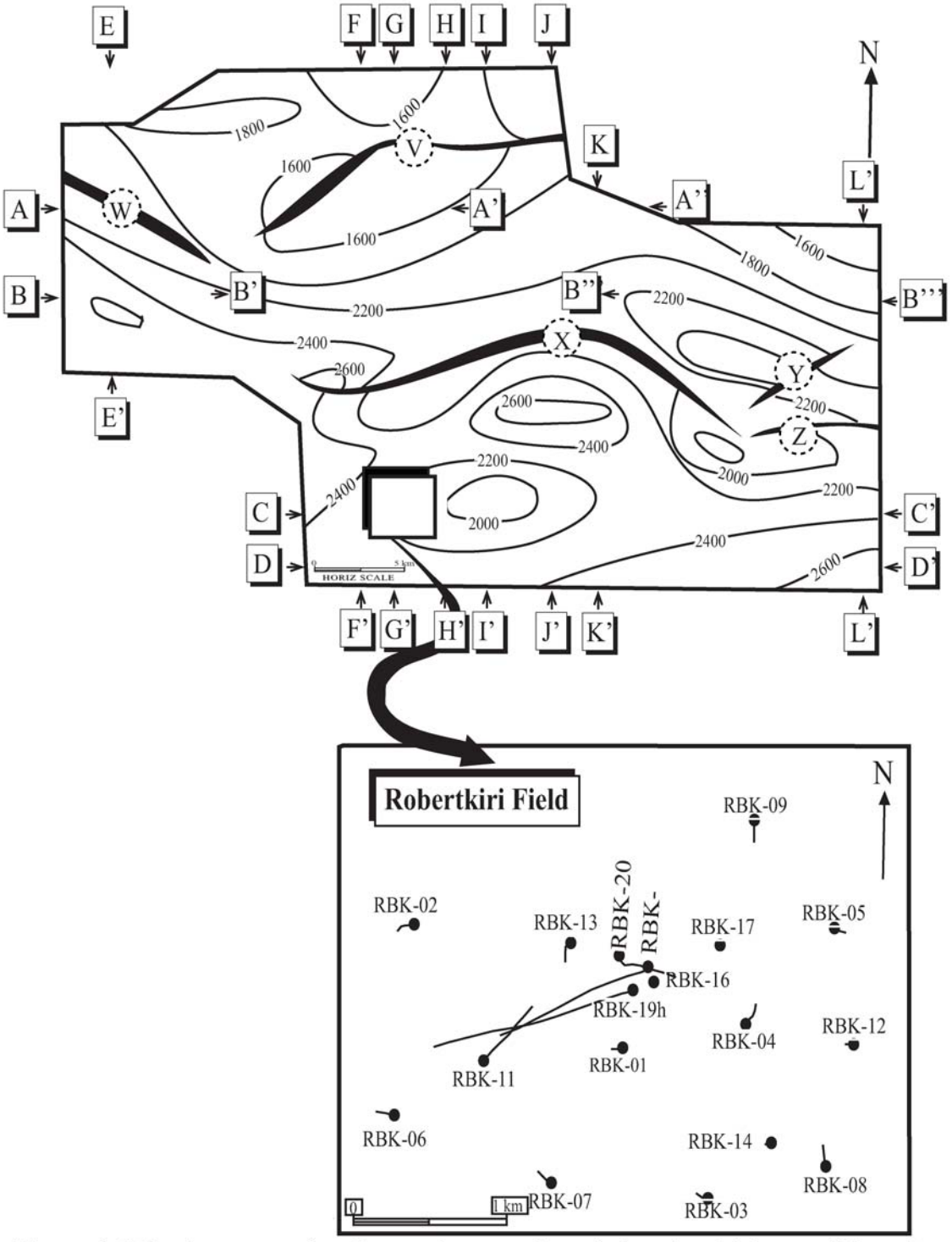

Figure 6. Seismic survey of study area (upper polygon) showing thickness of deposits addressed in this study and traces of major faults. Rectangles with arrows represent lines of seismic sections shown in Figure 9. Dotted circles denote traces of major faults. Insert map of Robertkiri field shows well locations (dots) and their deviated paths with depth.

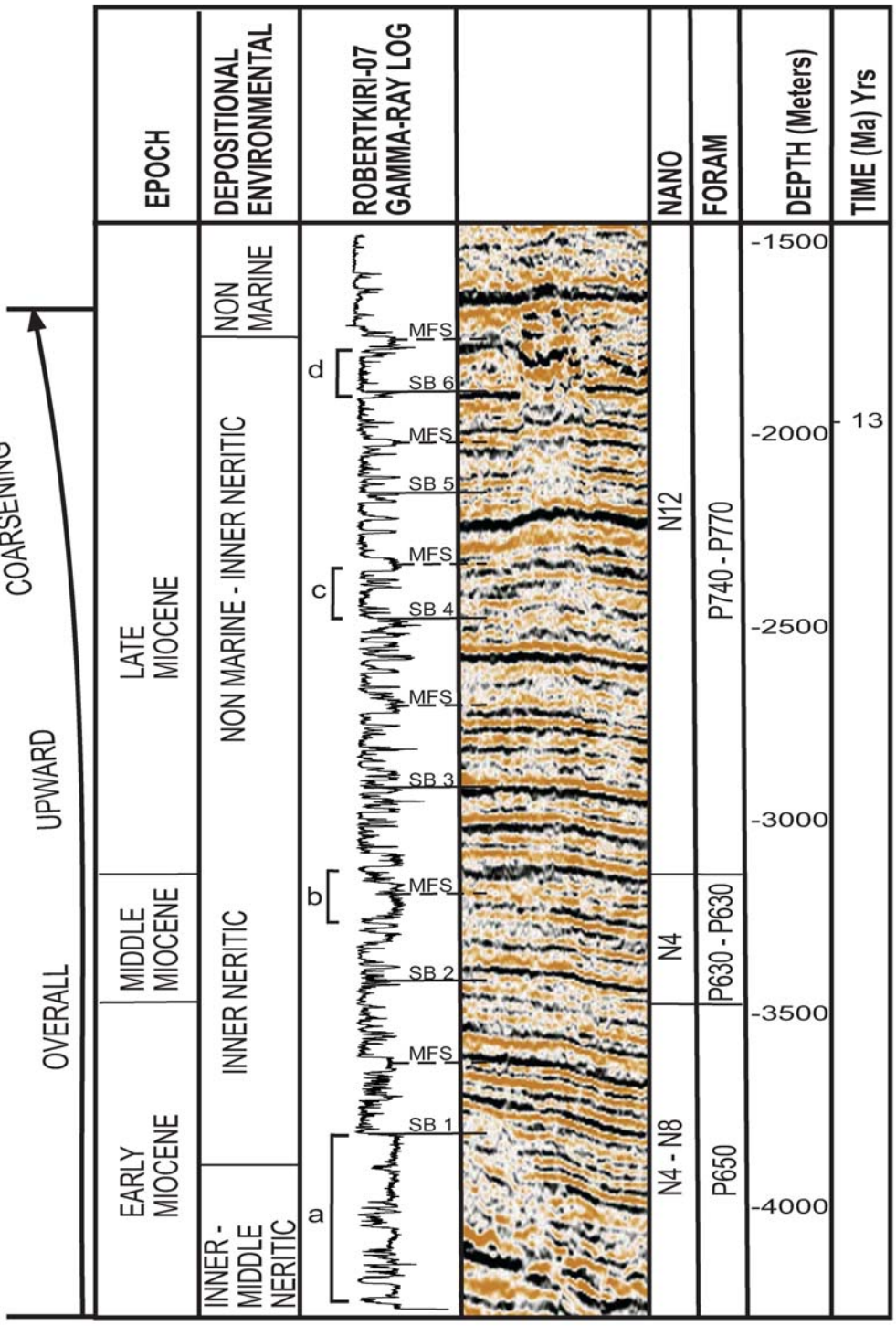

Figure 7a. Example of well log through the Niger delta in Robertkiri field showing overall upward coarsening trend and biostratigraphic zones, depositional environments and age estimated from unpublished Chevron report. Details of typical gamma ray patterns labelled a, b, c and d are described in figure 7b.

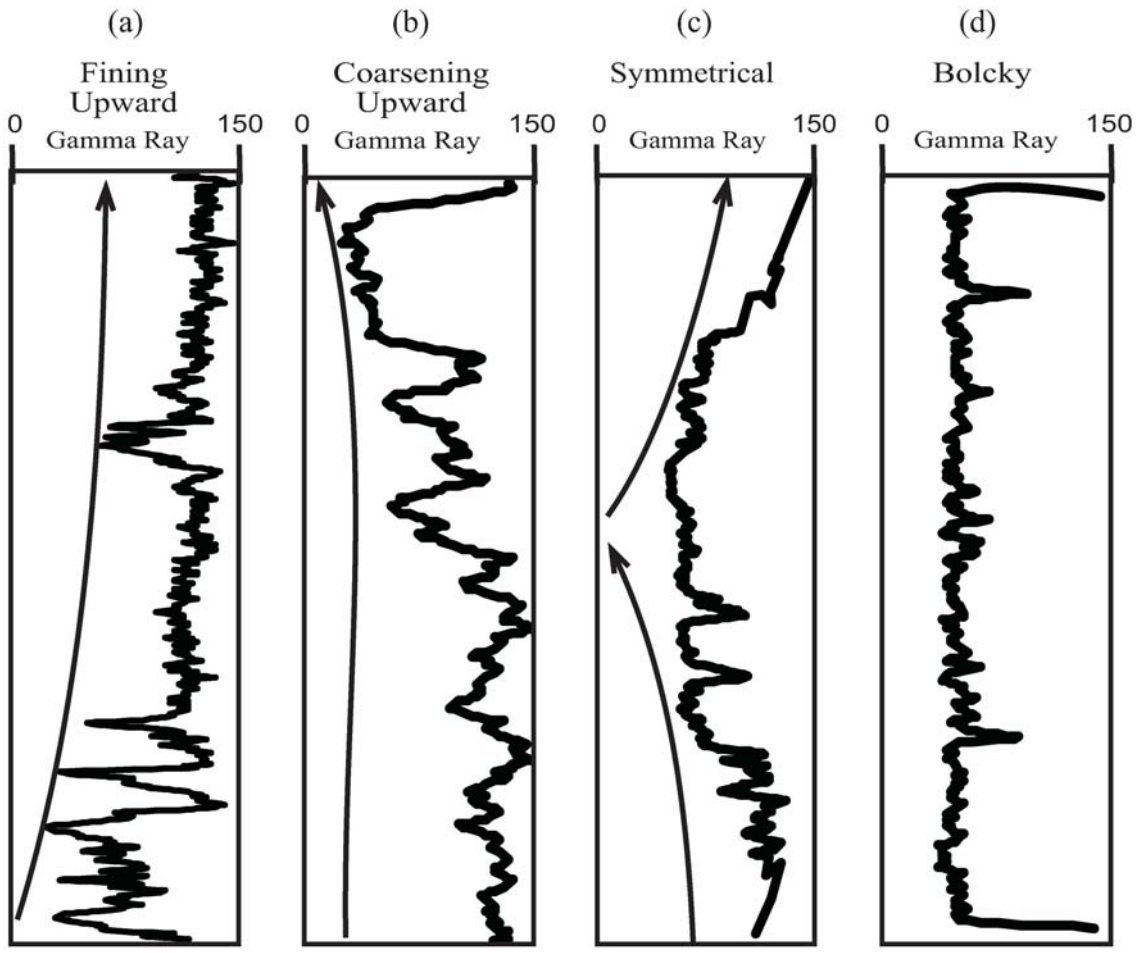

Figure 7b. Representative gamma ray patterns observed in Robertkiri field (a) Fining upward (b) Coarsening upward (c) Symmetrical and (d) Blocky log patterns.

coarsening and then gradual fining of deposits (Figure 7b, 3) and (4) “Blocky” intervals defined by abrupt decrease in gamma ray value overlain by an interval with uniformly low values, (Figure 7b, 4). Transitions between these characteristic log patterns are often abrupt; defined by a pronounced decrease of values at their base or increase of values at their top.

BIOSTRATIGRAPHY

Chevron's in-house biostratigraphic report of samples from Robetkiri-01 provides broad constraints on the age and depositional environments of the Agbada Formation (Figure 7a). Nano-fossil samples were related to the N4 to N8 biozones, and Foram samples to the P650 – 740 biozones. These biozones suggest deposits ranged from early to late Miocene in age. Depositional environments were interpreted to range from dominantly inner through middle neritic lower within the section and outer neritic through non-marine higher within the section.

SEISMIC VOLUME

Seismic data of the regional around Robertkiri field acquired by Western Geophysical has a dominant frequency of 60 Hz, and crossline and inline spacing of 12.5 meters. The seismic volume presented here extends to 3.5 seconds two way travel time (s twt), below which reflection continuity is generally poor. The seismic volume is characterized by a series of parallel reflections offset and deformed by major listric normal faults. The character of the seismic record changes with depth.

The basal part of the record (below 3 s twt) is disrupted by several zones with transparent to highly-discontinuous reflection patterns, which extend higher within the seismic volume under footwalls of major faults. This study focuses on reflections between 3.2 and 1.7 s twt, inferred based on regional studies to be from the Agbada Formation (Short and Stauble, 1967; Doust and Omatsola, 1990; Morgan, 2004). This interval corresponds to about 3 km of section. Reflections within this interval have moderate to good continuity and high amplitude variations. Reflections in the shallowest 1.7 s twt of the seismic volume are parallel, nearly horizontal, and less continuous.

Although few wells of Robertkiri field include logs of this interval, those that do show uniformly low gamma ray values characteristic of the fluvial Benin Formation.
The study interval is defined by the first and last continuous reflections that could be traced throughout the seismic volume. The seismic volume within this interval is divided into two interlayered seismic facies based on seismic reflection frequency and amplitude continuity (Figure 8; see also criteria used by Weimer et al., 1998). Facies 1 comprise several millisecond-thick intervals with lower-amplitude chaotic, discontinuous or inclined internal reflections (Figure 8). Facies 2 comprises higher-frequency, more continuous, parallel reflections. The vertical alternation of seismic facies defines thicker stratigraphic units (Figure 8).

Seismic facies 1 and 2 can be related in a general way to characteristic log trends described above (Figure 7a). The base of an interval of seismic facies 1 is defined by an abrupt change to relatively low-value gamma ray upward-fining or blocky log signatures; interpreted to reflect an abrupt coarsening. Seismic facies 2 deposits are generally finer-grained, and commonly comprise the basal parts of upward-coarsening or the upper parts of upward-fining well log successions. Particularly high amplitude and continuous reflections within facies 2 are commonly associated with relatively thick intervals with uniformly high gamma ray values, inferred to record thick shales.

SEQUENCE STRATIGRAPHIC DIVISION

Six stratigraphic sequences are defined within the Agbada Formation of Robertkiri field based on one or more of the following criteria: 1) Evidence in the seismic record of a surface that erosionally truncates underlying continuous reflections; 2) Abrupt change lower parts based on one of more of the following criteria: 1) Abrupt change from

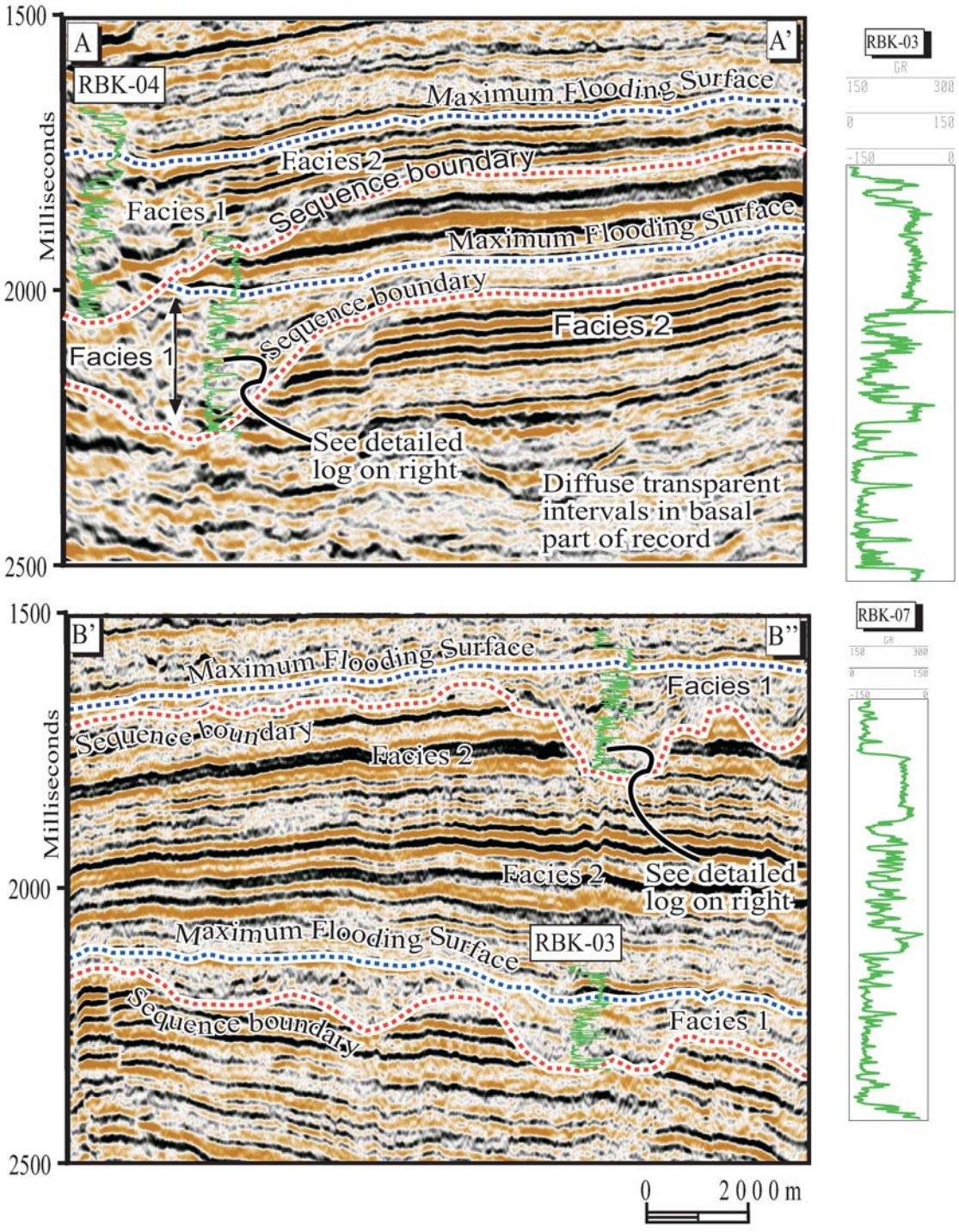

Figure 8. Seismic sections along A A' and B' B'' with well logs showing stratigraphic discontinuities, incisional features and general seismic facies character.

seismic facies 1 to 2; 2) A very high-amplitude or particularly continuous reflection within an interval of facies 2; 3) A thick interval with uniformly high gamma ray log values. Analysis of well logs suggests that lower parts of these sequences generally fine upward, whereas upper parts generally coarsen upward. Sequence boundaries and internal surfaces delineating lower and upper parts of sequences are interpreted to define stratigraphic discontinuities.

Erosion surfaces that define the base of sequences are interpreted to record abrupt basinward shifts in systems tracts. This definition of sequence boundaries is comparable with that of standard Exxon nomenclature (Posamentier et al., 1988, 1988, b; Van Wagoner et al., 1990; Mitchum and Van Wagoner, 1991). Parallel reflections of seismic facies 2 are inferred to record surfaces that were nearly horizontal following deposition (based on the small area covered by this seismic volume relative to the scale of depositional systems inferred from the modern Niger Delta). Abrupt vertical displacement of these reflections across the seismic volume are inferred to define faults and thickening of intervals between reflections across these faults are interpreted to record growth strata developed during syndepositional fault displacement and associated structural folding. Surfaces within sequences that divide lower and upper parts, defined by a pronounced increase in well log gamma ray values, are interpreted to record abrupt landward shifts in systems tracts. This division of sequences is compatible with the definition of “maximum flooding surfaces” (Posamentier and Vail, 1988; Posamentier et al., 1988; Van Wagoner et al., 1990; Mitchum and Van Wagoner, 1991). Thus deposits in lower parts of sequences are interpreted to be lowstand and transgressive system tracts and those in upper parts of sequences are inferred to be highstand system tracts. Spatial

changes in sequence thickness, the magnitude of basal incision, and the proportion of seismic facies are related in the discussion that follows to patterns of erosion and deposition during sequence development and observed patterns of structural deformation.

Sequence boundaries and maximum flooding surfaces were correlated between the wells of Robertkiri field by relating well log patterns to specific seismic reflections and vertical changes in seismic facies that could be traced between wells and by matching similar well log patterns within adjacent wells. The location of representative dip and strike oriented cross sections that show the correlation of these surfaces across sets of correlated well logs (Figures 9a, 9b, 9c and 9d) and through of the seismic volume (Figures 10a to 10l) is presented in Figure 6.

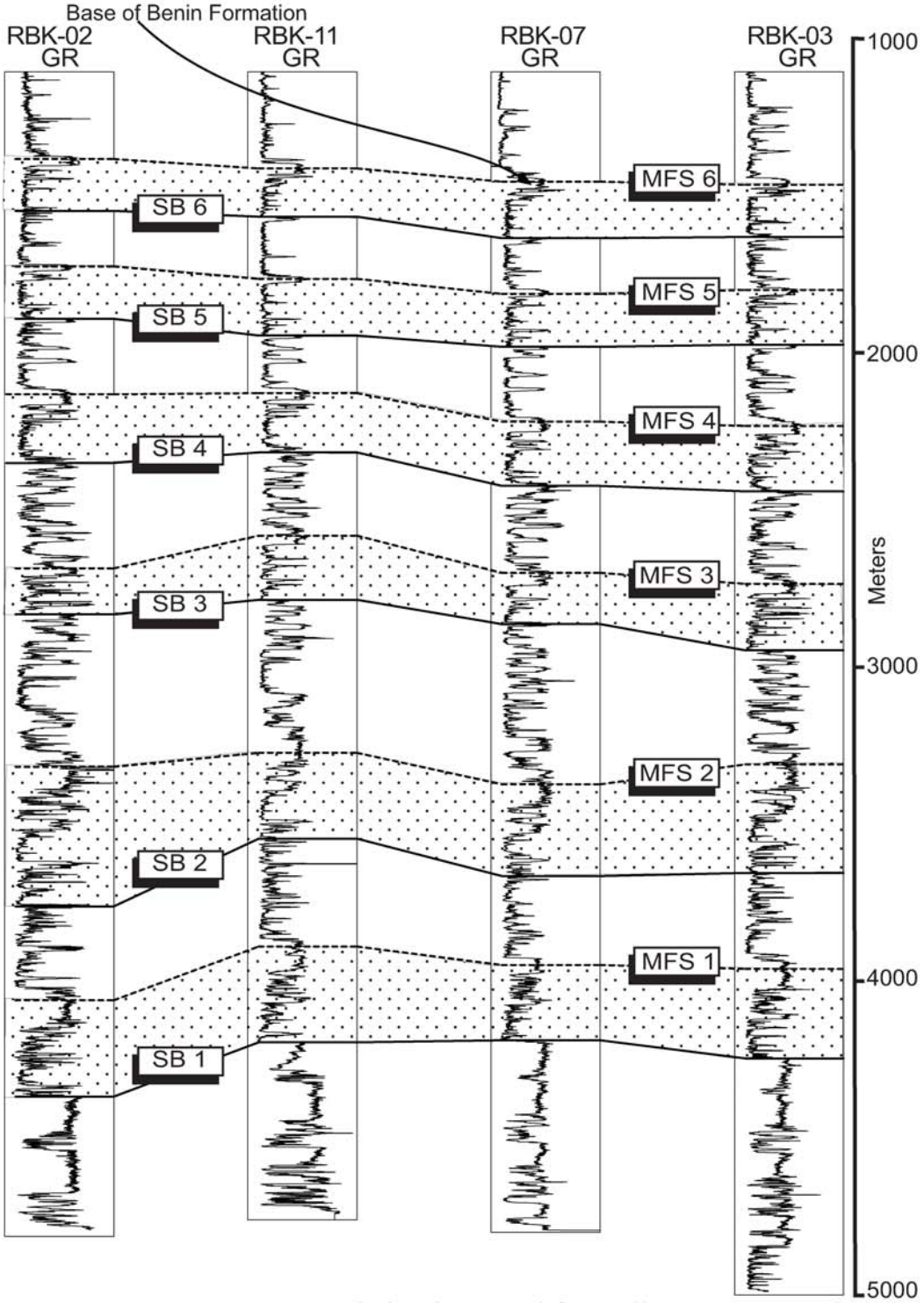

Figure 9a. Gamma ray correlation log panel for wells 02, 11, 07 and 03 indicating an overall upward weakly coarsening sequence. Sharp-based blocky and fining upward pattern are interpreted to be incised fluvial or estuary deposits, small scale coarsening upward units are inferred to be progradational highstand deltaic units while maximum flooding surfaces correspond to highest gamma ray interval. Sequence 1 is thicker at the western edge of the available well data.

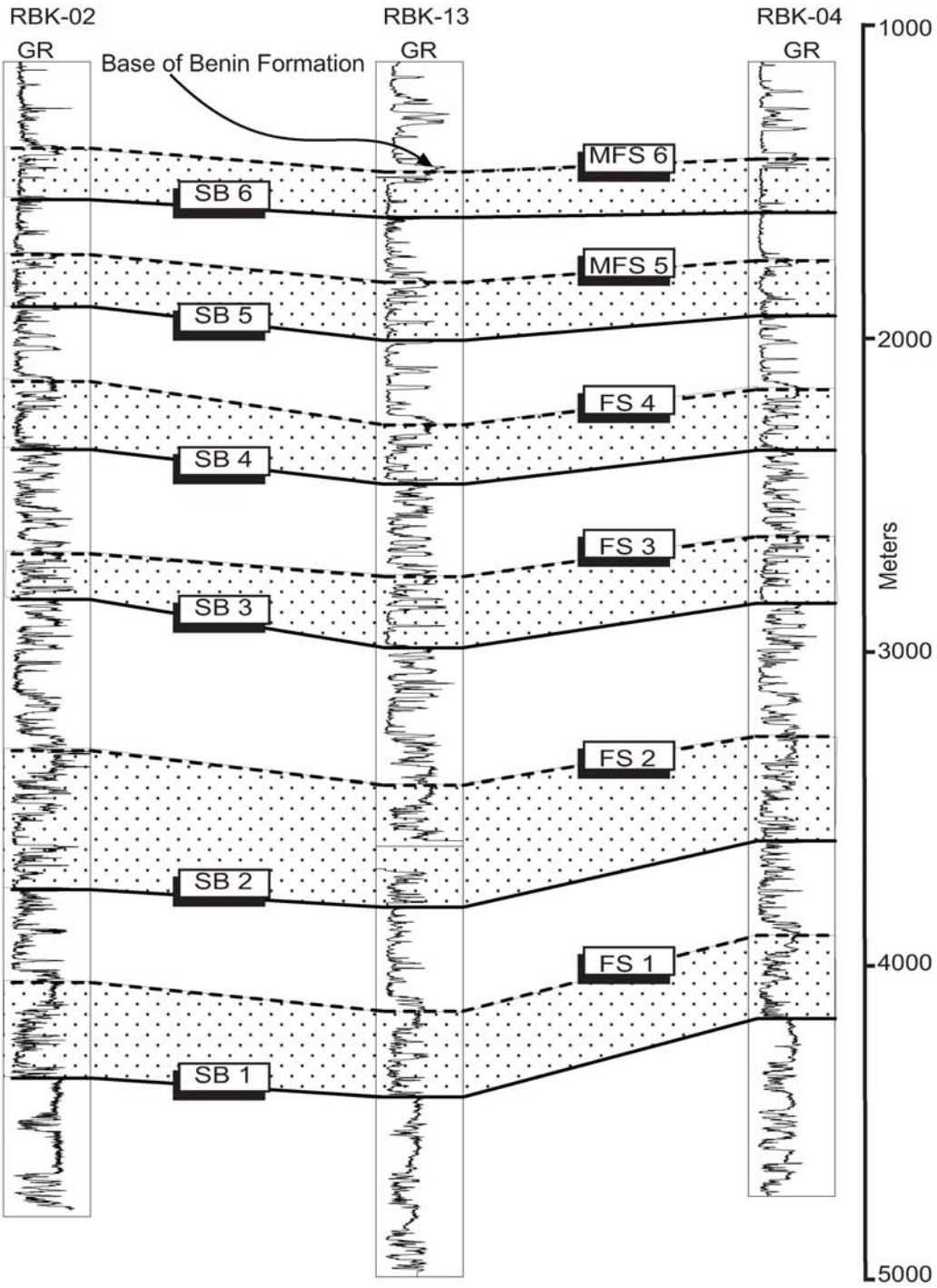

Figure 9b. Gamma ray correlation log panel for wells 02, 13 and 03 indicating an overall upward weakly coarsening sequence. Sharp-based blocky and fining upward pattern are interpreted to be incised fluvial or estuary deposits. Small scale coarsening upward units are inferred to be progradational highstand deltaic units while maximum flooding surfaces correspond to highest gamma ray interval.

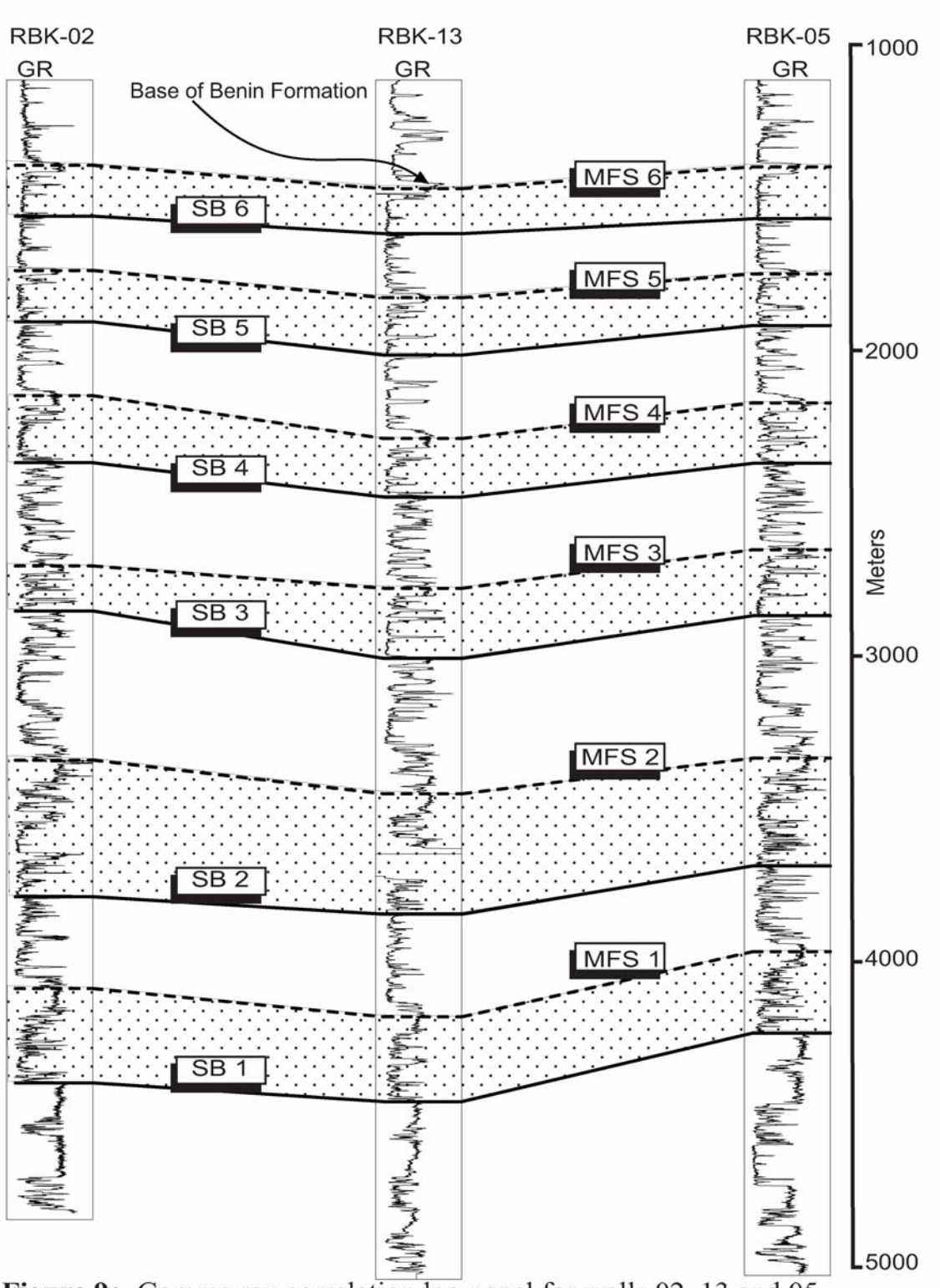

Figure 9c. Gamma ray correlation log panel for wells 02, 13 and 05 indicating an overall upward weakly coarsening sequence. Finer grained intervals are progressively thinner upsection.

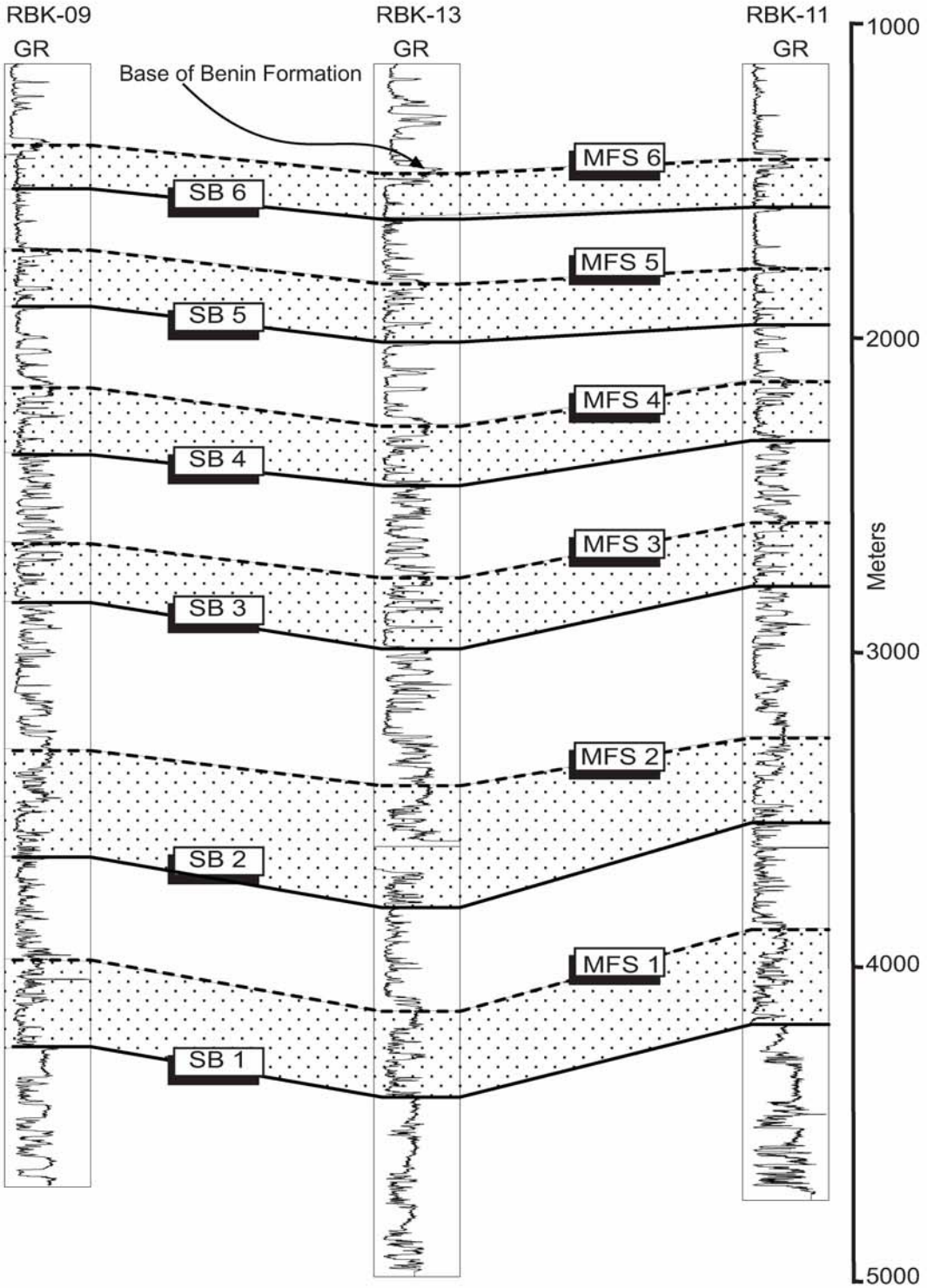

Figure 9d. Gamma ray correlation log panel for wells 09, 13 and 11 indicating an overall upward weakly coarsening sequence.Sequence 2 is thickest at the north central part of the available well log portion of the field.

STRUCTURE AND STRATIGRAPHY OF ROBERTKIRI FIELD

STRUCTURE

Structure in the area of Robertkiri field is dominated by three major normal faults that trend east-west and dip basinward (southward). These faults, each with broad convex basinward cuspate plain view geometry, are labeled V, W, and X on Figure 6 and seismic cross section (Figures 10a – 10l). Fault dips decline from 78-86 degrees in shallow parts of the section to less than 30 degrees in deeper parts. They become less apparent as the seismic record becomes obscured by larger transparent zones at depths greater than 2.5 seconds. Fault V divides into two distinct faults at shallow depths. Down-dropped blocks of major faults are deformed into broad anticlines, with double-plunging axes parallel to the adjacent cuspate fault trends. Small-scale synthetic and antithetic faults radiate from anticline crests, further complicating these structures. Although several hundred smaller-scale faults were delineated within the seismic volume, only those with greatest offset are shown in the seismic cross sections (Figures 10a – 10l).

Folding of reflections across anticlines and displacement of seismic facies across faults increase deeper in the seismic record. Within down-dropped blocks, reflections fan apart toward major faults, which is interpreted to record deposition of syndeformation growth strata. Reflections also fan apart basinward of anticline crests. Most depositional-dip oriented seismic cross sections traverse major faults V and X, and associated anticlines on down dropped blocks (Figures 10e – 10l). The cross section through the western edge of the field traverses fault W and associated anticline (Figure 10e). The one through the eastern edge of the field crosses a series of smaller faults, which

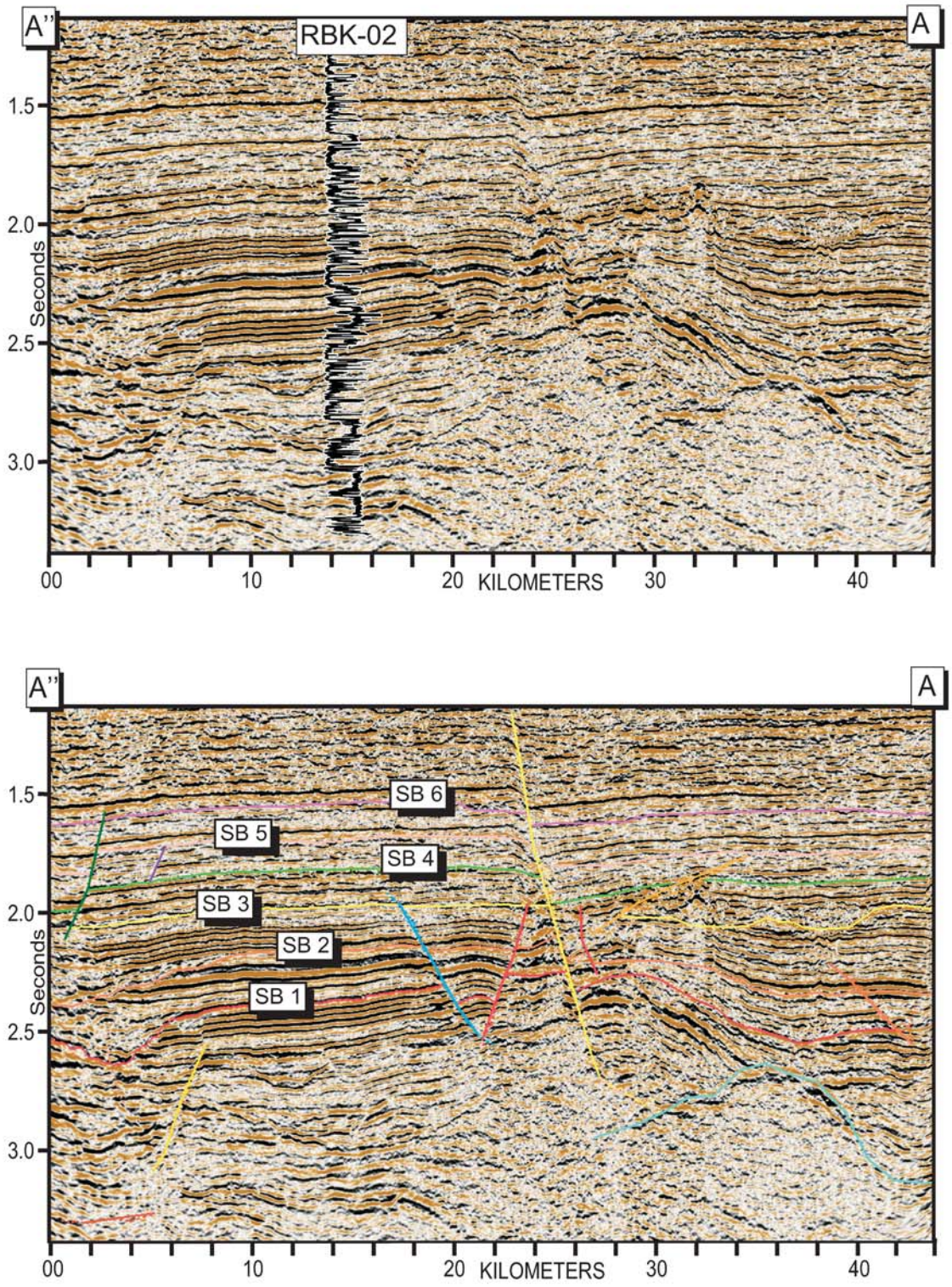

Figure 10a. Seismic cross section along line A A'' showing the six major sequence boundaries and the associated seismic facies. SB 1 and SB 2 (SB is Sequence Boundary) with lateral accretional feature are defined by seismic facies 1 at the western part of the cross section. SB 2 truncates the flooding surface of the underneath sequence 1.

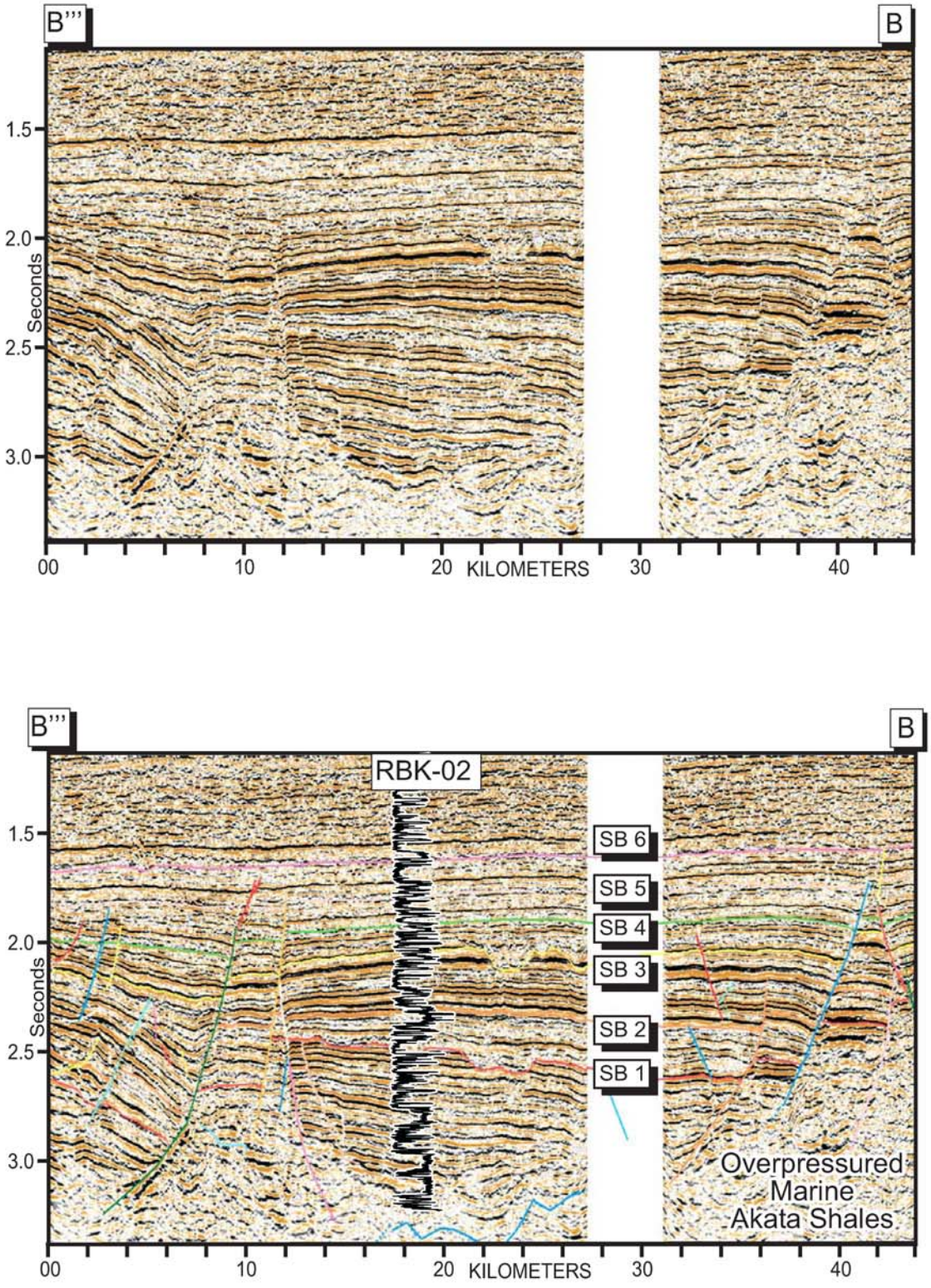

Figure 10b. Seismic cross section along line B B''' showing the six major sequence boundaries and the associated seismic facies. SB 1 and 3 (SB is Sequence Boundary) are defined by facies 1 at the central part of the cross section.

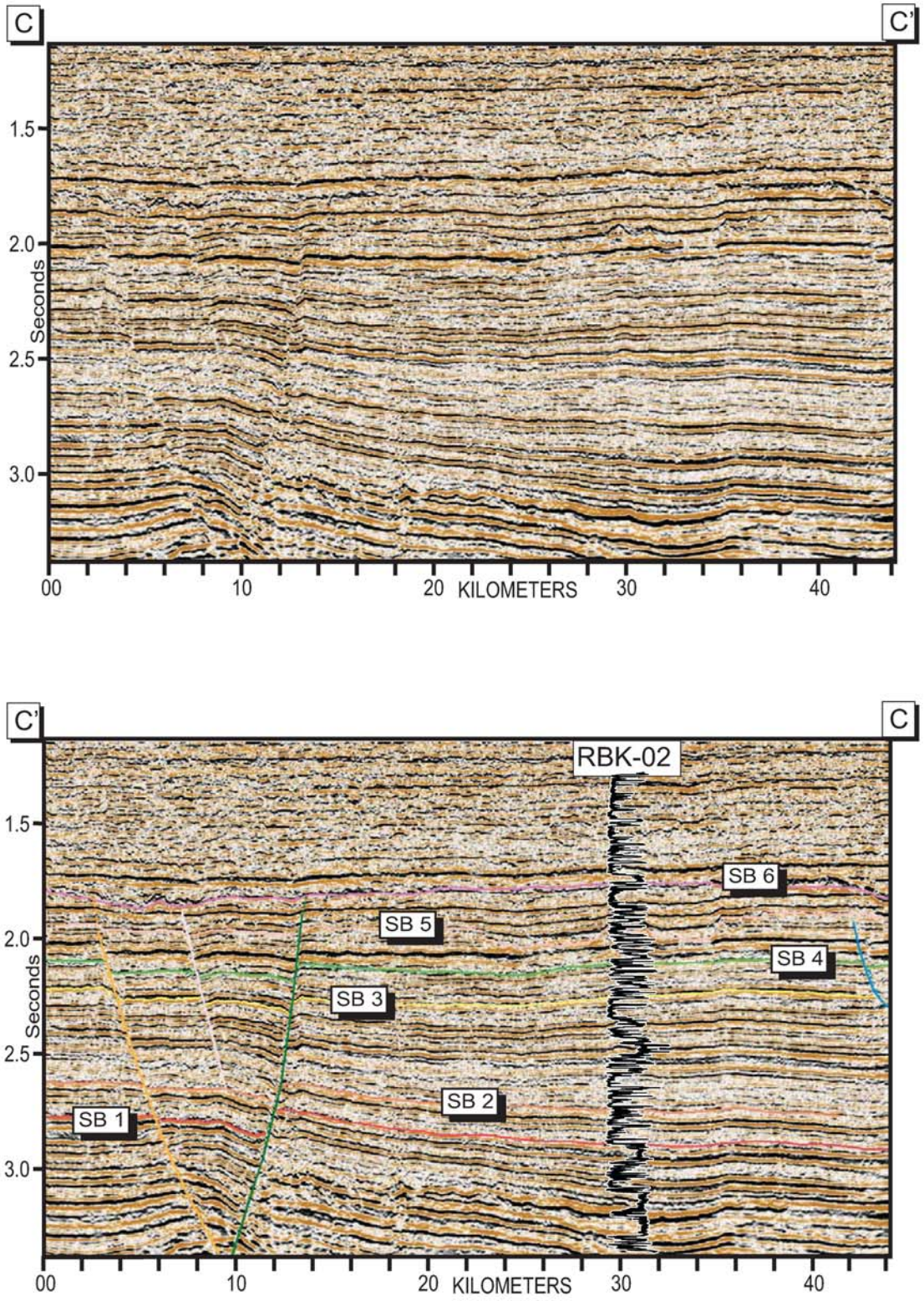

Figure 10c. Seismic cross section along line C C' showing the six major boundaries. Contact between seismic facies 1 and 2 are mostly gradational. Incisions on SB 5 and SB 6 are shallower and wider. A small embarkment divides incision on SB 5 into two seperate units.

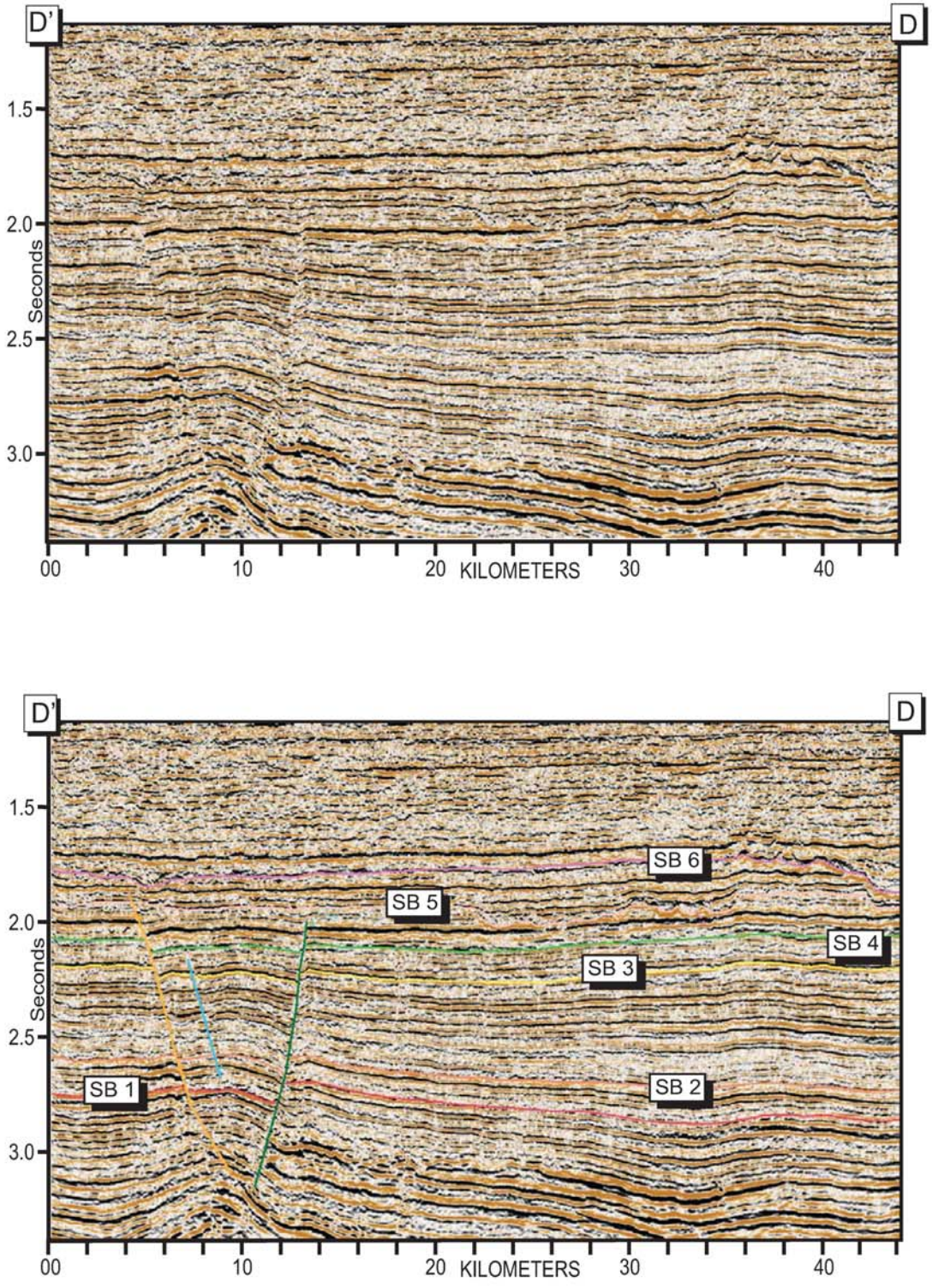

Figure 10d. Seismic cross section along line D D' showing the six major boundaries. Contact between seismic facies 1 and 2 are mostly gradational, Incisions on SB 5 and SB 6 are shallower and wider compared to sequences 1, 2 and 3. Incision on sequence 6 is deeper towards the eastern part of the field.

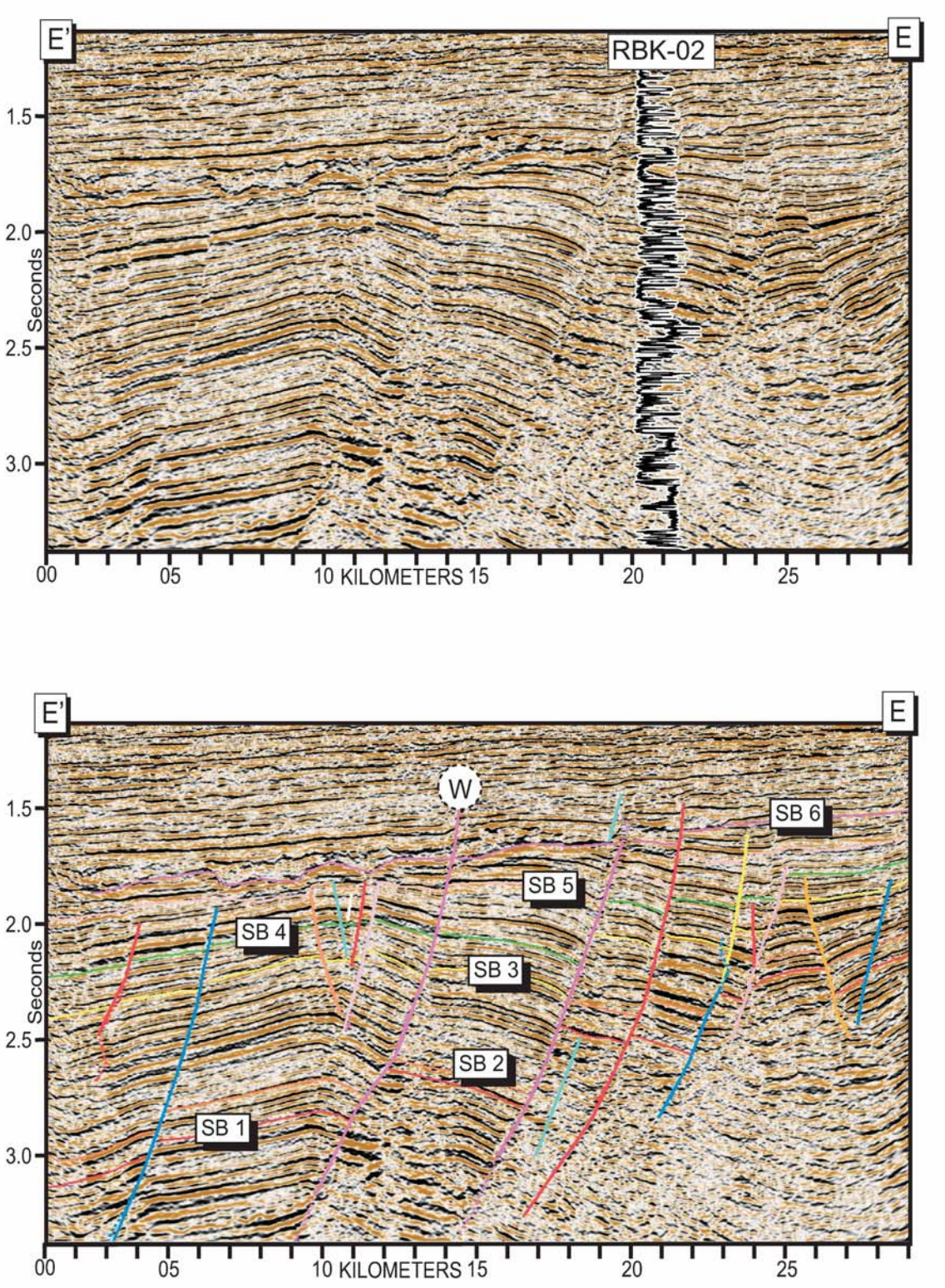

Figure 10e. Seismic cross section along line E E' showing the six major sequence boundaries and the seismic facies defining them. The incised feature of seismic facies 1 on SB 6 is shallow, wider and truncates most faults.

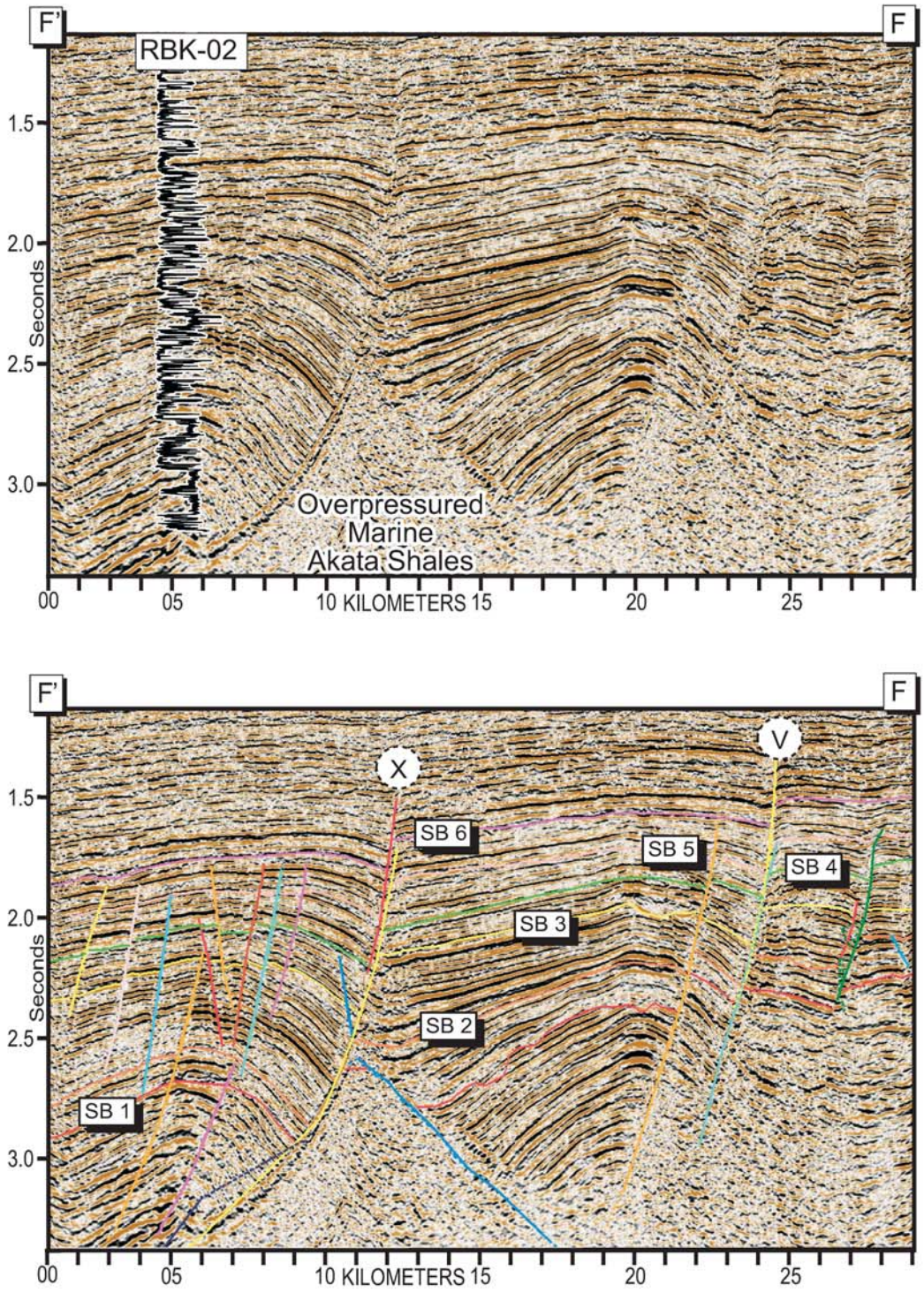

Figure 10f. Seismic cross section along line F F' showing prominent crestal incisions on SB 1 and SB 3 demostrating effect of undercompacted substrates on the sequence boundaries. Tilting of the incisions on SB 1 suggests a post-erosional deformation from the underlying mobile substrate .There is fanning of stratigraphy across anticline V towards fault X for sequences 1, 2 and 3.

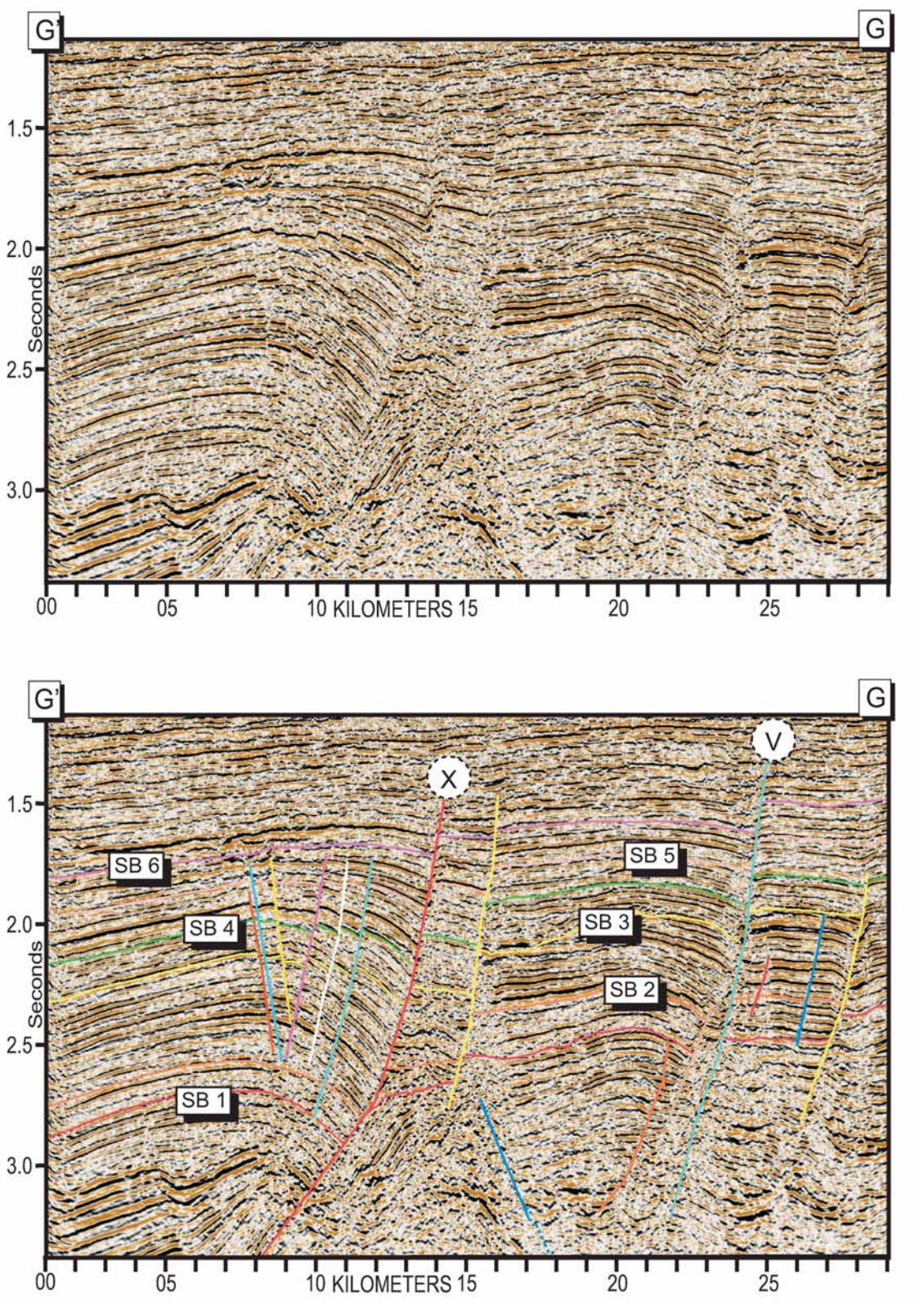

Figure 10g. Seismic cross section along line G G' showing crestal incision below SB 1 on the anticline adjacent to fault X.

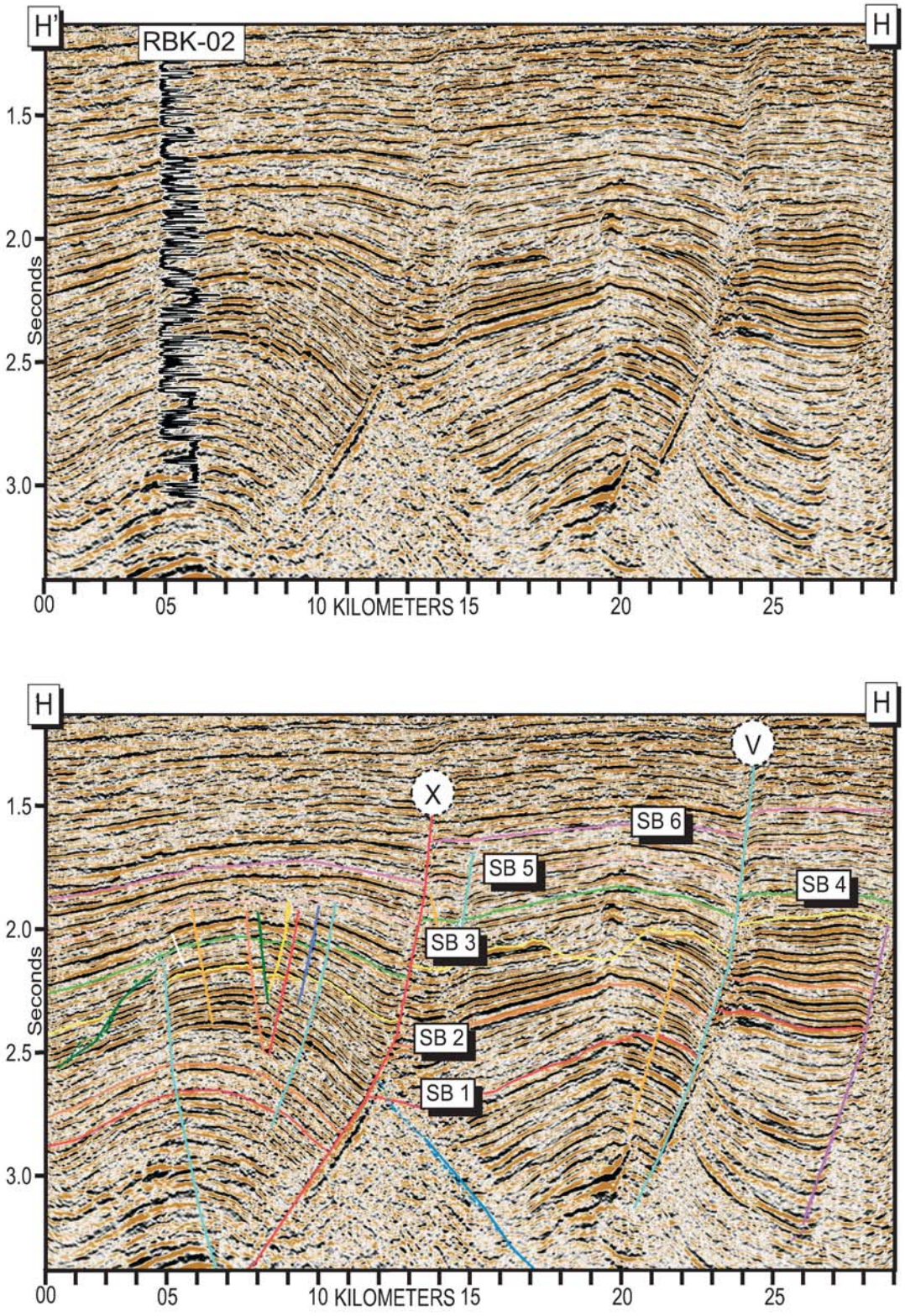

Figure 10h. Seismic cross section along line H H' showing evidence of inclined bedsets above SB 3 implying deltaic progradation, incised feature on SB 3 is 7 Km wide and 160 m deep. Diffuse and chaotic reflection event inferred to be mobile shales is shallower behind fault X.

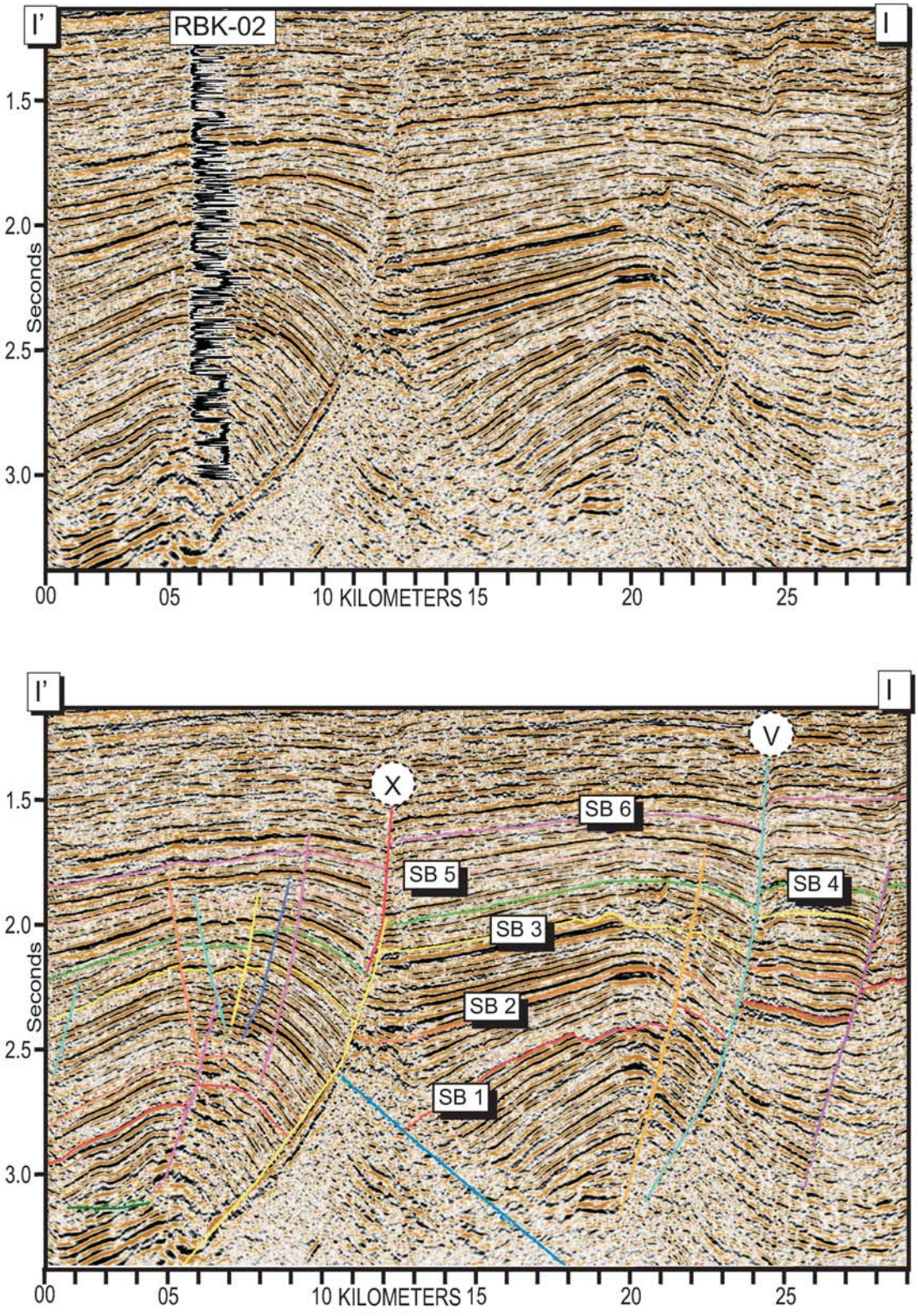

Figure 10i. Seismic cross section along line I I' showing the six major sequence boundaries and crestal incisions on SB 1 and SB 3. Fanning of strata across anticline V towards fault X is apparent in sequence 1 and 2.

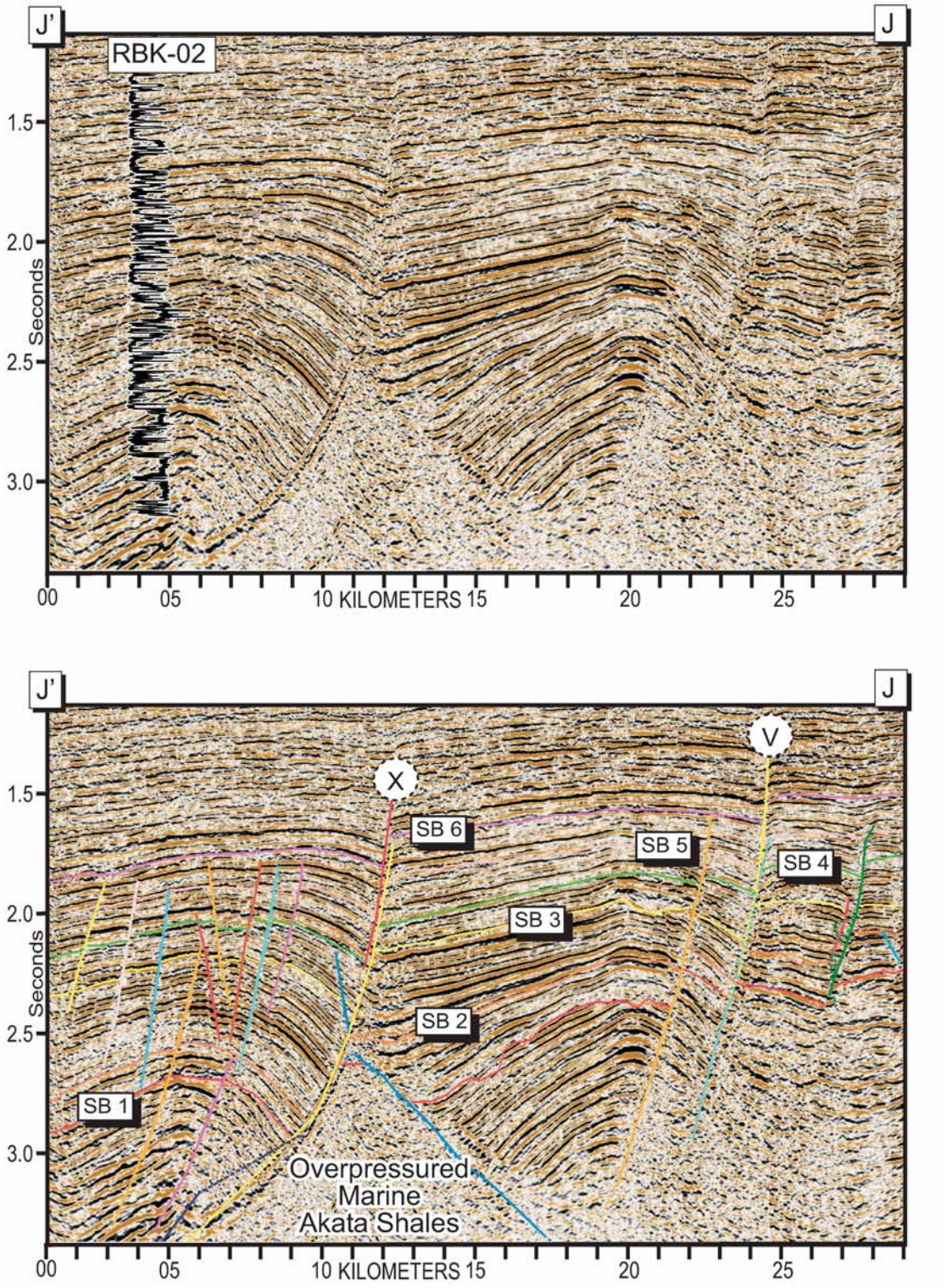

Figure 10j. Seismic cross section along line J J' showing stacked incised features of sequence boundaries 1 and 3 denoted by seismic facies 1 on anticline adjacent to fault V. Incisions across anticlines are shallower compared to the proximal center of the faults with greater throw. There is post-erosional tilting on SB 1. Reflection event inferred to be mobile shales is shallower behind fault X.

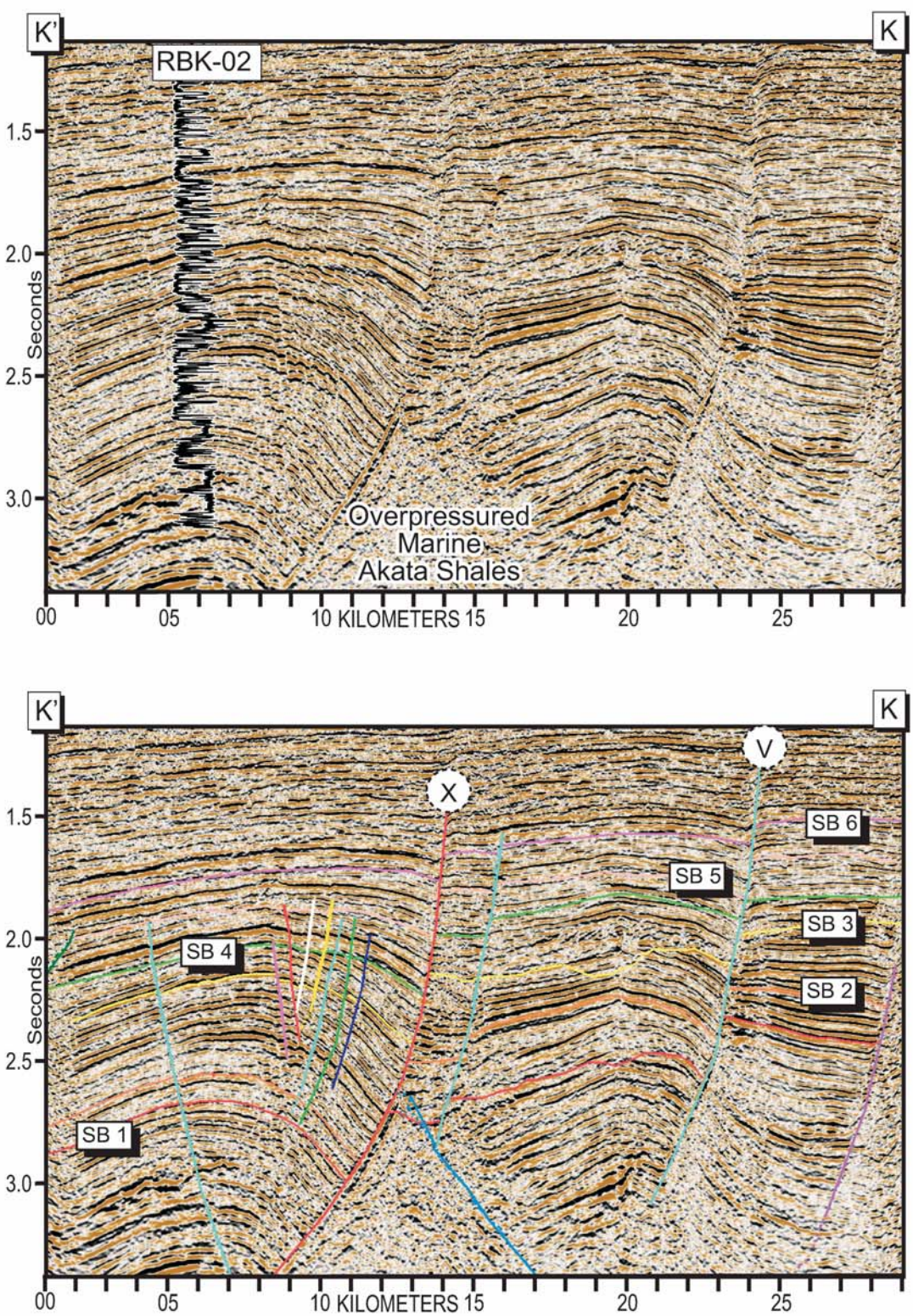

Figure 10k. Seismic cross section along line K K' showing inclined bedsets of seismic facies 1 above SB 1 and SB 3 on anticline V implying deltaic progradation. Incisions across anticlines are shallower compared to the more proximal center of the faults with greater throw. Incised feature on SB 3 is 7 Km wide and 160m deep.

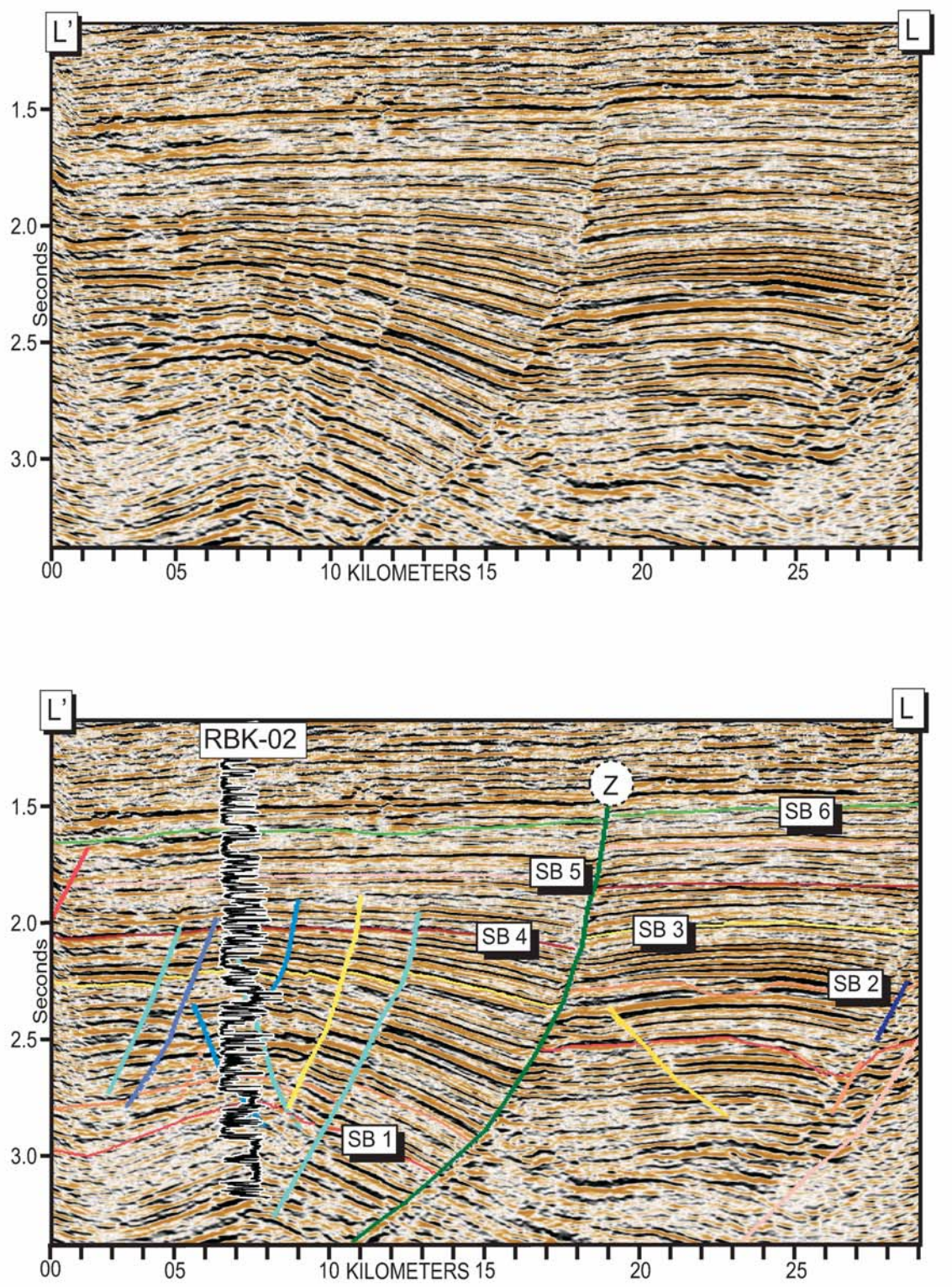

Figure 10l. Seismic cross section along line L L' showing the six major boundaries and the associated siesmic facies pattern. There is collapsed crest of rollover anticline adjacent to fault Z. Incisions on sequence boundary 1 and 2 across anticline upthrown of fault Z are shallower compared to the proximal center of the faults with greater throw.

successively down drop reflections basinward with comparatively little evidence for folding of down-dropped blocks (Figure 10l).

Lateral transitions from transparent seismic zones to more continuous reflections in basal parts of the seismic record occur at shallow levels under footwall blocks adjacent to major faults relative to under down-dropped blocks. Because these low-amplitude-discontinuous to transparent reflection zones can have variably abrupt or diffuse-gradational boundaries, they are interpreted to reflect deposits that have been fractured by overpressures and perhaps have moved upward under the weight of overlying strata during fault displacement. The occurrence of these transparent seismic patterns at shallower depths just landward of major faults may reflect isostatic rebound of footwall blocks as down-dropped blocks detached and shifted basinward.

Seismic cross sections perpendicular to depositional strike (Figures 10e – 10j) show reflections within anticlines are broadly horizontal parallel to fold axes. In the proximal (northern) part of the seismic volume, anticlines are separated by zones of folded reflections adjacent to the cuspate edges of major faults and by zones where transparent seismic patterns extend upward to shallow depth. Cross sections through more distal (southern) parts of the seismic volume are basinward of major anticlinal structures and these less deformed parallel seismic reflections extend to greater depths. Because maximum flooding surfaces within the Agbada Formation are inferred to define relatively flat depositional surfaces, top structure maps of these surfaces are used to define broad patterns of displacement across faults and deformation of fault blocks at different stratigraphic levels (Figures 11a and b). There is a regional basinward tilt of these surfaces, particularly pronounced for surfaces at deeper stratigraphic intervals.

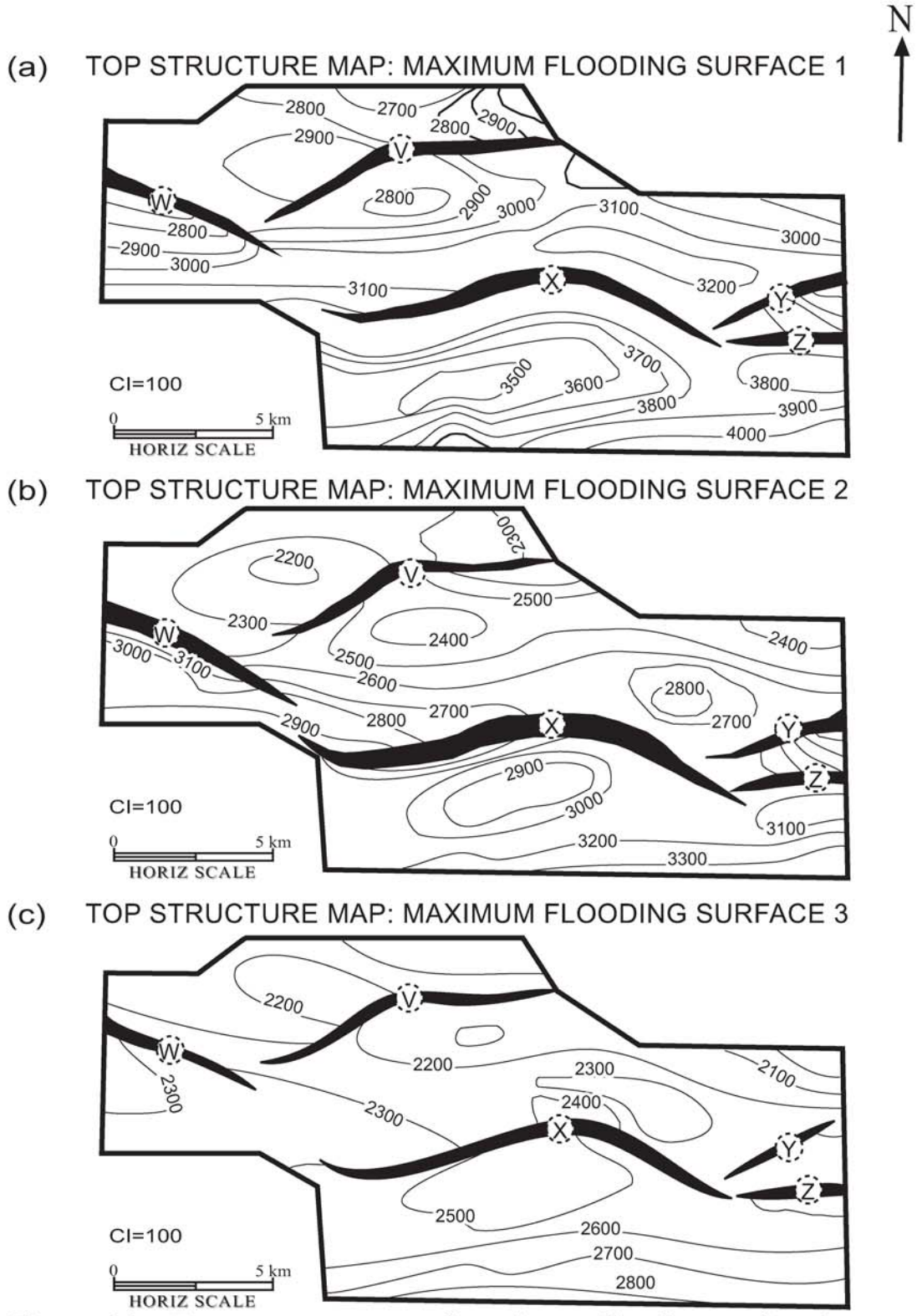

Figure 11a. Top structure maps of maximum flooding surface 1, 2 and 3 showing the main faults and changes in elevation across them, there is a regional east - west trend superimposed on the structure.

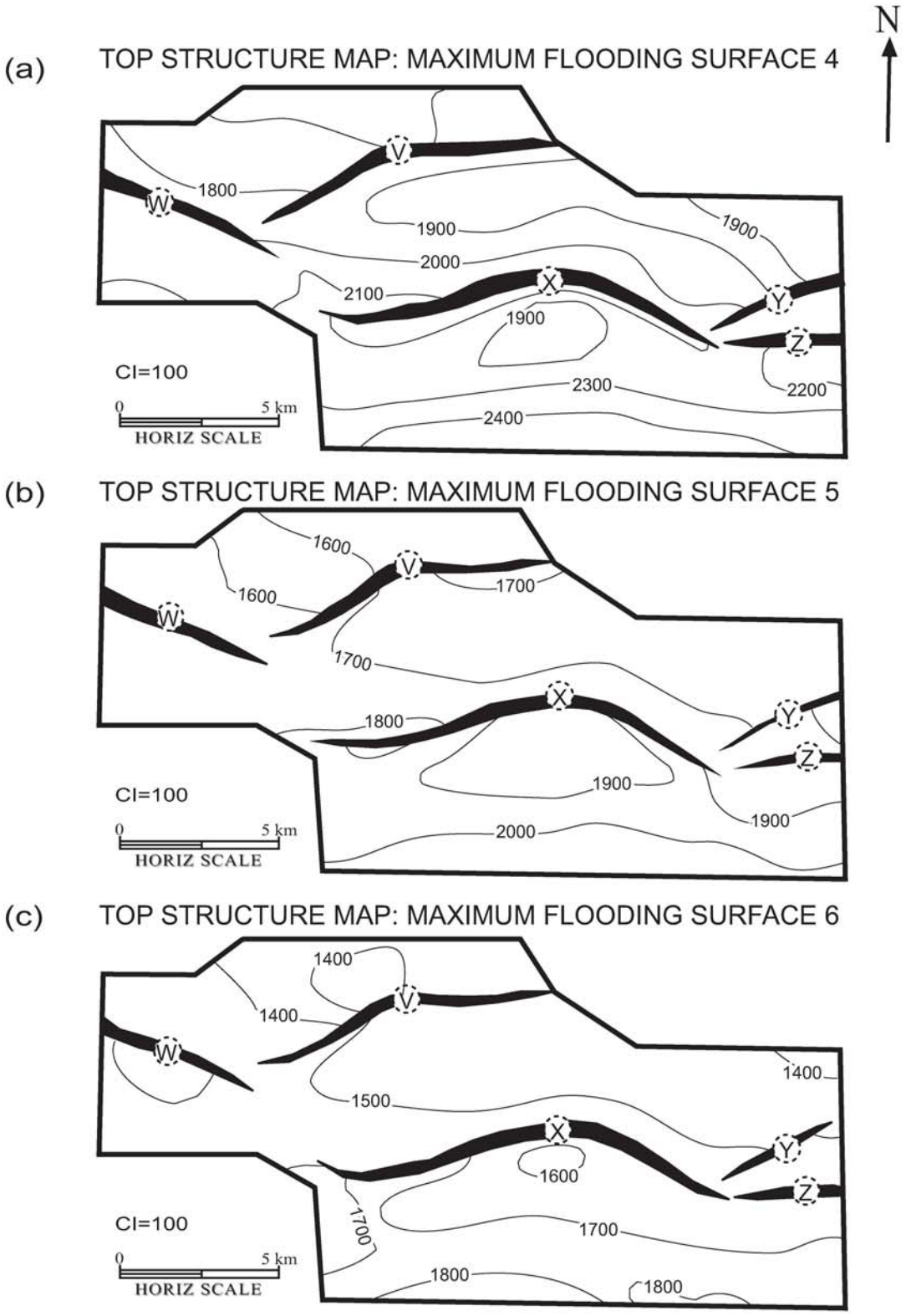

Figure 11b. Top structure maps of maximum flooding surface 4, 5 and 6 showing minor changes in elevation across major faults

Displacement across faults is greatest near apex of cuspate normal fault traces and is greater along older stratigraphic horizons. Anticlinal fold limbs are steeper near the center of fault traces and for older stratigraphic horizons.

STRATIGRAPHY

Vertical and lateral variations of seismic facies and well log patterns within the six sequences identified in the Agbada Formation of Robertkiri field are discussed separately in this section, before these variations are related to changes in erosion and depositional patterns across syndepositional structural topography. Sequence boundaries are directly overlain in most locations by chaotic reflection patterns of seismic facies 1 and they pass upward into more continuous, higher-amplitude, parallel reflections that comprise seismic facies 2. Wells of Robertkiri field are confined to the southwestern rollover anticline (Figure 6), which is the main structural play in the field. Although these well logs provide critical information relating lithic trends to seismic facies, they do not provide wide coverage of the area documented in the seismic record. The thickness of deposits between a sequence boundary and subsequent maximum flooding surface appear to mostly reflect the extent of incision along the base of the sequence (Figures 12a and b). The thickness of deposits between maximum flooding surfaces within successive sequences are inferred to mostly record variations in structurally generated accommodation and to a lesser extent the larger-scale progradation of the delta into the basin (Figures 13a and b). Seismic amplitude variation patterns examined in horizontal time slices or extracted along paths that parallel sequence boundaries or maximum flooding surface to generate “stratigraphic slices” provide additional information about lithic variations within sequences (Figures 14a – 14r).

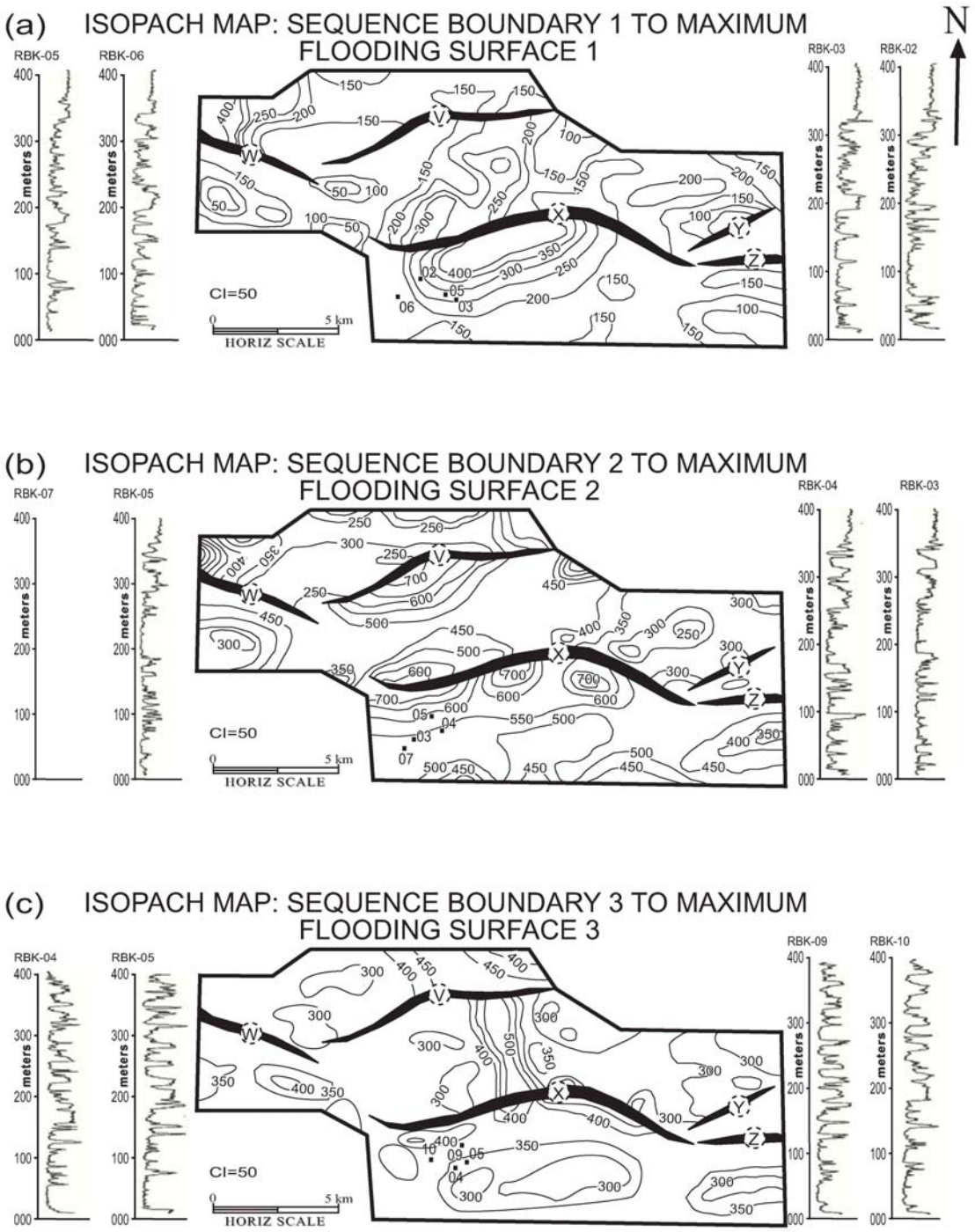

Figure 12a. Isopach maps of sequence boundary to maximum flooding surface for sequence 1, 2 and 3. Incisions in the northwestern and northcentral part of sequence 1 are represented as elongate steep sided contours. The northwestern-southeastern trending and southwestern trending belts merged in sequence 2 behind fault X. Incision is confined to the north central part of the field in sequence 3. The log pattern represents the sharp based incised feature to the fine grained maximum flooding surface. Growth stratigraphy is lesser on the eastern part of the map for sequence 2.

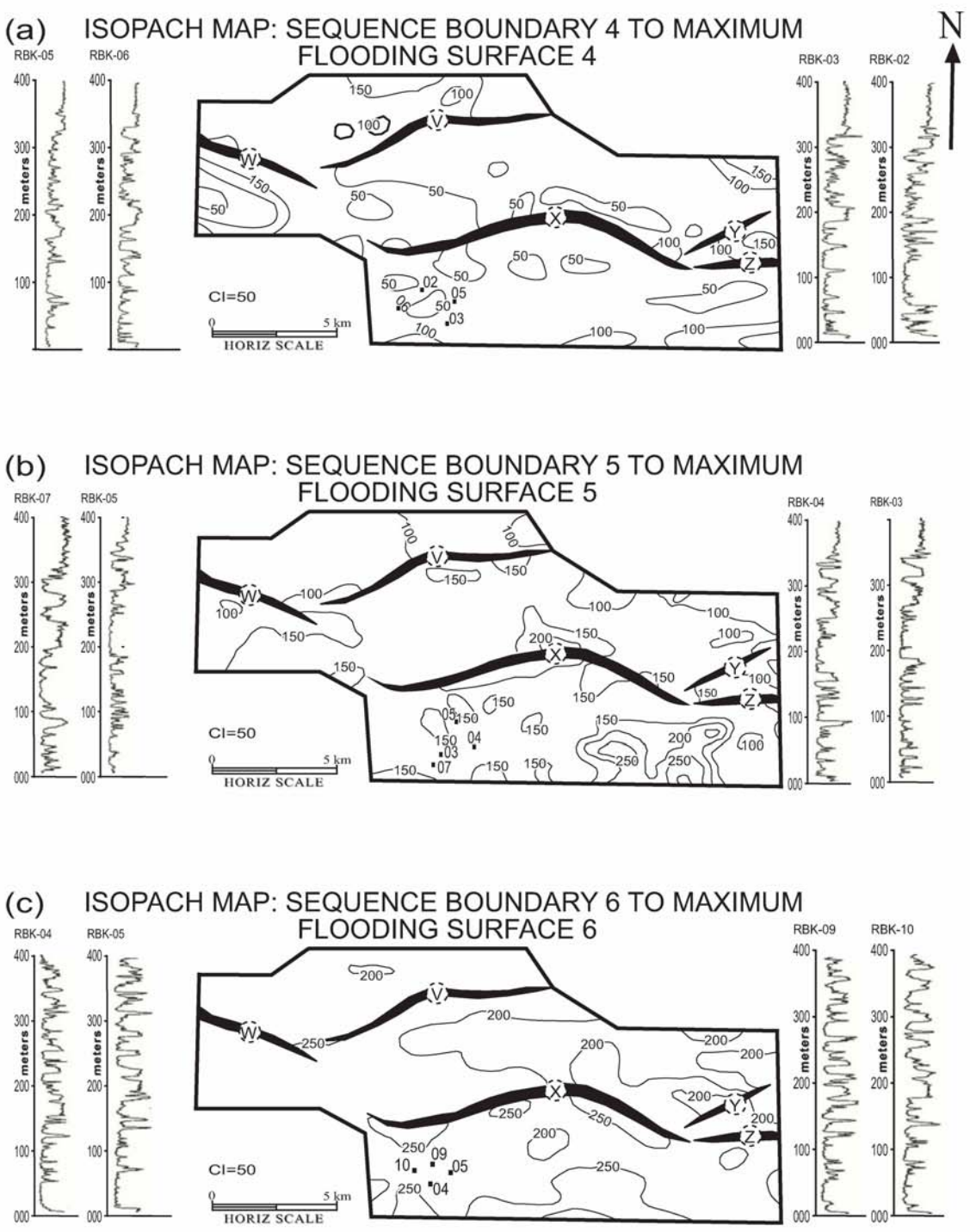

Figure 12b. Isopach maps of sequence boundary to maximum flooding surface for sequence 4, 5 and 6. Isopach thickness is more uniform in sequence 4 because of lack of distinct incision. Axis of incision has shifted to the southeastern part of the field in sequence 5 and 6.

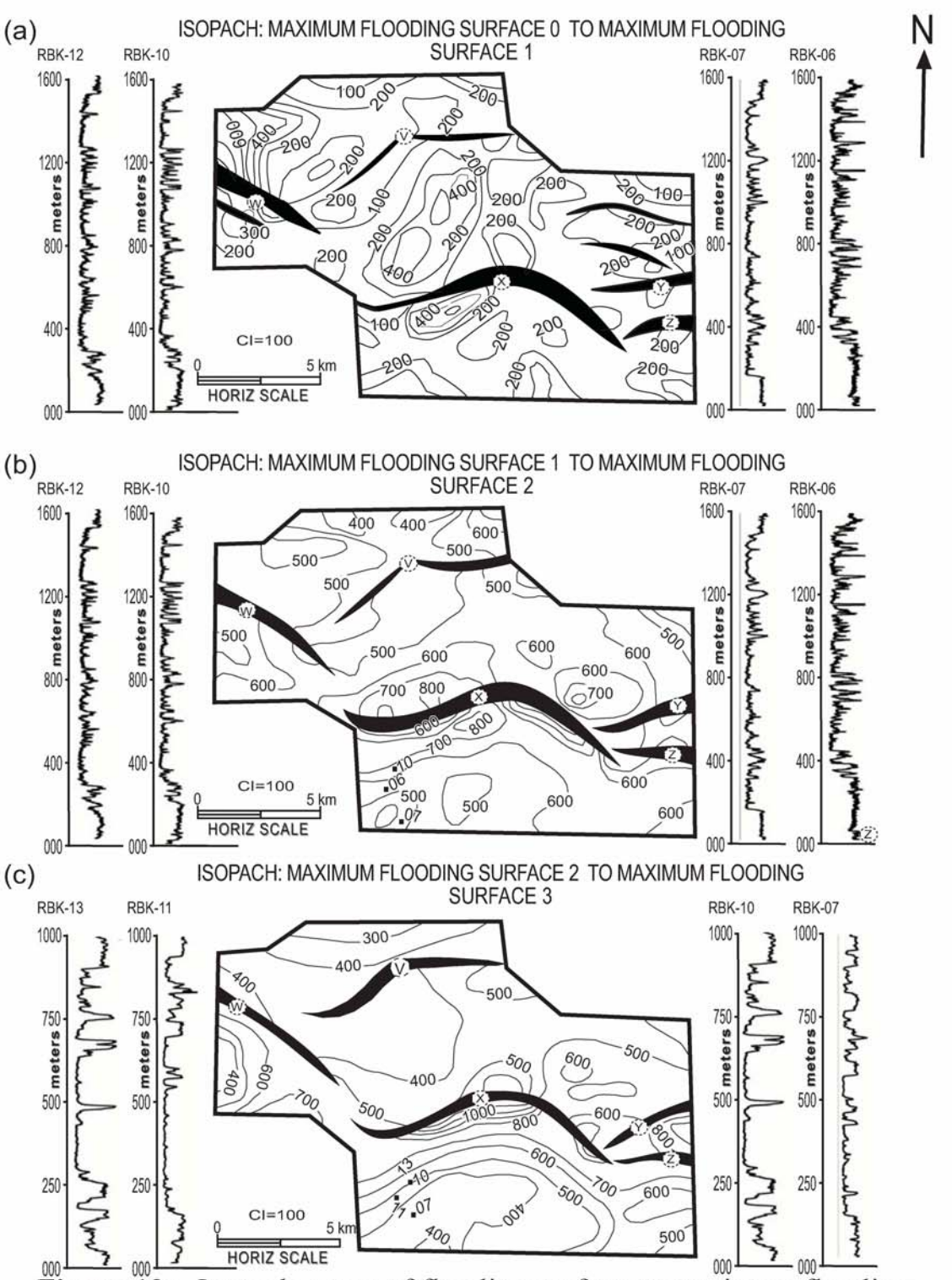

Figure 13a. Isopach maps of flooding surface to maximum flooding surface for sequence 1, 2 and 3 showing the nature of growth across the major syndepositional faults. Growth is less at the northwestern and mid eastern part of the field. Maximum flooding surface 0 to 1 has a prominent north central-southwestern trending elongate thickness belt across anticline adjacent to fault V.

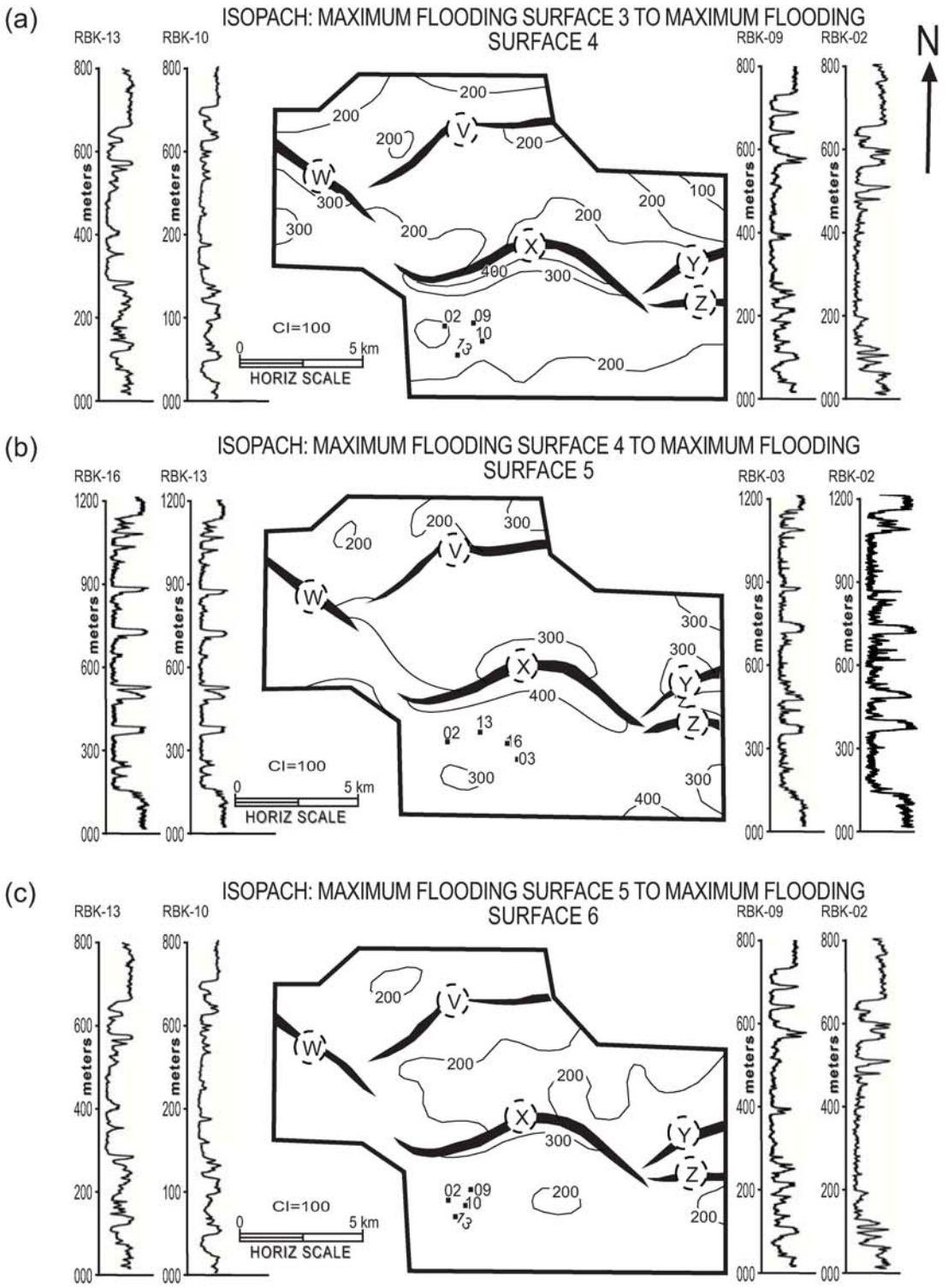

Figure 13b. Isopach maps of maximum flooding surface to maximum flooding surface for sequence 4, 5 and 6. Growth strata accumulation across the major syndepositional faults are less pronounced at this stratigraphic interval in the basin. There are 2 local relief features across anticline adjacent to fault V for isopach of sequence 6.

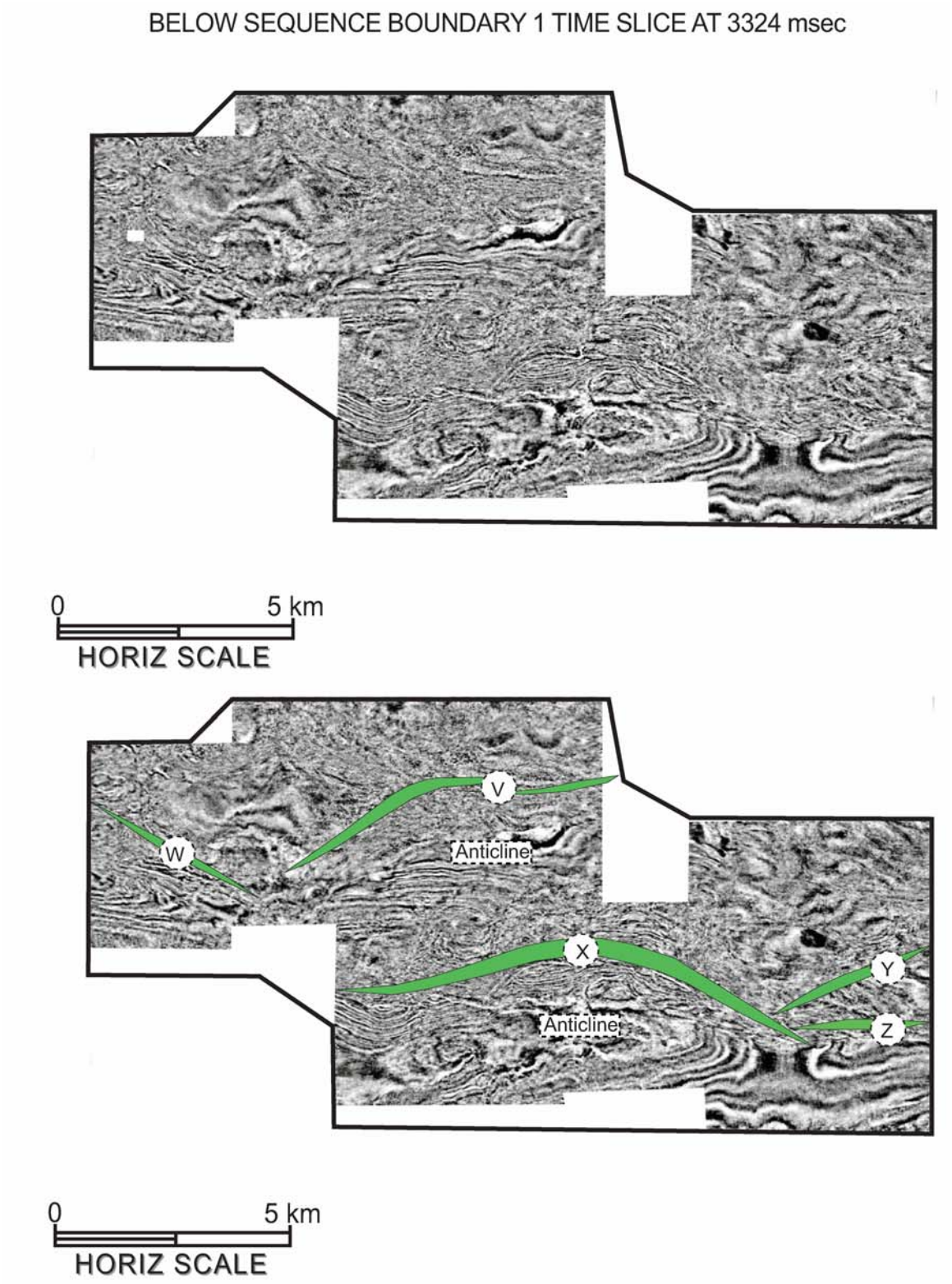

Figure 14a. Uninterpreted and interpreted seismic horizon slice below SB1 at 3.324 seconds showing major faults in Robertkiri with a general east - west regional trend of anticlines adjacent to the faults

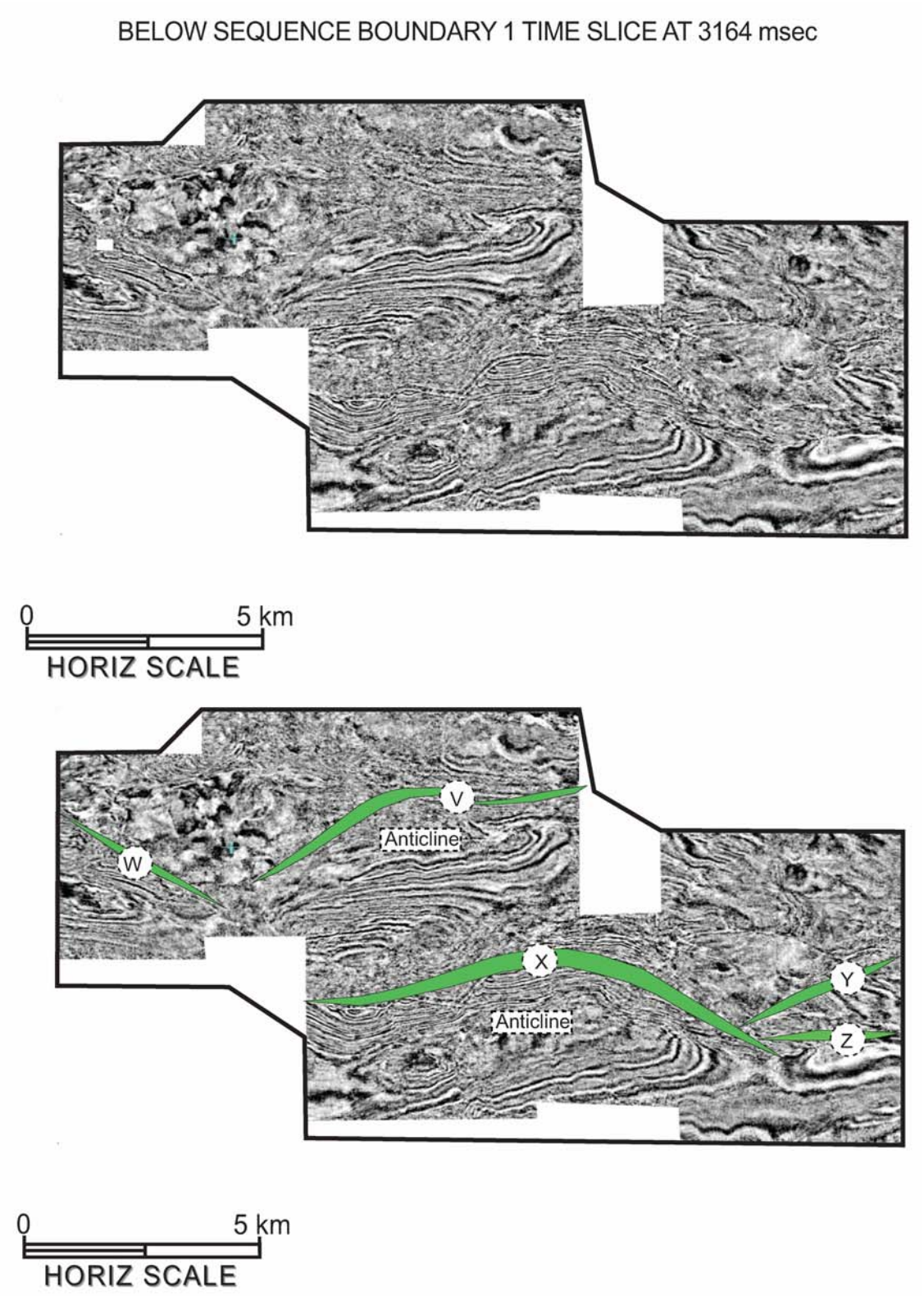

Figure 14b. Uninterpreted and interpreted seismic horizon slice below SB1 at 3.164 seconds showing major faults in Robertkiri with a general east - west regional trend of anticlines adjacent to the faults

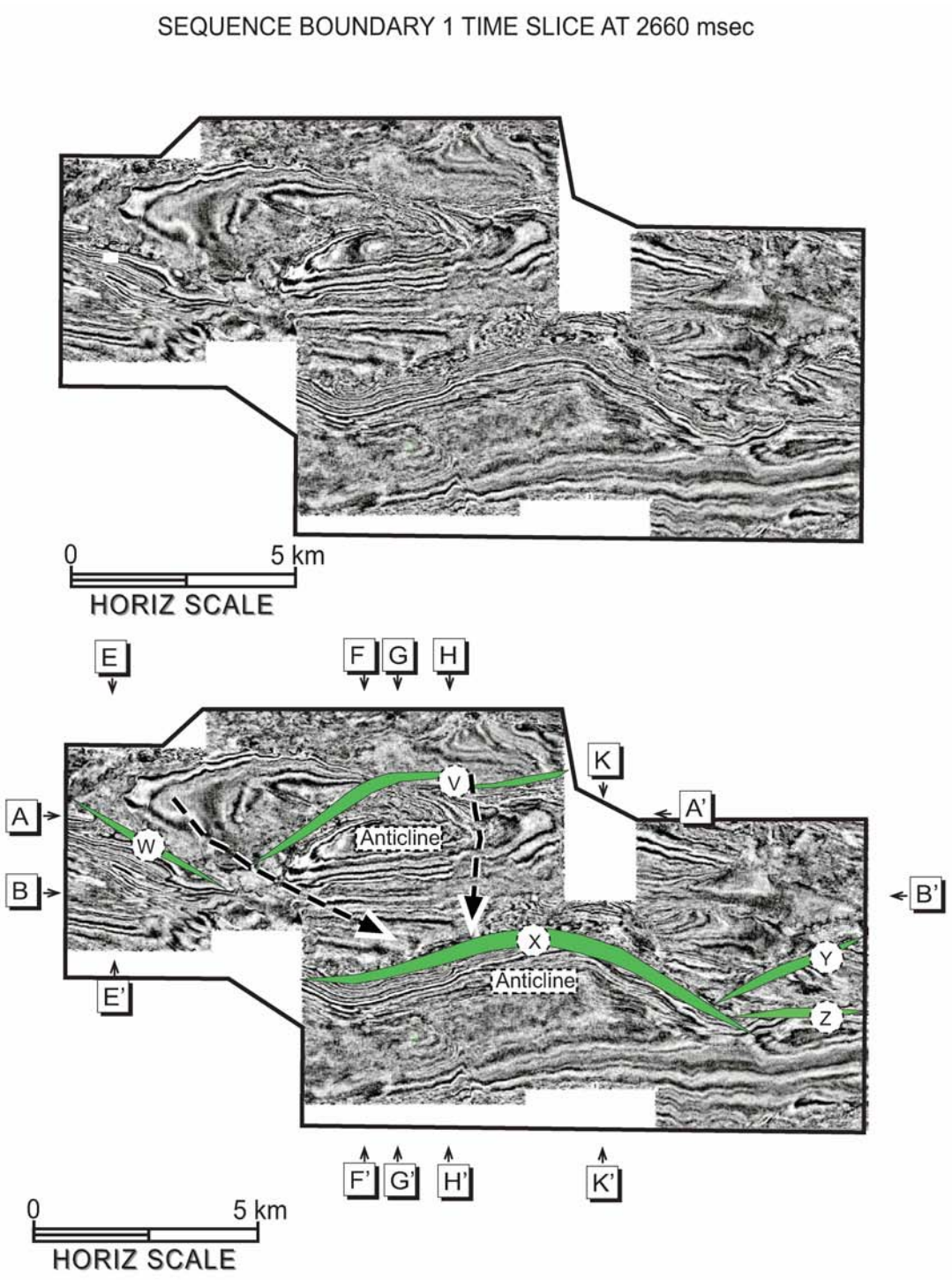

Figure 14c. Uninterpreted and interpreted seismic horizon slice on SB1 at 2.660 seconds showing the two main belts of incised features denoted by seismic facies 1 from the northwestern and north central parts of the field. Both belts are wider and seperate at this stratigraphic time slice than shallower in the sequence. Lines of seismic sections are denoted by rectangular boxes with little arrows.

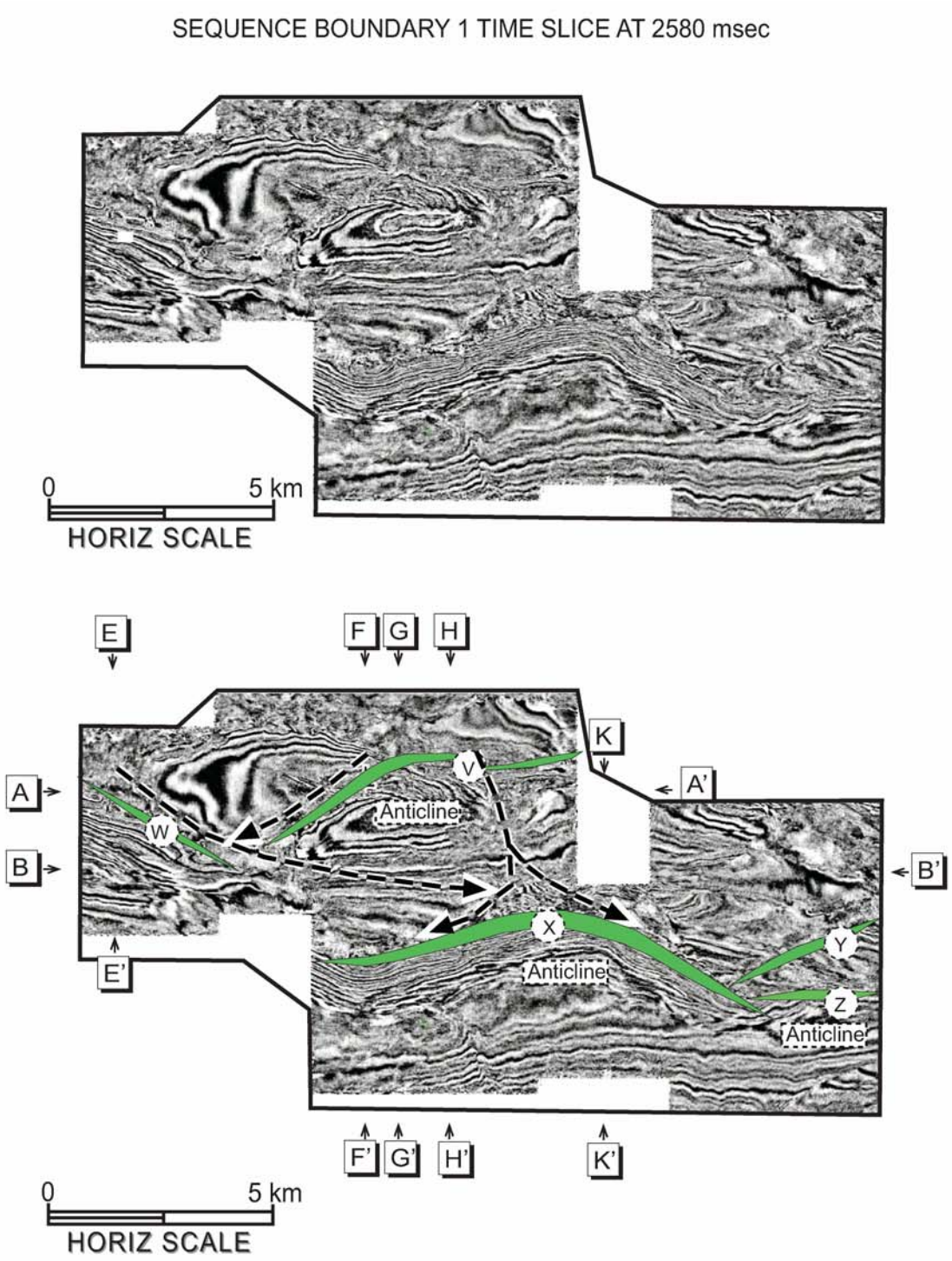

Figure 14d. Uninterpreted and interpreted seismic horizon slice on SB1 at 2.580 seconds. The belts of seismic facies 1 from the northwestern and north central parts of the field merged before bifurcating behind fault X. The belts are wider than observed deeper in the sequence. Lines of seismic sections are denoted by rectangular boxes with little arrows.

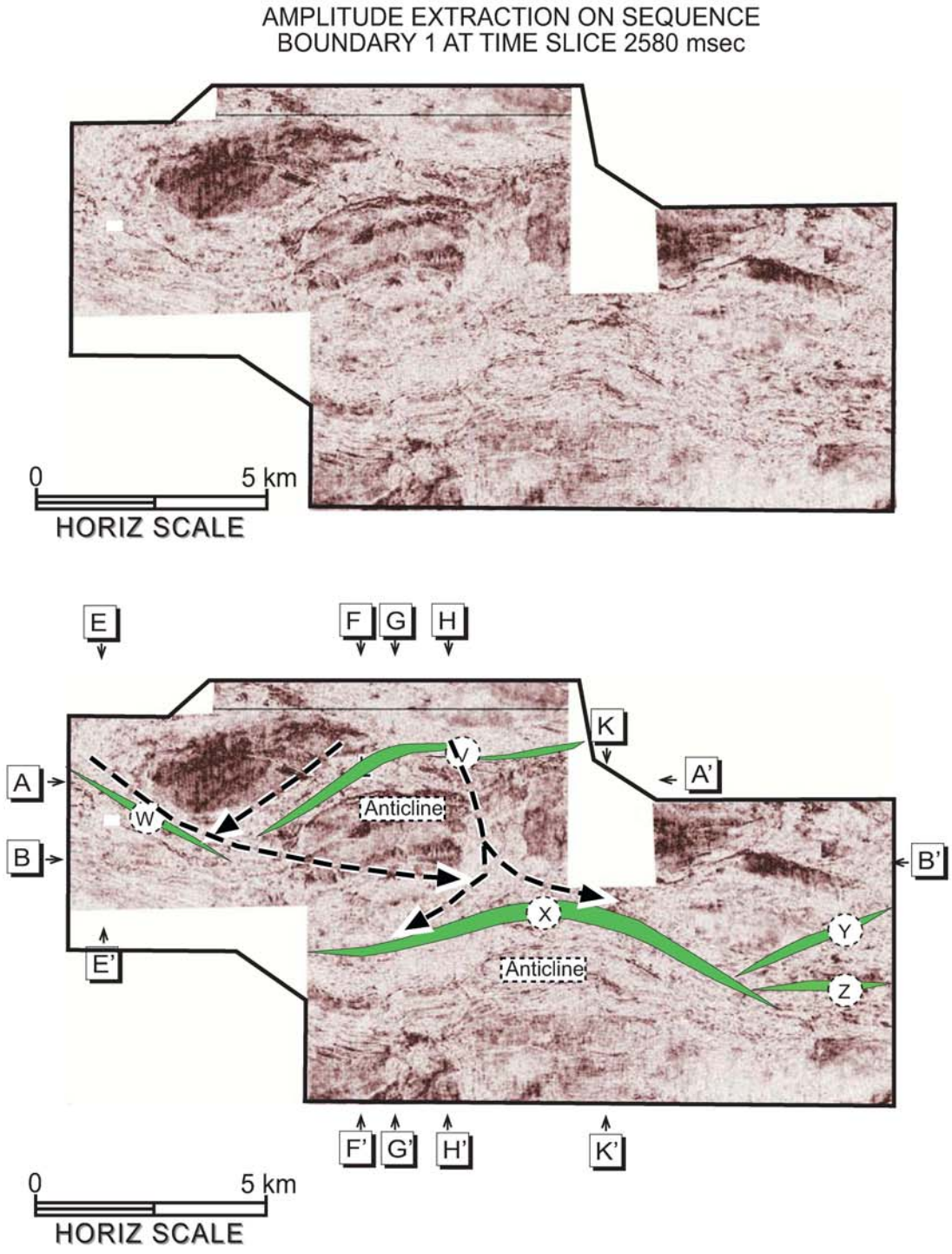

Figure 14e. Amplitude extraction on SB1 at 2.580 seconds. The belts of seismic facies 1 from the northwestern and north central parts of the field merged before bifurcating behind fault X. The belts are wider than observed deeper in the sequence. Lines of seismic sections are denoted by rectangular boxes with little arrows.

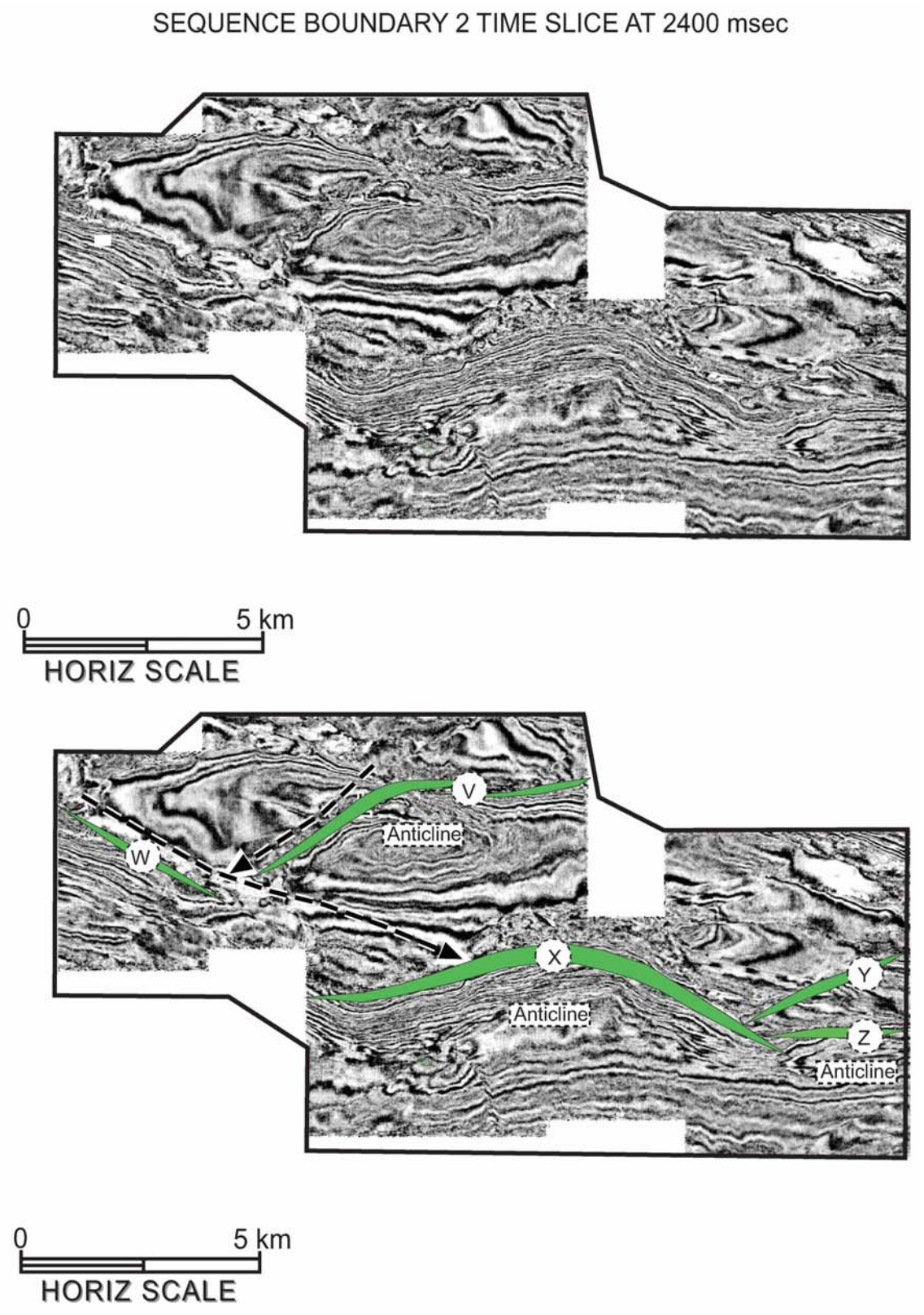

Figure 14f. Time slice at 2.400 seconds showing the two main incisional features on sequence boundary 2.

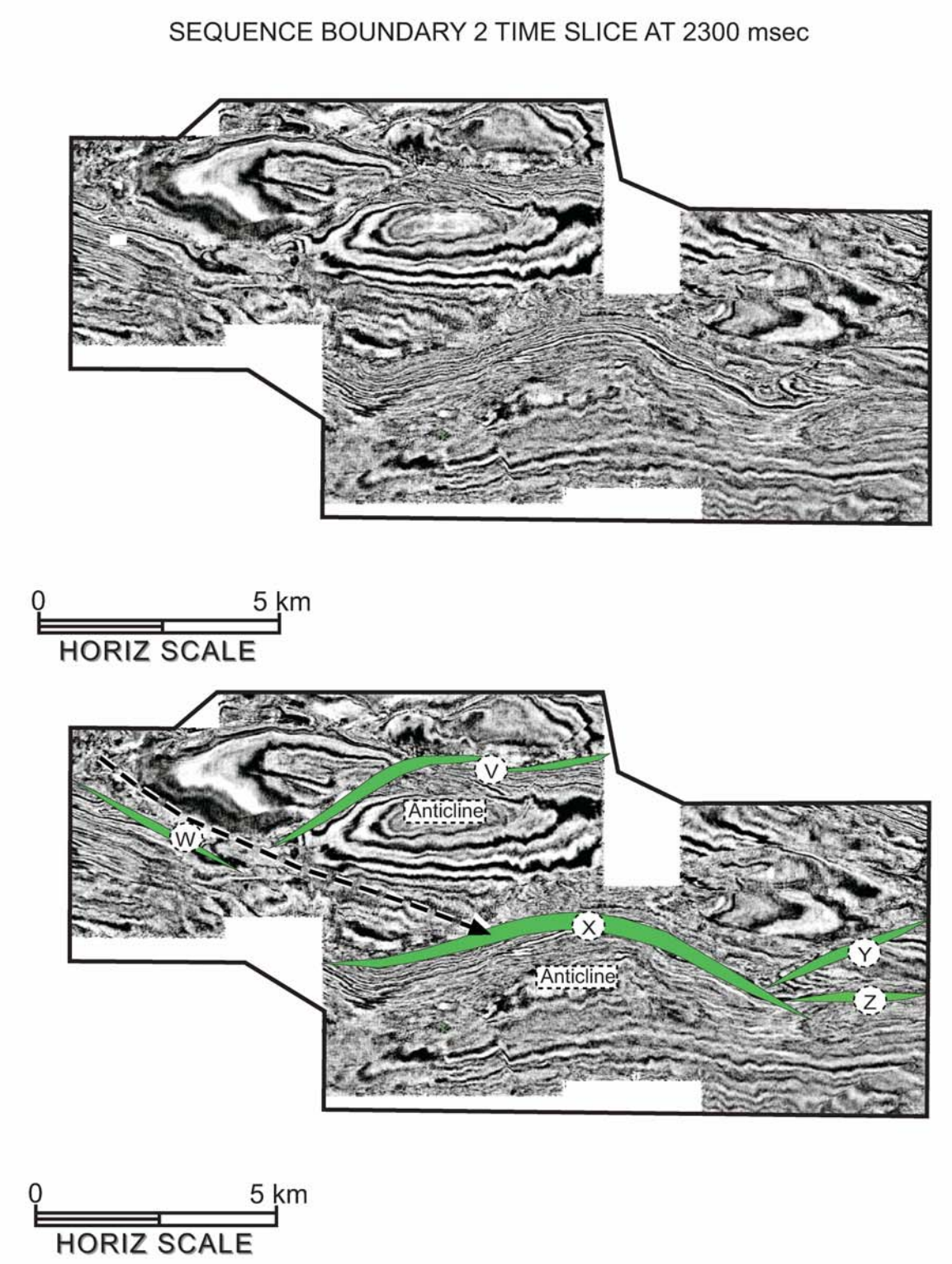

Figure 14g. Uninterpreted and interpreted seismic horizon slice on SB 2 at 2.300 seconds, showing the main incised feature from the northwestern part of the field. Incision adjacent to fault V at the northcentral part of the field is conspicously absent.

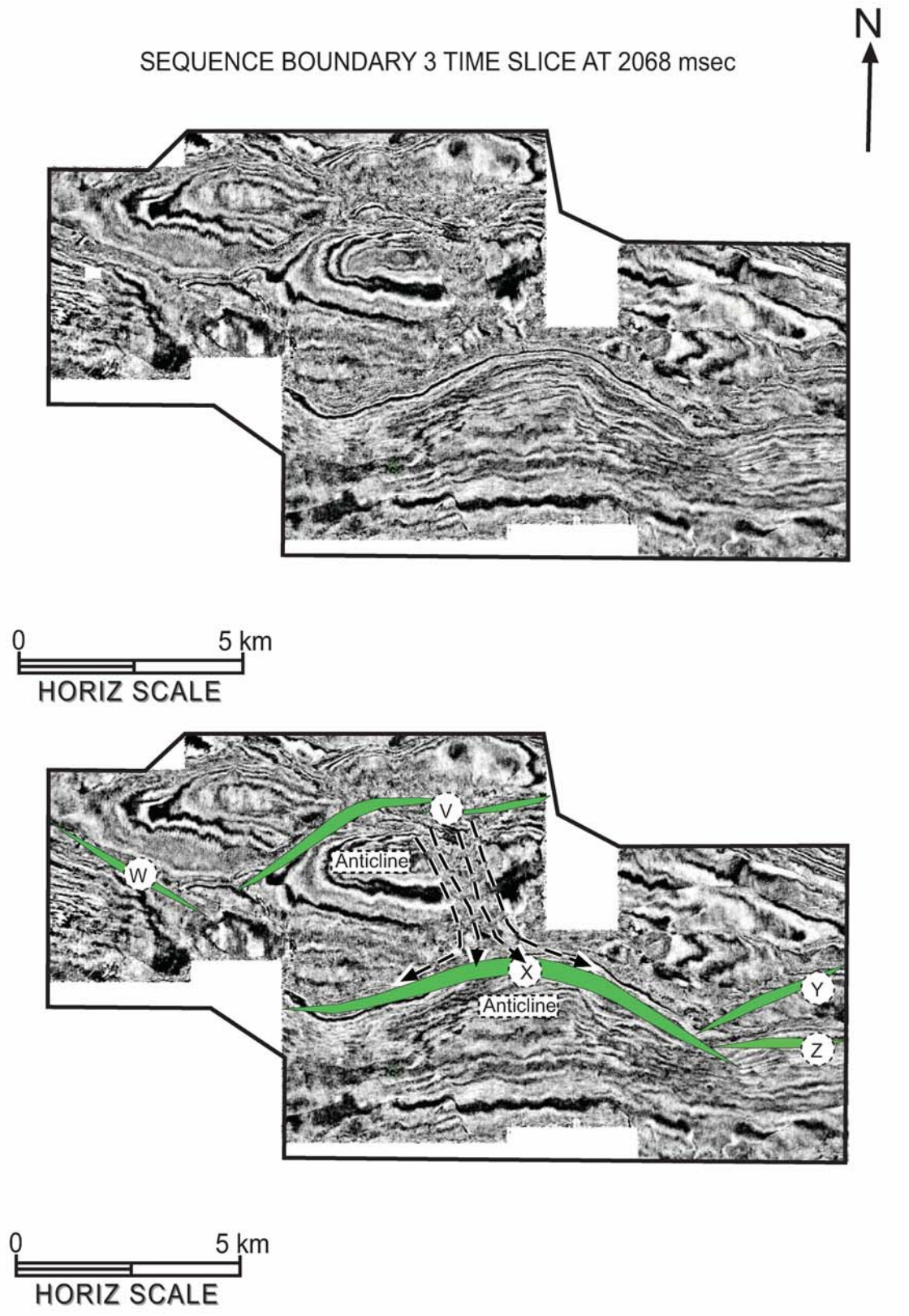

Figure 14h. Time slice of SB 3 at 2.068 seconds showing the main north central incision across anticline V bifurcating behind fault X.

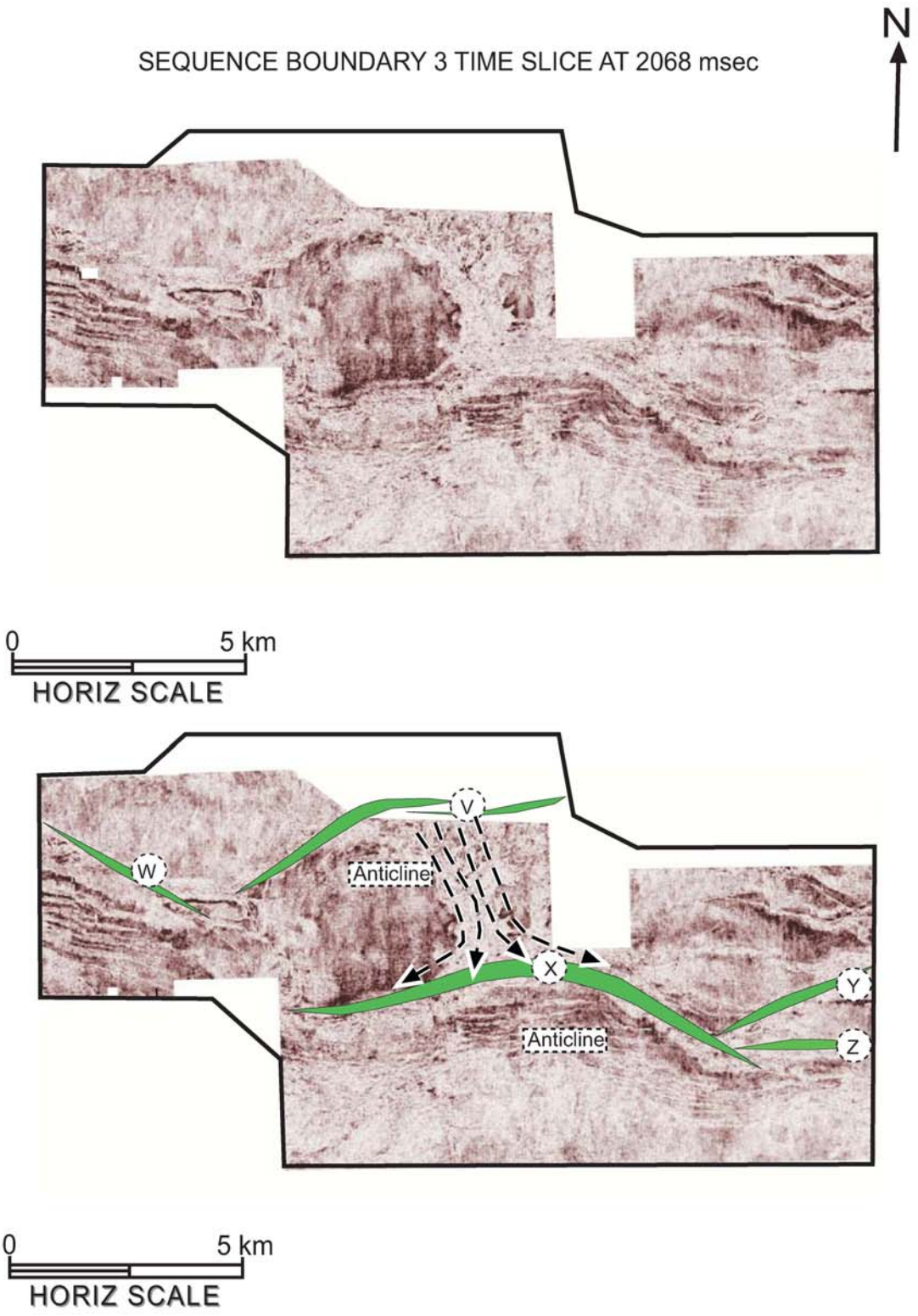

Figure 14i. Amplitude extraction of SB 3 at 2.068 seconds showing the main north central incision across anticline V bifurcating behind fault X. Antithetic and synthetic faults off main fault X are the small linear east-west trending feature on anticline X.

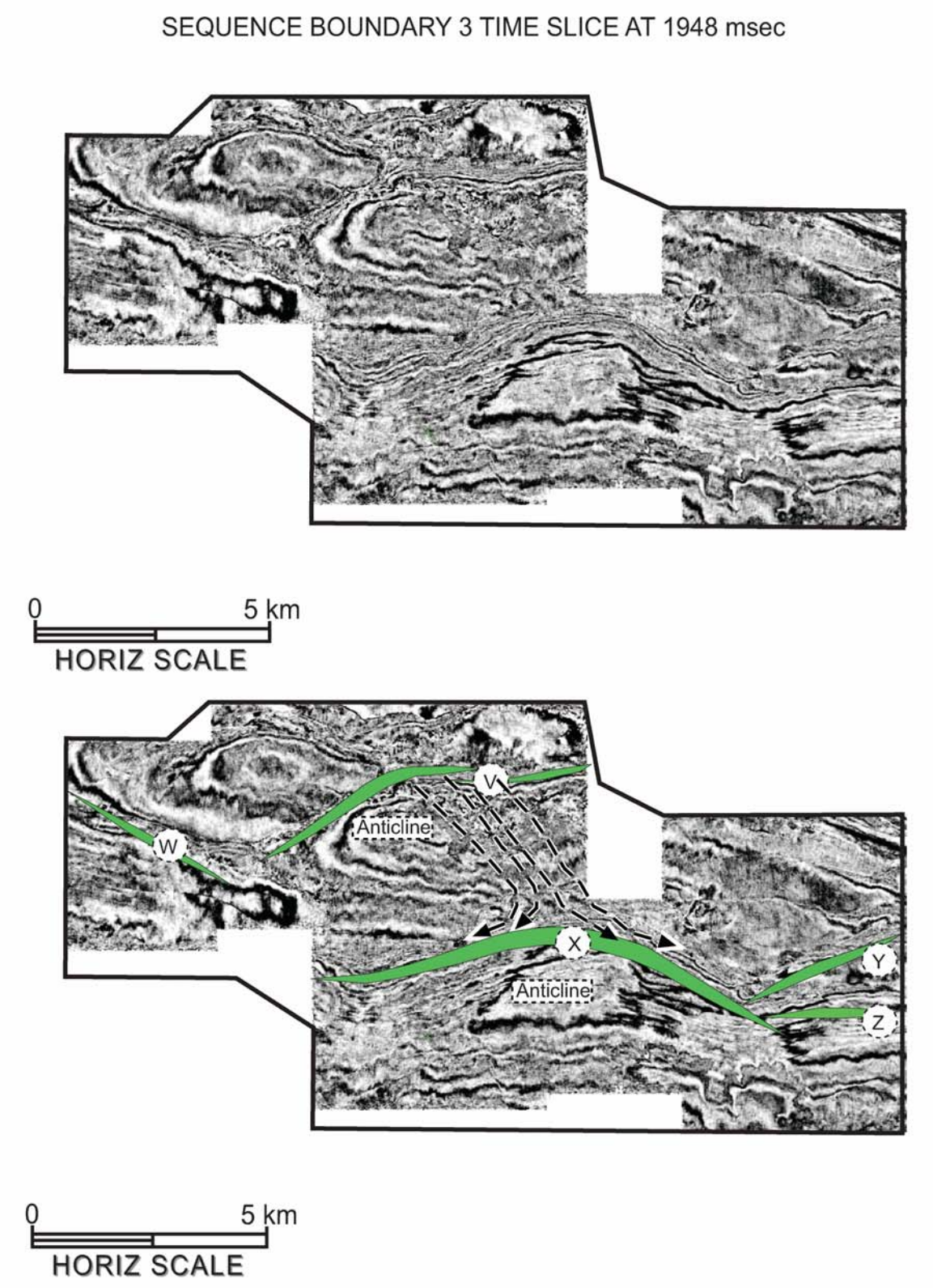

Figure 14j. Time slice of SB 3 at 1.948 seconds showing the main north central incision across anticline V bifurcating behind fault X.

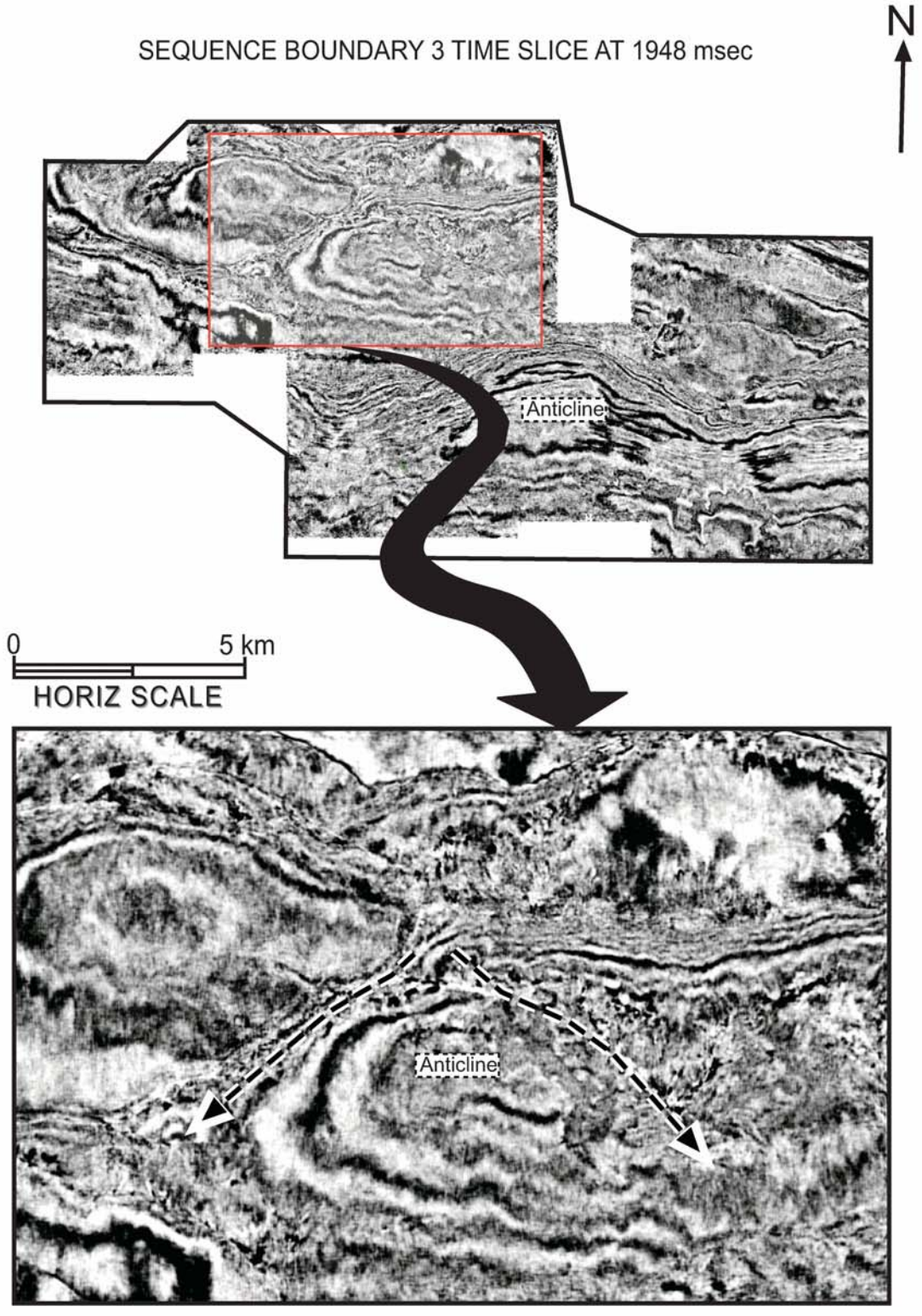

Figure 14k. Time slice of SB 3 at 1.948 seconds with nested smaller incised features inside the larger one on the hanging wall of anticline adjacent to fault V.

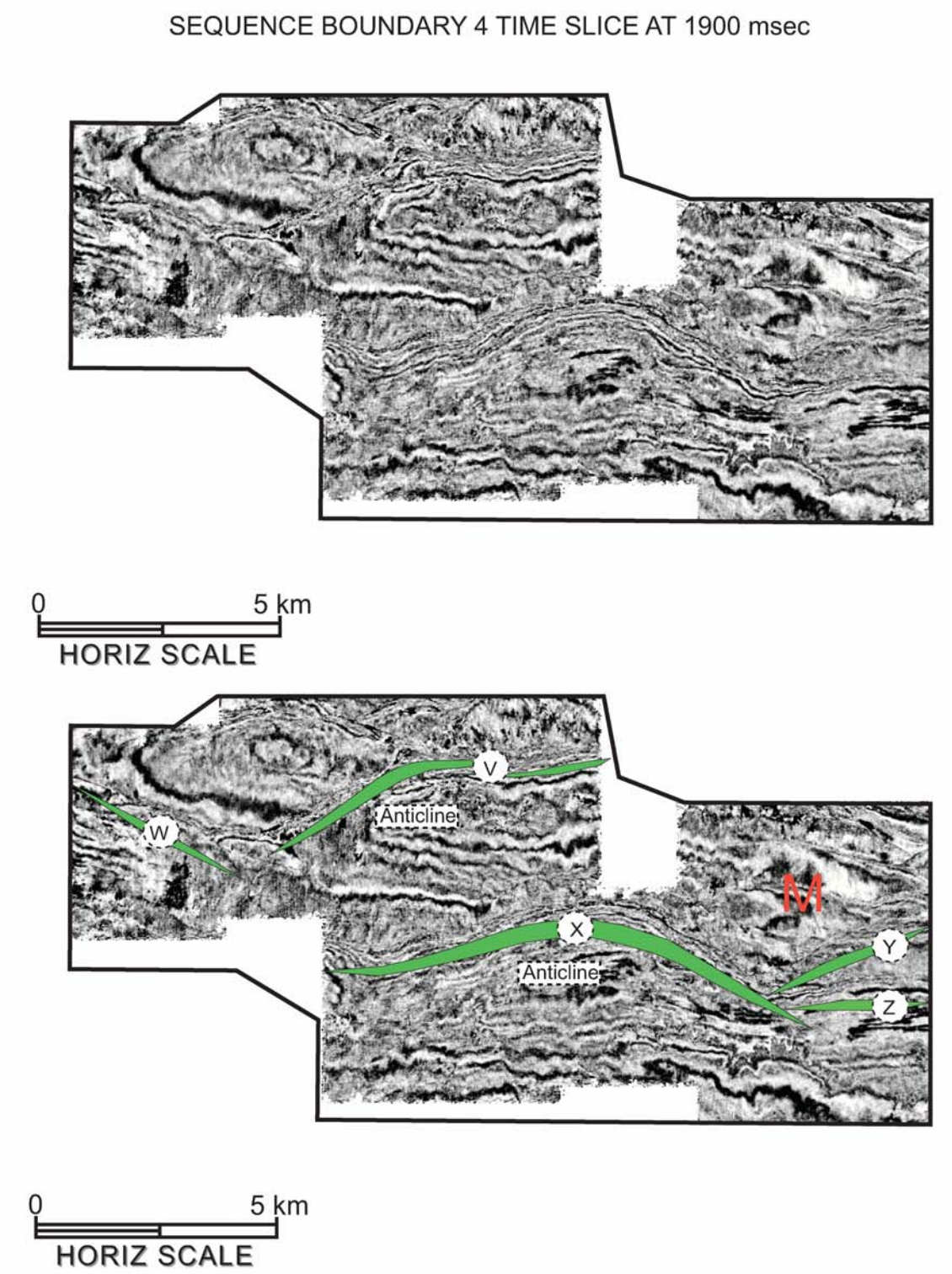

Figure 14l. SB 4 at time 1.900 seconds showing the major faults and their adjacent anticlines. The feature marked M on the footwall of fault Y could be inferred to be gas seepage effect.

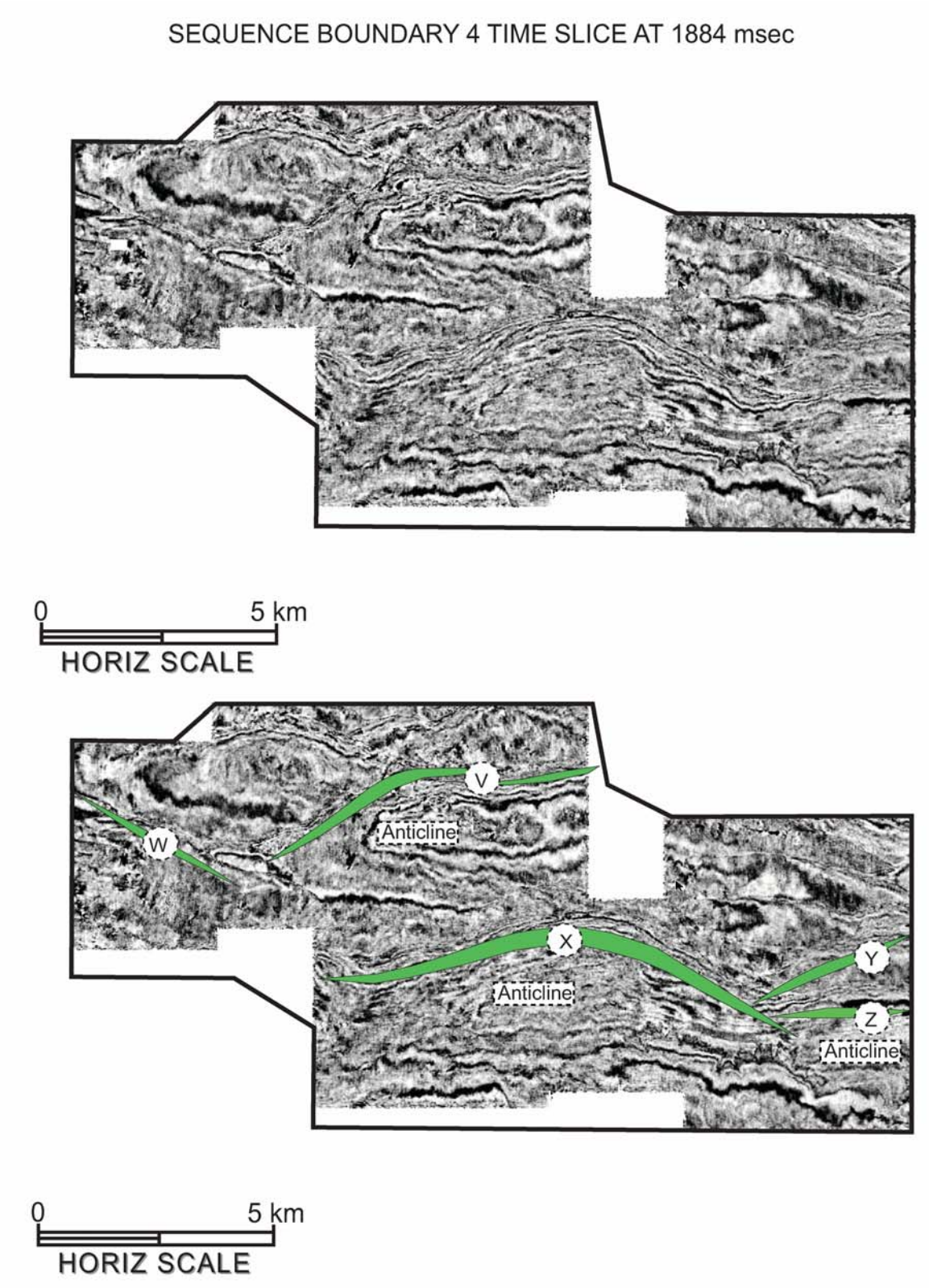

Figure 14m. SB 4 at time 1.884 seconds showing the major faults and their adjacent anticlines.

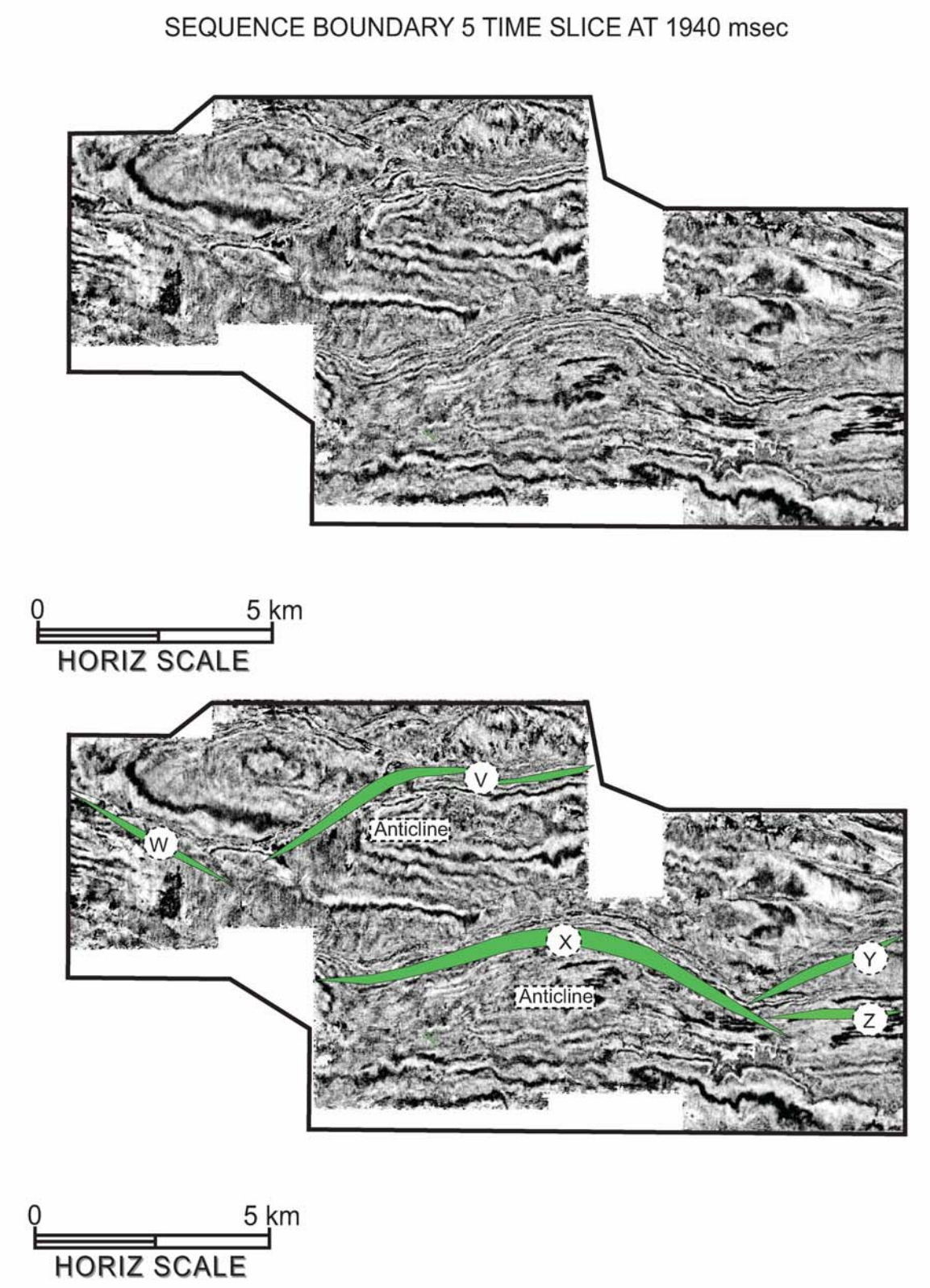

Figure 14n. SB 5 at time 1.940 seconds showing incision at the southeastern part of the field.

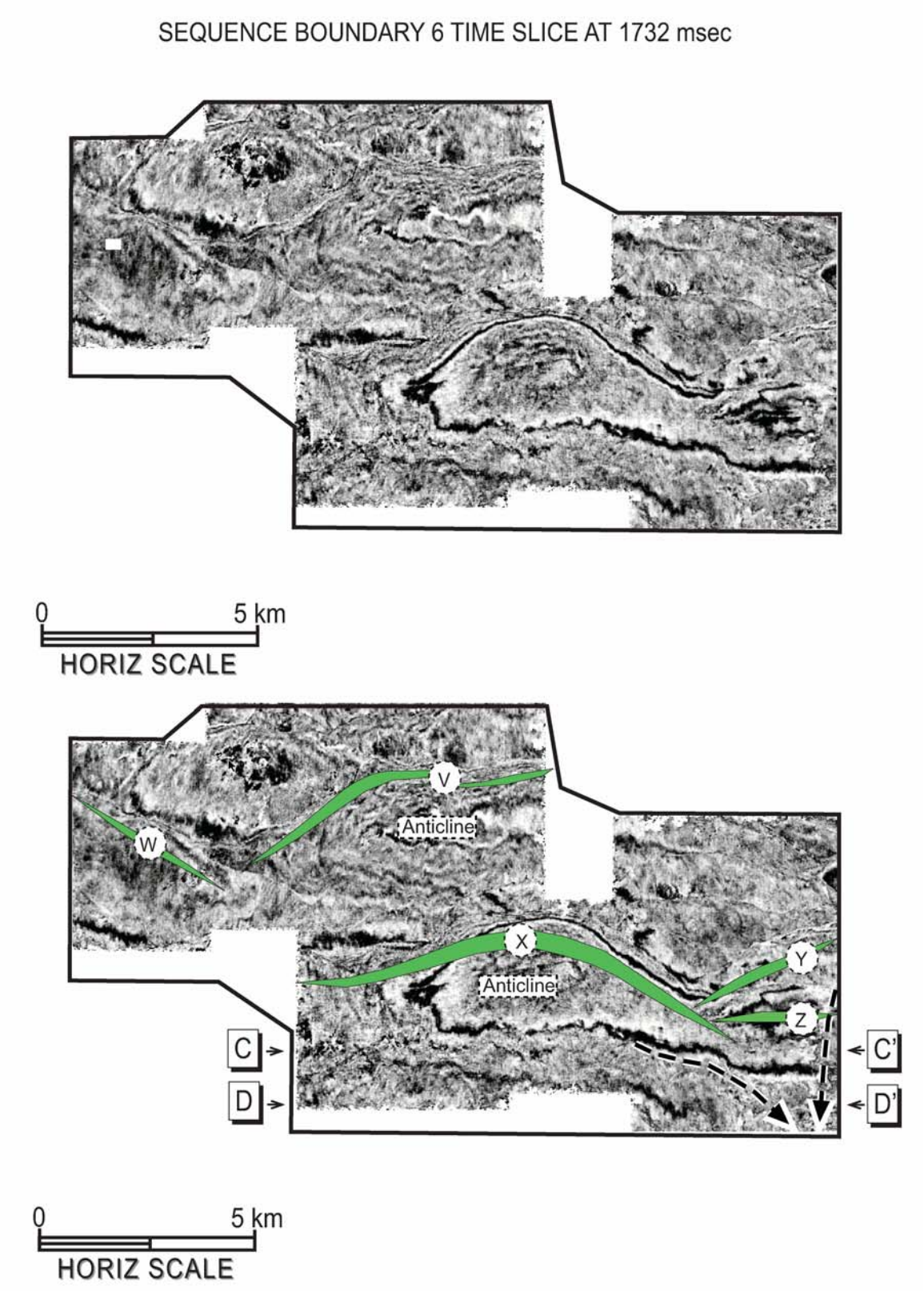

Figure 14o. SB 6 at time 1.732 seconds showing the incisions defined by seismic facies 1 at the southeastern part of the field.

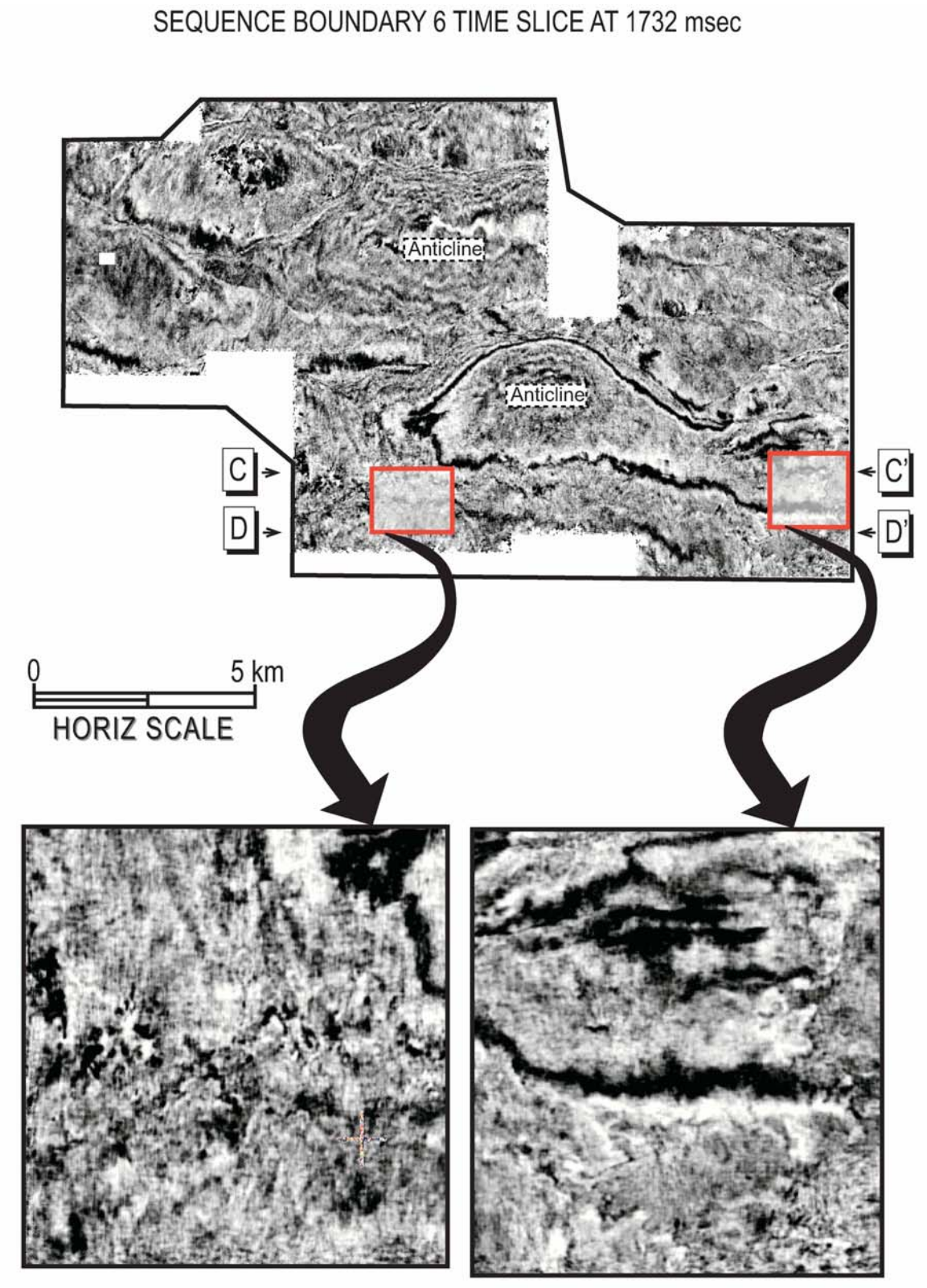

Figure 14p. SB 6 at time 1.732 seconds showing the incisions at the southwestern and southeastern parts of the field.

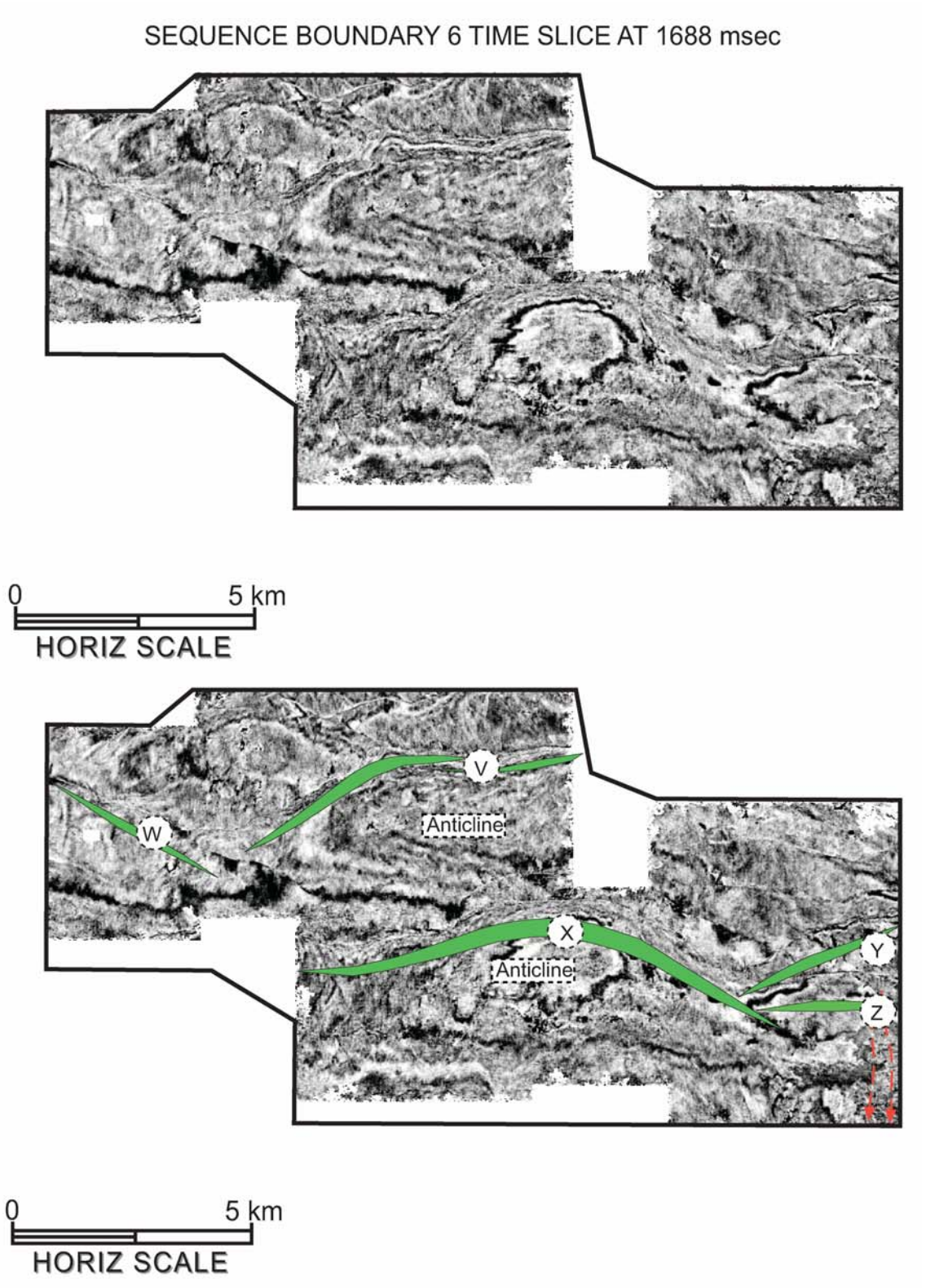

Figure 14q. SB 6 at time 1.688 seconds showing the channel incision at the southeastern part of the field.

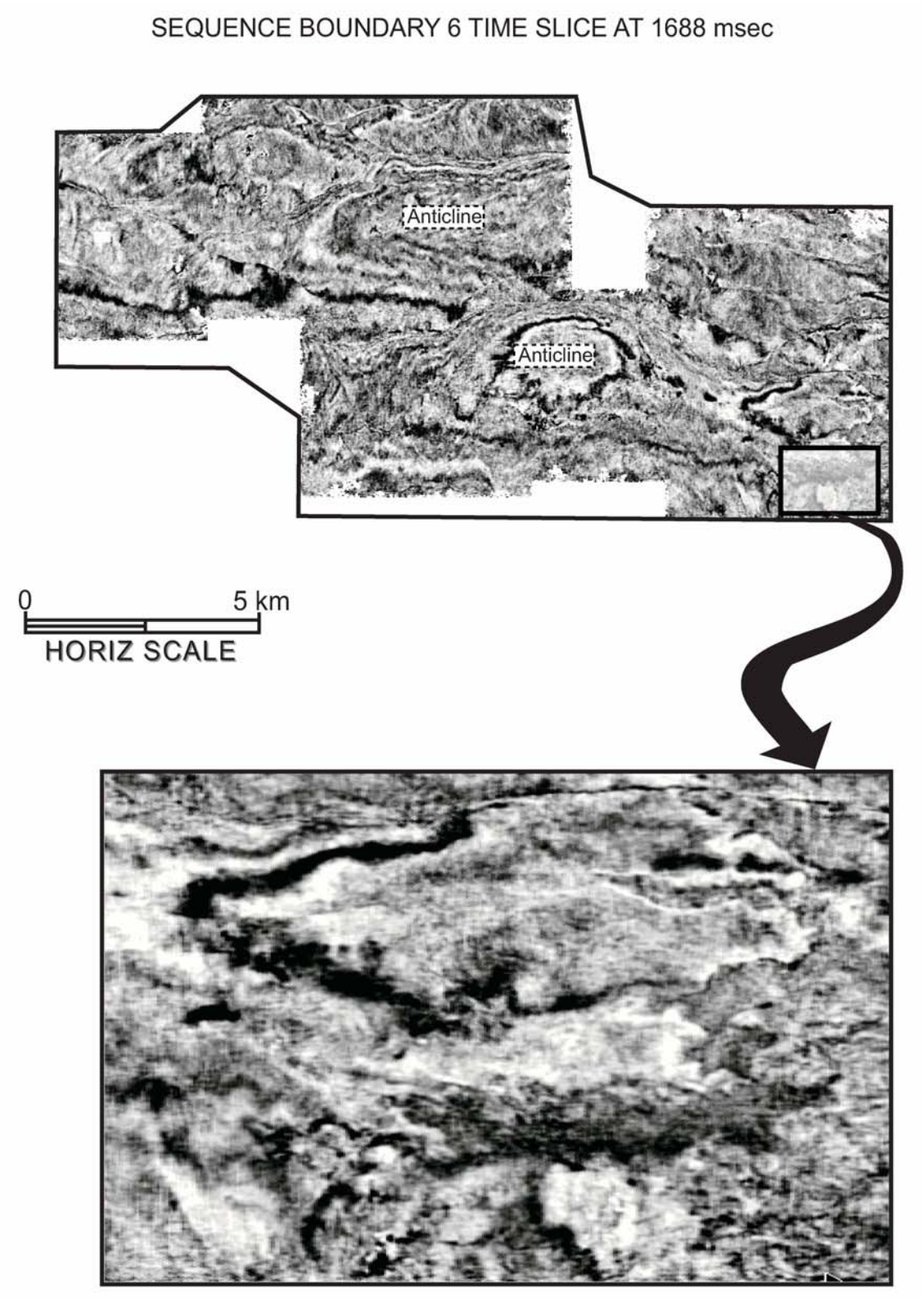

Figure 14r. SB 6 at time 1.688 seconds showing nested smaller incisions within a larger one at the southeastern part of the field.

Below Sequence Boundary 1

The interval below sequence boundary 1 is dominated by higher-frequency seismic facies 2 in basal parts of footwall blocks and broad diffuse transparent seismic patterns under footwall blocks. Although thicker chaotic seismic facies 1 interval are rare and can be difficult to distinguish from the diffuse edges of broader transparent zones, they occur locally above some surfaces that also show shallow incision into underlying reflections (e.g., Figure 10g, in the crest of the anticline basinward of Fault X). Logs of Robertkiri field penetrate only upper parts of this interval (Figure 9a), and record generally high gamma ray values and rarer low-value gamma ray intervals. The lower value intervals can be tens of meters thick, and generally have upward fining or blocky trends. Although vertical seismic facies variations and well log variations suggest there are additional sequences within these basal deposits, they are not addressed here. Tight folding and disruption of reflection continuity by the extensive transparent reflection zones did not allow the mapping of these variations across the seismic volume (Figures 14a and b).

Sequence 1

Sequence 1 (above sequence boundary 1) has an erosional base and averages 450 m thick. Areas of deeper incision are overlain by thicker belts of seismic facies 1. There, belts occur along two elongate trends, each a few kilometers wide. One belt extends Southeastward across the crest of the anticline on the down-dropped block of fault V to the block down dropped at fault X (Figure 12a, a). Erosion along this trend truncates about 110 m of underlying reflections at the anticline crest (Figures 10j and k). The second trend extends along fault W and then merges with the first along the western margin of fault X (including the area of Robertkiri field; Figure 14d). Reflection patterns

observed in horizontal time slices of the seismic volume dominantly record structural folding along anticlines (Fig. 14c and d). An amplitude extraction along a surface parallel to the sequence boundary more clearly shows the distribution of seismic facies 1 and 2 along the basal part of the sequence (Figure 14e). Belts of seismic facies 1 are narrower lower in the sequence and become wider stratigraphically higher within the sequence (Figures 10 a, b and j; also cf. horizontal slices in Figures 14c and d). Upward within the sequence, seismic reflections gradually become higher frequency, defining a transition into seismic facies 2.

Logs from Robertkiri field record vertical trends in the area where the two belts of facies 1 join down dip of fault X (c.f., Figures 6 and 9b). Gamma ray values abruptly decrease at the base of the sequence, and overlying deposits have low-gamma-ray-value, tens-of-meters-thick, blocky patterns (recording an abrupt coarsening). A 10 m thick internal with uniformly high gamma ray values occurs near the vertical transition from seismic facies 1 to 2. Gamma ray values initially gradually increase above this high gamma ray interval and then abruptly increase into several tens of meters thick blocky patterns (Figure 9c). Gamma ray patterns become thinner and more variable in the upper most part of the sequence, just below sequence boundary 2 (Figure 9d). The 10 m thick shale bed at the transition from seismic facies 1 and 2 defines a particularly high amplitude reflection, and is interpreted to be a maximum flooding surface. A structure map of this surface shows folding over anticlines and pronounced regional basinward dip (Figure 11a, a). Reflections within seismic facies 2 fan apart past the anticline crest on the footwall block of fault V (Figure 10i), but not past the crest of the anticline down dip of fault X. The thickness of deposits between a prominent reflection within an interval of

seismic facies 2 below sequence boundary 1 (labeled maximum flooding surface 0) and the maximum flooding surface within sequence 1 (labeled maximum flooding surface 1) show that deposits are thicker along belts of seismic facies 1 but do not thicken abruptly across major faults.

Sequence 2

Sequence 2 averages about 550 m thick. It has geometry and internal character similar to sequence 1. Although areas of deeper incision, overlain by thicker intervals of seismic facies 1, follow broadly similar elongate trends as those in sequence 1 (Figure 12a, b), the erosional trend along fault W is somewhat deeper (up to 130 m of erosion into underlying reflections; Figure 10e) and the erosional trend across the down-dropped block of fault V shifted to the western edge of the associated anticline (Figure 12a, b). Basal parts of seismic facies 1 belt are wider than shallower parts (c.f., Figures 14f and g). Like sequence 1, gamma ray logs show an abrupt decrease (coarsening) to blocky patterns in the basal part of the sequence, and a 25 m thick high-value interval near the vertical transition from seismic facies 1 and 2 (Figure 9a). Seismic facies 2, in the upper part of the sequence, is more uniform in thickness than the lower interval of facies 1.

Like in sequence 1, the high-value interval near the middle of the sequence is interpreted to record maximum flooding. It similarly changes in dip across anticlines above down dropped blocks and dips on average significantly offshore (Figure 11a, b). Fanning of reflections within seismic facies 2 is observed across the anticline crest down dip of fault V (Figure 10f, g, h). Although the interval between maximum flooding surfaces 1 and 2 thickens somewhat across all major faults, these changes are more prominent across the apex region of fault X than across faults W and Y (Figure 13a, b).

Sequence 3

Sequence 3 is about 330 m thick (Figures 10 a, j, h and k). A trend of deeper incision and associated belt of thicker seismic facies 1 is most pronounced across the crest of the anticline down dip of fault V (Figure 10f, g, h; Figure 12a, c). This erosional trend, locally cutting 300 m into underlying reflections, bifurcates onto the block down dropped across fault X (Figures 14h, i, j). In some locations this seismic facies 1 incision fill contains smaller-scale nested internal incision fills (Figure 14k). Where most deeply eroded, along the anticline crest below fault V, the incision fill comprises a several hundred meter thick set of inclined reflections that dip basinward toward fault X (Figure 10k).

Like the underlying sequences, gamma ray values abruptly decrease at the base of the sequence, and basal deposits have low-value blocky patterns. The basal interval with low gamma ray values is vertically divided by several 5 to 10 m thick intervals with high gamma ray values (Figure 9b). Gamma ray values increase abruptly in the middle of the sequence, at an interval interpreted to define the maximum flooding surface. The interval of seismic facies 2 above this maximum flooding surface is really thin. Fanning of reflections within facies 2 across anticline crests is less pronounced than that observed in earlier sequences. The maximum flooding surface has lower regional dip toward the basin and folding of this surface across anticline crests is more gentle (Figure 11a, c). Although thickening of the interval between maximum flooding surfaces 2 and 3 across fault V is also less pronounced than observed in older sequences, there is significant thickening of this interval across fault X. (Figures 11a, c and 12a, c).

Sequence 4

Sequence 4 averages 250 m thick. Although the base of this sequence is defined by an abrupt coarsening, basal erosion and associated seismic facies 1 are restricted to a few localized areas along the hanging wall of faults V and X (Figure 12b, a). Reflections within seismic facies 2 in the upper part of this sequence are nearly parallel across anticlines. Intervals between these reflections have little offset across faults relative to that observed in sequences below (Figure 14d). The basal deposits fine upward from the sequence boundary to a thick interval with high gamma ray values, interpreted to be the maximum flooding surface. Gamma ray values abruptly change above this maximum flooding surface to a succession with low-value blocky patterns.

Sequence 5

Sequence 5 averages 250 m thick. Several widespread shallow incisions (< 50 m of erosion into underlying reflections) along north-south elongate trends define the base of the sequence: 1) across fault W to the west side of the seismic volume; 2) along the block down dropped at fault V to the apex of fault X; 3) through the eastern part of seismic volume across faults Y, and Z (Figure 12b, b). There are multiple laterally connected shallow incisions cutting into the footwall of fault X (Figure 11b, b; Figure 12b, b). Seismic facies 1 are confined mainly to the southeastern part of the field (Figure 14n), and thus most of the sequence is composed of seismic facies 2. Logs through sequence 5 show an abrupt coarsening at the base of the sequence and basal deposits have low-gamma-ray-value, blocky patterns separated by thinner (<3 m) high-gamma-ray intervals. The maximum flooding surface, defined by a 20 m thick interval with uniformly high

gamma ray values, occurs within the interval of seismic facies 2. The maximum flooding surface shows low regional dip into the basin (Figure 11b, b).

Sequence 6

Sequence 6 is about 130 thick. Two elongate areas of deeper incision are recognized across the anticline down dip of fault X; One along its eastern limb and the other nearly directly across its crest (Figure 11b, c). Both are overlain by thick successions of seismic facies 1. Belts of seismic facies 1 within these incisions locally contain nested internal incised fills (Figure 14p) and elsewhere 100 m thick sets of inclined reflections (Figures 10, e; 14o). Wider, shallow inclusions define this surface elsewhere within the seismic volume (Figures 10c, d and l). The maximum flooding surface was defined by a pronounced reflection within the gradual upward transition from seismic facies 1 to 2 and by high gamma ray emissions recorded by well logs. Facies 2 reflections in upper parts of this sequence fan apart across the area between faults V and X, but not across the block down dropped across fault X. There are only minor variations in the thickness of the interval between maximum flooding surfaces 5 and 6 across the seismic volume (Figure 13b, b).

INTERPRETATION OF STRATIGRAPHIC TRENDS

Truncation of reflections under sequence boundaries records fluvial incision during relative sea level lowstands. Seismic facies 1, associated with low-value blocky gamma ray well log patterns, records accumulation of sandy fluvial channel deposits within incised valley fills. High gamma ray spikes within these intervals may record preservation of overbank deposits within valleys or estuarine deposits preserved as the valley was transgressed. The high gamma ray intervals, commonly associated with

vertical transitions from seismic facies 1 to 2, are interpreted to have formed during maximum flooding following sea level rise. Upward coarsening patterns through seismic facies 2 intervals record progradation of shorelines following maximum flooding. Blocky patterns lower within these successions may indicate sharp-based shoreface deposits formed as relative sea levels began to fall, whereas those higher in successions probably record distributary or fluvial channel deposits. The fining of deposits recognized in the upper most part of some sequences may be paralic deposits formed along tide-influenced coastlines. These depositional interpretations suggest that seismic facies 1 mostly comprise lowstand and transgressive system tracts and seismic facies 2 comprise highstand system tracts.

Two distinct drainages in the oldest sequences 1 and 2 (the western one following the trend of fault W and the eastern crossing the apex of fault V) each appear to be influenced by structural movements. Deeper incisions across faults V and W suggest these features were associated with syndepositional topography. The path of the eastern drainage directly across the crest of the anticline basinward of fault V suggests this feature was not a structural high during highstand. Deeper incision across the crest of this anticline at the base of sequences, however, suggests that it became a topographic high when most sediment was being bypassed farther basinward during lowstand. Fanning apart of reflections away from the anticline crest within overlying facies 2 intervals records the filling of topography and accumulation of growth strata during subsequent highstand progradations. Basinward tilts of all stratigraphic surfaces within this interval reflects the longer term seaward collapse of this basin margin (figure 10f).

Sequence 3 does not record evidence for a western drainage along fault W, suggesting that this sediment source avulsed elsewhere during the intervening highstand: It may have joined the eastern drainage up dip or avulsed laterally out of the study area. Although this sequence is thinner than the previous two, suggesting lower average accommodation, deeper incision suggests the greatest relative sea level fall. The fill directly above the sequence boundary show distinct smaller reflection truncation, interpreted to image individual river channels with size near the lower limit of seismic resolution. Local thicker sets of inclined reflections, nearly 100 m thick, may be bayhead delta deposits formed where more incised areas of valleys were rapidly flooded. Relative to previous sequences, mean sediment accumulation clearly shifted basinward to the down dropped side of fault X.

Sequence 4, with no obvious basal erosion, is interpreted to be a progradational interval formed when relative sea level never fell faster than regional subsidence (a “type 2” sequence boundary, using standard Exxon terminology; Mitchum and Van Wagoner, 1991). Limited seismic facies 1 and uniform thickness also suggest that deposition was spread widely along the basin margin. Progressive thinning of younger sequences, associated with less offset across major faults, suggests accommodation development slowed as deformation ceased.

A broadening of incisions under the final two sequences (5 and 6), the blocky nature of their well log signatures, and very-thin, local seismic facies 2 intervals suggest they dominantly record fluvial bypass of sediment to basinward areas with more accommodation remaining. These nearly horizontal sequences, truncating tilted reflections of underlying sequences and major faults, record deposition after structural

deformation had greatly slowed or stopped within the study area. Deeper incisions along sequence boundary 6 in the most distal parts of the seismic volume suggest that patterns of episodic incision and fill observed within the older sequences in this study area continue in areas more basinward. Overlying deposits with more transparent, discontinuous reflections (upper 1.5 s twt in the seismic record), interpreted earlier to be fluvial deposits of the Benin Formation, record continued bypass of sediment to more basinward areas within the basin.

DISCUSSION

Syndepositional structural collapse of the Niger Delta clastic wedge significantly complicates development of internal stratigraphic sequences. As discussed previously, Niger Delta progradation is punctuated at the regional scale by the development of depobelts formed as sediment loads underlying shales, which in turn become overpressured and unstable. Normal faults along the proximal edge of a depobelt displace prograding delta deposits downward and basinward into underlying mobile shales, which in turn move upward in more distal areas along a counter-regional fault (Figure 15). The character of sequence development and depositional facies of sediments preserved depend on relative rates and patterns of regional structural collapse across depobelts in response to accumulating sediments, as well as shifts in the position of deposition produced by relative sea level changes.

Knox and Omatsola (1989) presented an “escalator” model of regional regression to describe depositional patterns within Niger Delta depobelts (Figure 16). In this model, rates of structural collapse and associated rise of diapirs in more basinward areas closely balanced rates of sediment supply. The depobelt is thus filled by relatively horizontal sheets of shallow marine deltaic, paralic and fluvial strata, which are successively displaced downward after deposition during continued structural collapse. Delta regression stalls behind rising shale structures along the distal edge of the depobelt, as the thick succession of shallow water sediments accumulate. This pattern continues until underlying overpressured mobile shales are depleted, structural subsidence under the depobelt slows, and the delta front again progrades basinward. As the delta front moves

past the shale diapirs along the distal edge of the depobelt, more distal areas are loaded, and a new depobelt begins to form.

Robertkiri field is located within the proximal edge of the Coastal Swamp I depobelt (Figure 2), fairly near the area of maximum progradation of the modern Niger Delta. This presumably was an area of continuous relatively high sediment supply, where depositional pattern across the depobelt should be similar to those predicted by the "escalator" model. Sequences observed within Robertkiri field record smaller-scale stratigraphic variations within this depobelt, which might reflect shorter-term displacement across faults or sea level variations.

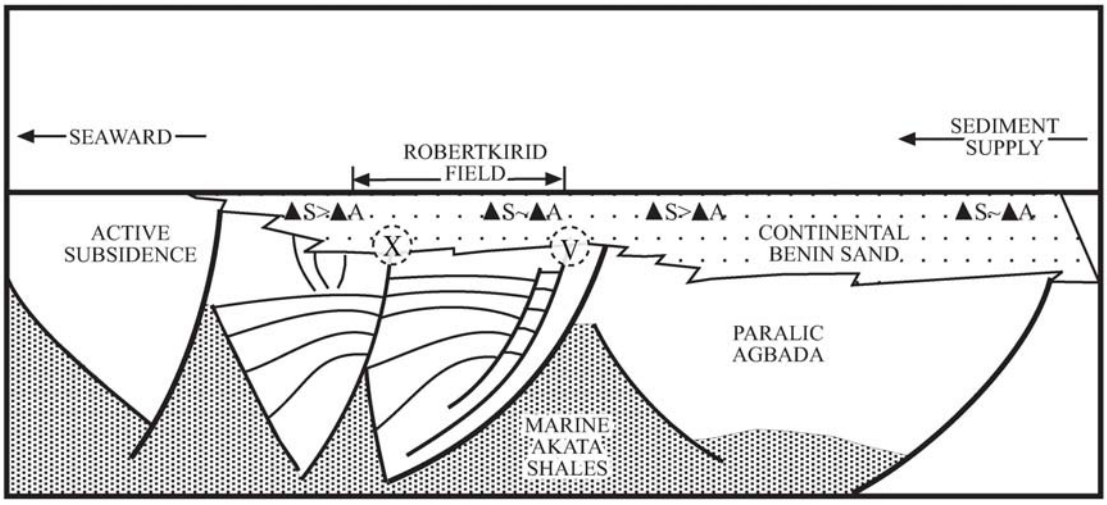

Figure 15. Shematic diagram of adjacent depobelts around Robertkiri field showing influence of geopressured mobile Akata shale on the paralic Agbada unit. Shale withdrawal provided greater accommodation at the distal end of the depobelts and are closely related to formation of the landward diping counter-regional faults. Modified from Doust and Omatsola (1990).

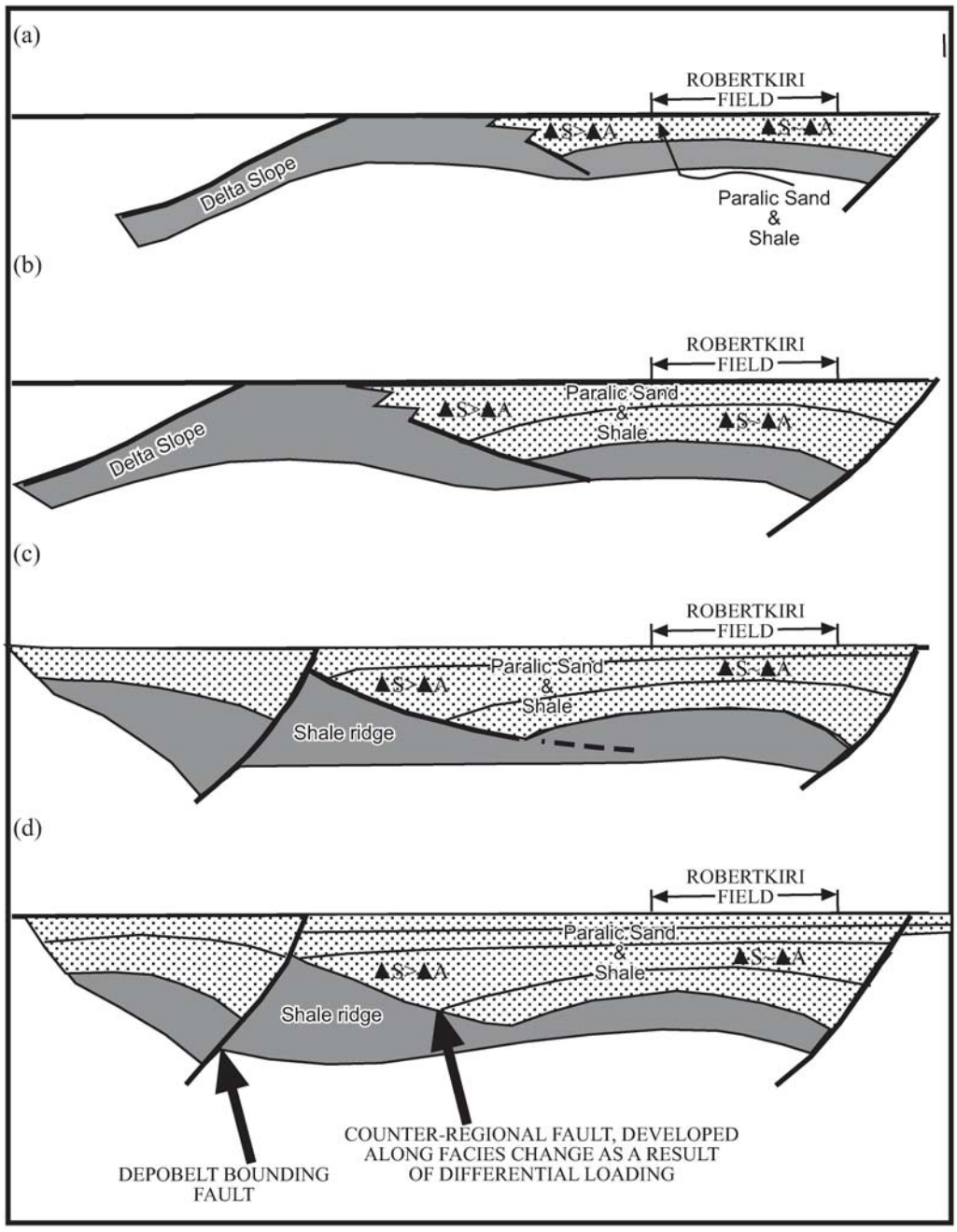

▲S = RATE OF SUBSIDENCE ▲A = RATE OF ACCUMULATION

Figure 16: Escalator regression model of regional regression for depositional patterns within Niger Delta depobelts. (a) Shallow marine shelf to deltaic coastal plain deposition of sand and shales progrades over a depobelt . (b) The depobelt matures with decreased subsidence at its distal part. (c) Paralic sedimentation diachronously slows down in the depobelt as a newer depobelt develops basinward and (d) The paralic facies eventually advances rapidly over the younger depobelt as it structurally matures. Modified after Knox and Omatsola (1987).

Structure under Robertkiri field indicates that the proximal edge of the Coastal Swamp I depobelt is defined by a succession of major cuspate normal faults. Thickness changes between stratigraphic surfaces lower within the formation (Sequences 1-3) show greater structural influence, with layers clearly thickening directly adjacent to faults along basinward tilted fault blocks and thinning over the crests of rollover anticlines. Stratal patterns across down-dropped fault blocks have broad similarities with larger-scale depobelts. Strata are clearly displaced downward and basinward across these faults. Transparent seismic zones mark distal ends of a down-dropped block, in the footwall of a succeeding major fault. Locally abrupt contacts between areas with coherent reflections within a down-dropped block and adjacent transparent zones basinward may indicate counter-regional faults underlain by shale diapirs. Unlike larger-scale depobelts, however, transparent zones rise upward through only the basal most stratigraphic interval. Although there is evidence for a progressive basinward shift in areas of thickest sediment accumulation within sequences (Figures 12 and b; 13a and b) and evidence for greater sediment bypass during deposition of successive sequences, for the most part reflection patterns can be traced across multiple fault blocks. This suggests that several adjacent blocks were being buried simultaneously, and thus any upward movement of basal shales along the footwalls of faults did not create major bathymetric barriers to sediment transport basinward. This pattern is different from minibasins that form on slopes over mobile salt layers, which tend to more completely restrict sediment bypass until they are nearly completely filled, producing more pronounced “fill and spill” histories of basin-filling. Deeper narrower incisions and course-grained facies belts along boundaries of lower sequences, relative to broader, less deeply incised surfaces that

characterize upper sequence boundaries, probably also reflect more rapid rates of structural deformation early in the history of depobelt filling.

The broadly-defined upward-coarsening trend, less evident for significant accumulation of growth strata up section, and thinning of successive sequences suggest that rates of tectonic subsidence relative to sediment supply decreased over time. It may be that structural collapse was more rapid during initial stages of depobelt development or that sediment supply was initially restricted to more proximal areas and loading effects on subsidence were more widespread. Despite the decrease in shale upward, blocky and upward-fining log patterns in basal deposits (below sequence boundary 1), and evidence for fluvial incision at the base of even the oldest sequences suggest shallow water to fluvial deposition. Thus, the vertical succession may indicate decreasing rates of aggradation rather than progradation of systems tracts and associated depositional environments.

Separating structural and stratigraphic controls on sequence development can be difficult in this setting, where sediment loading controls rates of local subsidence of fault blocks, which in turn control sediment transport pathways into the basin. Depobelts nearly filled with sediment, as predicted by Knox and Omatsola (1989), might be rapidly flooded when rising sea levels flood extensive, shallow, delta-top areas. Maximum flooding surfaces that can be traced across multiple fault blocks, like those traced across Robertkiri field, might indicate a similar sequence stratigraphic setting. Mechanisms that produced incisions along sequence basal erosion surfaces are more difficult to constrain, as these surfaces vary significantly in character across individual fault blocks and associated down dropped blocks; In general, erosion along sequence boundaries is greater

into footwalls and crests of roll over anticlines. Brown et al. (2004) recently proposed a model to explain sequence erosion within deltaic successions that prograded onto mobile shale substrates off the northern Gulf of Mexico shelf. They suggested that falling sea level would force deposition to rapidly shift basinward, initiating a new area of sediment loading. Build up of a lowstand wedge initiates the development of a new fault and associated concentration of growth strata above the adjacent down dropped block. Stratal relationships observed within Robertkiri field, specifically relatively gradual changes in sequence thickness across several fault blocks, does not support this mechanism for the development of sequences on Niger Delta; at least not at the scale that we examined. The depth of incisions at the base of sequences (>100-200 m) is difficult to explain in terms of sea level falls alone, as 3rd order eustatically driven variations during the Miocene are generally reported to be only several tens of meters (Posamentier and Vail 1988; Van Wagoner et al. 1990; Talling,1998). Deepest incisions, in the footwalls of major faults and over crests of rollover anticlines suggests local structural uplift, even within the areas dominated by clastic wedge collapse along normal faults. Footwall blocks may isostatically rebound under rising mobile shales as the weight of adjacent hanging wall blocks is shifted basinward. Fluvial incision over anticline crests many be enhanced even in areas above down dropped fault blocks.

CONCLUSIONS

Sequence stratigraphic framework for a growth faulted delta deposit was constructed using a 3D seismic volume and well logs through the Agbada Formation within Robertkiri field, offshore Nigeria. The main conclusions are:

1. Six major 3rd order sequence boundaries and intervening maximum flooding surfaces were mapped. The sequences developed above a succession of basinward-dipping normal faults, where hanging walls were displaced basinward during deposition.
2. Upsection the deposits broadly coarsen, but depositional environments appear to have been consistently fluvial to shallow marine. Blocky sandstones that occur abruptly within intervals above maximum flooding surfaces may indicate falling stage "forced" regression. Sequences become thinner and contain less evidence for the accumulation of growth strata down dip of major faults and away from rollover anticline crests.
3. Sequences lower within the succession are defined by narrower and deeper incisions (hundreds of meters deep), whereas boundaries of those higher within the succession are broader and less deeply incised. The youngest two sequences are largely horizontal and truncate underling faulted and deformed strata below, suggesting they were deposited after structural collapse in this area had ended.
4. Incisions along sequence boundaries can be hundreds of meters deep, which exceed expected 3rd order eustatic falls in sea level during the Miocene. Thus, these incisions must have been structurally enhanced, despite the overall extensional nature of deformation along this shelf margin.

5. Robertkiri field strata were deposited along the proximal side of the Coastal Swamp I depobelt, in an area that received relatively high rates of sediment supply. Rates of structural collapse decreased over time, as more sediment was bypassed seaward. Interpretation of mechanisms that formed high-frequency sequences is difficult in this setting, where rates of sediment loading control structurally generated accommodation, which in turn controls paths of sediment transport into the basin.

REFERENCES CITED

Adeogba, A.A., T.R. McHargue, and S.A. Graham, 2005, Transient fan architecture and depositional controls from near-surface 3-D seismic data, Niger Delta continental slope: American Association of Petroleum Geologists Bulletin, v. 89, p. 627-638.

Cathles, L.M., E.L. Colling, A. Erendi, G.D. Wach, M.W. Hoffman, and P.D. Manhardt, 2003, 3-D flow modeling in complex fault networks: Illustration of new methods with an exploration application in offshore Nigeria, *in* S. Duppenbecker and R. Marzi, eds., Multidimensional Basin Modeling: AAPG/Datapages Discovery Series no. 7, p. 177– 195.

Cohen, H.A., and K. McClay, 1996, Sedimentation and shale tectonics of the northwestern Niger DeltaNiger Delta front: Marine and Petroleum Geology, v. 13, p. 313–328.

Corredor, F., J.H. Shaw, and F. Billoti, 2005, Structural styles in the deep-water fold and thrust belts of the Niger Delta: American Association of Petroleum Geologists Bulletin, v. 89, p. 753–780.

Daily, G.C., 1976, A possible mechanism relating progradation, growth faulting, clay diapirism and overthrusting in a regressive sequence of sediments: Bulletin of Canadian Petroleum Geology, v. 24; p. 92-116.

Damuth, J.E., 1994, Neogene gravity tectonics and depositional processes on the deep Niger Delta continental margin: Marine and Petroleum Geology, v. 11, p.320-346.

Doust, H. and E. Omatsola, 1989, Niger Delta: American Association of Petroleum Geologists Memoir 48, p. 201-238.

Doust, H., and E. Omatsola, 1990, Niger Delta, in J.D. Edwards and P.A. Santogrossi, eds., Divergent/passive margin basins: American Association of Petroleum Geologists Memoir 48, p. 239-248.

Evamy, B.D., J. Haremboure, R. Kammerling, W.A. Knaap, F.A. Molloy, and P.H., Rowlands, 1978, Hydrocarbon habitat of tertiary Niger Delta: American Association of Petroleum Geologists Bulletin, v. 62, p. 1-39.

Edwards, M. B., 2000, Origin and significance of retrograde failed shelf margins; Tertiary Northern Gulf Coast Basin: Transactions of the Gulf Coast Association, v. 50, p. 81-93.

Hooper, R.J., R.J. Fitzsimmons, N. Grant, and B.C. Vendeville, 2002, The role of deformation in controlling depositional patterns in the South-Central Niger Delta, West Africa: Journal of Structural Geology, v. 24, p. 847-859.

Khalivov, N.Y., and A.A. Kerimov, 1983, Origin of mud volcanism and diapirism: International Geological Review, v. 25, p. 877-881.

Knox, G. J., and E. Omatsola, 1989, Development of the Cenozoic Niger Delta in terms of 'Escalator Regression" Model and impact on Hydrocarbon distribution, *in* Proceedings KNGMG Symposium "Coastal Lowlands Geology and Geotechnology," 1987: Dordrecht, Kluwer, p. 181-202.

Lawrence, S.R., S. Munday, and R. Bray, 2002, Regional geology and geophysics of the eastern Gulf of Guinea (Niger Delta to Rio Muni): The Leading Edge, v. 21, p. 1112–1117.

Mitchum, R.M., Jr., and J.C. Van Wagoner, 1991, High-frequency sequences and their stacking patterns: Sequence stratigraphic evidence of high-frequency eustatic cycles: Sedimentary Geology, v. 70, p. 131-160.

Morgan, R., 2004, Structural controls on the positioning of submarine channels on the lower slopes of the Niger Delta: Geological Society, London, Memoir 29, p.45- 51.

Morley, C.K., 1992, Notes on Neogene basin history of the Western Alboran Sea and its implications for the tectonic evolution of the Rif-Betic Orogenic Belt: Journal of African Earth Sciences, v. 14, p. 57-65.

Morley, C.K., P. Crevello, and Z.H. Ahmad, 1998, Shale tectonics and deformation associated with active diapirism: The Jerudong Anticline, Brunei Darussalam: Journal of the Geological Society of London, v. 155, p. 475–490.

Petters, S.W., 1978, Stratigraphic evolution of the Benue trough and its implications for the Upper Cretaceous paleography of West Africa: Journal of Geology, v. 86, p. 311-322.

Posamentier, H.W., M.T. Jervey, and R.R. Vail, 1988, Eustatic controls on clastic deposition I - Conceptual Framework, *in* C.K., Wilgus, , B.S. Hastings, C.G. St.C. Kendall, H. Posamentier, C.A. Ross, J. Van Wagoner, eds., Sea-Level Changes - An Integrated Approach: Society of Economic Paleontologist and Mineralogists Special Publication 42, p. 109-124.

Posamentier, H. W., and P. R. Vail, 1988, Eustatic controls on clastic deposition II – Sequence and systems tracts models, *in* C.K., Wilgus, , B.S. Hastings, C.G. St.C. Kendall, H. Posamentier, C.A. Ross, J. Van Wagoner, eds., Sea-Level Changes - An Integrated Approach: Society of Economic Paleontologist and Mineralogists Special Publication 42, p. 125-154.

Postma, G., 1995, Sea-level related architecture trends in coarse grained delta complexes, *in* S.K. Chough and G.J.Orton, eds., Fan Deltas: Depositional Styles and Controls: Sedimentary Geology, v. 98, p. 3-12.

Rensbergen, P.V., C.K Morley, D.W. Ang, T.Q. Hoan, and N.T. Lam, 1999, Structural evolution of shale diapirs from reactive rise to mud volcanism: 3D seismic data from the Baram delta, offshore Brunei Darussalam: Journal of The Geological Society, v. 156, p. 633-650.

Rensbergen, P.V., and C.K. Morley, 2000, 3D Seismic study of a shale expulsion syncline at the base of the Champion delta, offshore Brunei and its implications for the early structural evolution of large delta systems: Marine and Petroleum Geology, v. 17, p. 861–872

Reijers, T.J.A., S.W, Petters, and C.S, Nwajide, 1997, The Niger Delta Basin, in R.C. Selley, ed., African Basins-Sedimentary Basin of the World 3, Amsterdam, Elsevier Science, p. 151-172.

Short, K.C., and A.J. Stauble, 1967, Outline of Geology of Niger Delta: American Association of Petroleum Geologists Bulletin v. 51, p. 761-779.

Stacher, P.,1995, Present understanding of the Niger Delta hydrocarbon habitat, in M.N. Oti, and G. Postma, eds., Geology of Deltas: Rotterdam, A.A. Balkema, p. 257-267.

Talling, P.J., 1998, How and where do incised valleys form if sea-level remains above the shelf edge?: Geology, v. 26, p. 87 90

Thorne, J.A., and D.R. Swift, 1991, Sedimentation on continental margins VI: A regime model for depositional sequences, their component systems tracts, and bounding surfaces, in D.J.R, Swift, G.E. Oertel, R.W. Tillman, J.A. Thorne, eds., Shelf Sand and Sandstones Bodies: Geometry, Facies and Sequence Stratigraphy: Special Publication International Association of Sedimentologists 14, p. 189-255.

Tuttle, L.W., R.R Charpentier and M.E. Brownfield, 1999, The Niger Delta Petroleum System: Niger Delta Province, Nigeria, Cameroon, and Equatorial Guinea, Africa: U.S. Geological Survey World Energy Project, Open-File Report 99-50-H.

Vail, R.R., R.M. Mitchum, and S. Thompson, 1977, Seismic stratigraphy and global changes of sea level, Part 3. Relative changes of sea level from coastal onlap, in , C.E. Payton, ed., Seismic Stratigraphy - Applications in Hydrocarbon Exploration. American Association of Petroleum Geologists Memoir 26, p. 63-82.

Van Wagoner, J.C., R.M. Mitchum, K.M. Campion, and V.D. Rahmanian, 1990, Siliciclastic sequence stratigraphy in well logs, cores and outcrops: American Association of Petroleum Geologists Methods in Exploration Series, v. 7. pp. 1-55

Weber, K.J. and E.M. Daukoru, 1975, Petroleum geology of the Niger Delta: Proceedings of the 9th World Petroleum Congress, Tokyo, v. 2, p. 202- 221.

Weber, K.J., 1986, Hydrocarbon distribution patterns in Nigerian growth fault structures controlled by structural style and stratigraphy: American Association of Petroleum Geologists Bulletin, v. 70, p. 661-662.

Weimer, P., P. Varnai, F.M. Budhijanto, Z.M. Acosta, R.E. Martinez, A.F. Navarro, M.G. Rowan, B.C. McBride, T. Villamil, C. Arango, J.R. Crews, and A.J. Pulham, 1998, Sequence stratigraphy of Pliocene and Pleistocene turbidite systems, northern

Green Canyon and Ewing bank (offshore Louisiana), northern Gulf of Mexico: American Association of Petroleum Geologists Bulletin, v. 82, p. 918– 960.

VITA

NAME:	Olusola Akintayo Magbagbeola
EDUCATION:	Texas A&M University College Station, Texas M.S., Geology, 2004. University of Ibadan Ibadan, Nigeria M.Sc., Geophysical Exploration, 1995. University of Ilorin Ilorin, Nigeria B.Sc., Geology & Mineral Exploration, 1991.
PROFESSIONAL EXPERIENCE:	Chevron Nigeria Limited Lagos, Nigeria Earth Scientist, 1997-present. University of Ibadan Ibadan, Nigeria Assistant Lecturer, 1995-1997. Federal University of Technology Akure, Nigeria Graduate Assistant, 1992-1993
PERMANENT ADDRESS:	Chevron Nigeria Ltd. (Pouch Mail) 6001 Bollinger Canyon Road San Ramon, California 94583